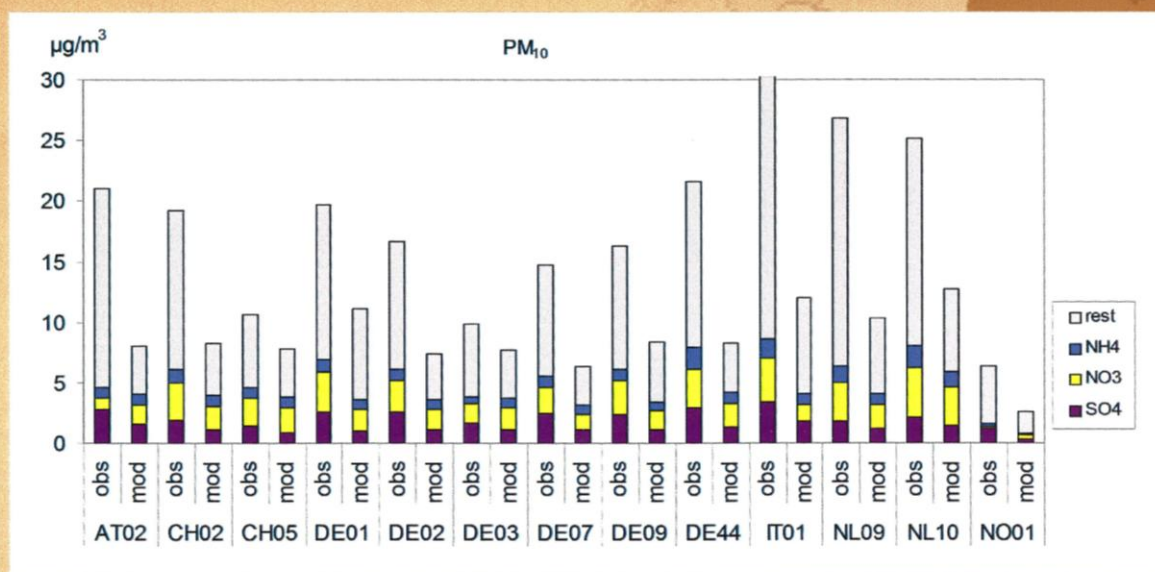


# Transboundary particulate matter in Europe

Status Report 4/2009





NILU: EMEP Report 4/2009  
REFERENCE: O-98134  
DATE: AUGUST 2009  
ISSN: 1504-6109 (print)  
1504-6192 (online)

**EMEP Co-operative Programme for Monitoring and Evaluation of the  
Long-Range Transmission of Air Pollutants  
in Europe**

**Transboundary particulate matter in Europe  
Status report 2009**

**Joint  
CCC, MSC-W, CEIP and CIAM  
Report 2009**



**Norwegian Institute for Air Research**  
P.O. Box 100, NO-2027 Kjeller, Norway



**Norwegian Meteorological Institute**  
P.O. Box 43 Blindern, NO-0313 Oslo, Norway



**Umweltbundesamt GmbH**  
Spittelauer Lände 5, AT-1090 Vienna, Austria



**IIASA – International Institute for Applied  
Systems Analysis**  
Schlossplatz 1, AT-2361 Laxenburg, Austria



## List of Contributors

Karl-Espen Yttri<sup>1</sup>, Wenche Aas<sup>1</sup>, Kjetil Tørseth<sup>1</sup>, Kerstin Stebel<sup>1</sup>,  
Svetlana Tsyro<sup>2</sup>, David Simpson<sup>2</sup>,  
Katarina Merckova<sup>3</sup>, Robert Wankmüller<sup>3</sup>  
Zbigniew Klimont<sup>4</sup>, Robert Bergström<sup>5</sup>,  
Hugo Denier van der Gon<sup>6</sup>,  
Thomas Holzer-Popp<sup>7</sup> and Marion Schroedter-Homscheidt<sup>7</sup>

- 1) Norwegian Institute for Air Research, Kjeller, Norway
- 2) Norwegian Meteorological Institute, Oslo, Norway
- 3) Umweltbundesamt, Vienna, Austria
- 4) International Institute for Applied Systems Analysis, Laxenburg, Austria
- 5) Swedish Meteorological and Hydrological Institute, Norrköping, Sweden
- 6) TNO Netherlands Organisation for Applied Scientific Research, Utrecht, The Netherlands
- 7) German Aerospace Center (DLR), German Remote Sensing Data Center (DFD), Oberpfaffenhofen, Germany

<sup>1</sup> EMEP Chemical Coordinating Centre

<sup>2</sup> EMEP Meteorological Synthesizing Centre – West

<sup>3</sup> EMEP Centre on Emission Inventories and Projections

<sup>4</sup> EMEP Centre on Integrated Assessment Modelling



# Contents

	Page
<b>Executive Summary .....</b>	<b>7</b>
<b>1 Status of emissions, 2007 .....</b>	<b>13</b>
1.1 PM emission reporting under LRTAP Convention .....	13
1.1.1 Status of reporting .....	13
1.1.2 PM emission trends .....	13
1.1.3 PM key categories .....	17
1.1.4 Emission data used for modelling .....	19
1.2 Assessment of PM emissions using GAINS .....	20
1.3 Improved emission estimates of EC/OC .....	26
<b>2 Measurement and model assessment of particulate matter in Europe, 2007 .....</b>	<b>30</b>
2.1 Particulate matter mass concentrations .....	30
2.1.1 Introduction .....	30
2.1.2 The EMEP model and runs setup .....	30
2.1.3 Status of particulate matter mass observations .....	31
2.1.4 Spatial distribution of PM <sub>10</sub> and PM <sub>2.5</sub> .....	32
2.1.5 Temporal trends in PM <sub>10</sub> and PM <sub>2.5</sub> .....	33
2.1.6 Differences in model results, 2007 vs. 2006 .....	33
2.1.7 Particulate matter size distributions .....	35
2.2 Exceedances of WHO AQGs by regional background PM mass .....	38
2.3 Contribution of secondary inorganic species to PM mass .....	42
2.3.1 Introduction .....	42
2.3.2 Measurements and modelling of secondary inorganic aerosol (SIA) .....	42
2.3.3 Evaluation of the model performance for PM mass and SIA .....	45
2.4 Elemental and Organic Carbon .....	49
2.4.1 Status of sampling and measurement, and quality of observation data .....	49
2.4.1.1 EC and OC levels at the Norwegian site Birkenes (NO01) .....	51
2.4.1.2 EC and OC levels at the Italian site Ispra (IT04) .....	53
2.4.1.3 EC and OC levels at the German site Melpitz (DE44) .....	55
2.4.1.4 EC and OC levels at the Spanish site Montseny (ES17) .....	57
2.4.1.5 Concluding remarks .....	58
2.4.2 Improvements in modelling Secondary Organic Aerosols: Experiments with the VBS Approach .....	58
2.4.2.1 Introduction .....	58
2.4.2.2 The volatility basis set (VBS) approach .....	59
2.4.2.3 EC and OC emissions .....	59
2.4.2.4 EMEP-VBS OA models, and results .....	60
2.4.2.5 Caveats, Conclusions and Future Work .....	63
2.4.2.6 Acknowledgements .....	63
2.5 EMEP Intensive Measurement Periods .....	63

<b>3</b>	<b>Aerosol optical properties and special events occurring during 2007.....</b>	<b>67</b>
3.1	Remote sensing.....	67
3.1.1	Introduction.....	67
3.1.2	Model calculations of AOD.....	68
3.1.3	Further testing of model AOD: Agricultural fires in spring 2006.....	70
3.1.4	SYNAER measurements of Particulate Matter.....	73
3.2	Special events in 2007.....	76
3.2.1	Wild fires in Greece.....	76
3.2.2	Dust episode in Ukraine observed across Europe.....	77
<b>4</b>	<b>References.....</b>	<b>81</b>
	<b>APPENDIX A Overview of PM emissions reporting.....</b>	<b>87</b>
	<b>APPENDIX B Tables and figure to Chapter 2.....</b>	<b>91</b>

## **Executive Summary**

The current report presents the status of the emission reporting, observations and modelling activities undertaken under EMEP in relation to particulate matter in the European rural background environment. It also includes a section related to the application of satellite remote sensing data in validation of model results and it presents two distinct episodes of transboundary fluxes of particulate matter taking place during 2007.

### **Emission reporting**

Only 33 Parties provided primary particulate matter emissions data in 2009, but compared to the year 2002, where only 27 Parties reported PM emissions, it is considered an improvement from 53% to 65% of Parties. The reported trends in PM emission fluxes vary quite considerably among the Parties. In the period from 2000 to 2007, the PM emissions in EU-27 region have decreased. Due to a lack of data from the other regions, it is not possible to assess the overall trend for the whole EMEP area. Since 2000, PM<sub>10</sub> and PM<sub>2.5</sub> emissions have increased in 10 and 8 Parties, respectively. From 2006 to 2007 emissions increased in 11 Parties.

The distribution of key emission categories identified for Eastern and Western Europe is different and the total number of key categories is higher in Western Europe for both PM<sub>10</sub> and PM<sub>2.5</sub>. Residential Stationary Combustion is the most significant key source for PM<sub>10</sub> and PM<sub>2.5</sub> in both regions. In Eastern Europe, Public Electricity and Heat Production and Stationary Combustion in Manufacturing Industries and Construction-Other follow in importance. Road Transport contributes also significantly to PM<sub>10</sub> and PM<sub>2.5</sub> in both Eastern and Western Europe; in the latter, large population of diesel vehicles plays a major role.

Completeness of sectoral PM emissions needs improvement. While more or less complete data are available for Europe (except for some Balkan countries), no PM emissions were reported by the EECCA countries, Turkey and for the “Russian Federation extended EMEP domain”.

### **Modelling emissions of primary PM**

A comparison of national submissions to the CLRTAP and GAINS model estimates for the EU-15 shows a relatively good agreement on a national level as well as for key sectors. However, review of the time series of submissions indicates that there may have been significant changes in the methodology used by national experts to estimate emissions. Analysis of various discrepancies is under way and the results will be communicated to the national experts and used to improve the GAINS model. Only limited comparison can be done for several UNECE countries (specifically for a number of non-EU-27 countries) since submissions are either missing or are incomplete.

Total anthropogenic emissions (for the period 2000-2005) of primary BC and OC in Europe (excluding international shipping) have been estimated in GAINS model at about 0.6 and 0.75 Tg, respectively. For both carbonaceous species the largest single contributing sector is residential combustion with share of 40 and

50% for BC and OC. For BC, road transport is nearly as important as residential combustion and combined with off-road makes a share of 50%. Total primary carbonaceous particles represent about 42% of primary emissions of PM<sub>2.5</sub> in Europe. For all sectors but transport BC/OC emissions ratio is below 1. There are large uncertainties in basic data needed for calculation of emissions of carbonaceous emissions, especially in countries where emission reporting and other statistical data collection focuses on large industrial installations.

It is expected that the total European PM<sub>2.5</sub> emissions will decline in the coming decades by about 20% compared to the year 2005. Most of the decline will take place in the EU countries, especially EU-15. For Russian Federation, Ukraine, and Turkey a significant growth of emission is expected, provided no additional legislation is introduced in the considered period. Future emissions of BC and OC are expected to decline by about 25% mostly due to already implemented and envisaged policies in transport sector as well as structure of fuel use in domestic sector (less solid fuels). Total number for the EMEP regions shows still a rather pessimistic picture as it assumes rather conservative air pollution policies in FSU and EECCA countries resulting in increase of emission in these regions mostly due to rapid motorization.

## **Concentration Measurements and Modelling**

### *Spatial and temporal variability of PM<sub>10</sub> and PM<sub>2.5</sub>*

For the first time, modelled PM concentrations are presented for the EMEP extended area, including the EECCA countries. Another important change this year is that the calculations have been performed with a more recent version of the EMEP model. It applies a revised scheme for night-time formation of nitric acid and results in an appreciable decrease in the concentrations of nitrate and ammonium compounds. As a consequence, concentrations of PM<sub>10</sub> and PM<sub>2.5</sub> decreased, and in particular for central Europe. A third important change is the use of a new meteorological driver. In general, air concentrations calculated with the new HIRLAM meteorology indicates lower values than those calculated with the previous PARLAM meteorology. The reason for that is to be further investigated.

For 2007, mass concentrations of PM are reported for 52 sites (50 for PM<sub>10</sub> and 26 for PM<sub>2.5</sub>), which are 3 more than for 2006. 18 countries reported mass concentrations for 2007, which is one more compared to the previous year. The inclusion of the two French sites (FR0009 and FR0013) makes an important extension to a part of Western Europe, which previously has not reported PM mass concentration levels to EMEP.

The spatial pattern seen for PM<sub>10</sub> and PM<sub>2.5</sub> in 2007 corresponds to that reported for previous years, and reflects both population density and other major anthropogenic sources. There are large spatial gradients illustrated e.g. by the annual means of PM<sub>2.5</sub> with the lowest annual mean reported for Birkenes (NO01) (3.3 µg m<sup>-3</sup>) and the highest for Ispra (IT04) (25.7 µg m<sup>-3</sup>). The majority (78%) of the sites which reported levels of PM<sub>10</sub> both for 2006 and 2007 experienced lower annual mean concentrations in 2007 compared to the previous year. The decrease in PM<sub>10</sub> experienced by the majority of the sites going from 2006 to 2007 appears

to be attributed mostly to PM<sub>2.5</sub>. Six sites reporting concentrations of PM<sub>2.5</sub> for 2007 have time series that extend five years. Both for PM<sub>10</sub> and PM<sub>2.5</sub> none of these sites show any evident year-by-year reduction or increase in the concentration.

There are quite substantial differences (exceeding 30%) between model results for PM<sub>10</sub> and PM<sub>2.5</sub> obtained for 2007 compared to the calculations performed for previous years due to the updates in the model and changes in meteorological and emission data. In general, the model calculated concentrations of anthropogenic PM<sub>10</sub> and PM<sub>2.5</sub> that were 5-30% lower in 2007 than in 2006 for most of the EMEP area except from Spain, France, northern Italy, the northernmost part of Scandinavia, and in the extended areas of EMEP. Meteorological variability and the new meteorological driver used to prepare the data for 2007 have likely affected the differences seen for PM when comparing model results for 2006 and 2007. Large parts of southern and south-eastern Europe, and Scandinavia experienced more precipitation in 2007 than in 2006, while it was drier in Spain, northern France, the UK and most of Russia and Central Asia compared to 2006. A particularly warm and wet winter was observed in most of Europe in 2007, causing lower PM<sub>10</sub> and PM<sub>2.5</sub> concentrations. The overall effect of emission changes on PM was a decrease of PM<sub>10</sub> and PM<sub>2.5</sub> concentrations by up to 30% for most of Europe and an increase of PM<sub>10</sub> and PM<sub>2.5</sub> by up to 30% for the northern most part of Scandinavia and Central Asia. The observations show that the contribution of fine particles to PM<sub>10</sub> is less in spring and summer (65% on average), increasing to 70% in autumn and to 79% in winter. The observations show that PM<sub>2.5</sub> typically account for a larger fraction of PM<sub>10</sub> in central Europe, reflecting the strong influence of anthropogenic sources.

Model calculated annual mean regional background concentrations of PM<sub>10</sub> in 2007 were below the EU limit value of 40 µg m<sup>-3</sup> in most of Europe, with the exception of the Central Asian countries. However, the calculated annual mean PM<sub>10</sub> exceeded the WHO recommended AQG of 20 µg m<sup>-3</sup> pr year in several polluted areas, among others in the Benelux countries, the Po Valley, Slovakia, and also in a number of grid cells associated with large cities or other greater emission sources. In a rather extensive area, except from parts of central Europe, Scandinavia and the north of Russia, PM<sub>10</sub> exceedance of 50 µg m<sup>-3</sup> occurred more than 3 days, which is the maximum number of days recommended by the WHO. Furthermore, the WHO AQG for PM<sub>2.5</sub> was exceeded by regional background concentrations in more than 3 days in most of the European countries, except northern Europe and northern Russia. For most sites, the model under-predicts the number of exceedance days compared to observations, although with some exceptions.

## **Concentration Measurements and Modelling**

### *Chemical speciation*

The relative contribution of SO<sub>4</sub><sup>2-</sup> to PM<sub>10</sub> and NO<sub>3</sub><sup>-</sup> to PM<sub>10</sub> based on the data reported for 2007 are quite similar; 14±4% for SO<sub>4</sub><sup>2-</sup> and 13±4% for NO<sub>3</sub><sup>-</sup>. However, the spatial distributions are quite different. For several of the sites which reported a decrease in the concentration of PM<sub>10</sub> for 2007 compared to the previous year, there is a correspondingly strong decrease in SIA. SIA is currently

underestimated by 34% by the model. The model underestimation of SIA contributes to the model's negative bias for PM<sub>10</sub> and particularly for PM<sub>2.5</sub>, which is larger than what has been reported for previous years. PM<sub>10</sub> is currently underestimated by 43%, while PM<sub>2.5</sub> by 41%. As the relative contribution of SIA to PM varies across Europe, the recent updates of the model affected the calculated PM to a various extent. Therefore, the changes have caused a somewhat different regional distribution of calculated PM<sub>10</sub> and PM<sub>2.5</sub> over Europe compared to previous years. The spatial correlation between calculated and measured PM<sub>10</sub> and PM<sub>2.5</sub> is somewhat lower than that seen in the earlier reports, the correlation coefficient being 0.60 for PM<sub>10</sub> and 0.70 for PM<sub>2.5</sub>. The model performance seems to be better for the warm season compared to the cold season when compared to observations.

There is still a lack of comparable EC/OC data in Europe, which makes it difficult to address the spatial and temporal variation of these variables on the regional scale. This situation did not improve from 2006 to 2007, but a substantial increase in the number of countries and sites reporting levels of EC and OC is however expected in the coming years. This is due to the ongoing development of the unified protocol for sampling and measurement of the ambient aerosol content of EC and OC within the EUSAAR project.

Only four countries reported measurements of EC and OC for 2007, which is one more than for 2006. The sites are Birkenes (NO01) in Norway, Melpitz (DE44) in Germany, Ispra (IT04) in Italy, and Montseny (ES17) in Spain. A brief overview of the data reported for these sites are presented and show that there are large regional differences in the carbonaceous aerosol concentration. Results further show large inter-annual variations in the levels of carbonaceous aerosol. This calls for a rapid increase in the number of sites performing such measurement on a continuous basis.

Complementary analyses of e.g. organic tracers and <sup>14</sup>C, along with AMS-measurements are necessary to reveal the sources of particulate carbonaceous matter. The sources and formation mechanisms of SOA are still very uncertain, with many plausible pathways but still no reliable estimates of their relative importance. In such a situation one cannot expect a model to reliably capture measurements. The EMEP model has been extended to build on some of the recent ideas inherent in the so-called volatility-basis set (VBS) approach. Using the VBS, different SOA-forming reactions can be mapped onto the same set of bins over the range of organic aerosol mass concentration typical of ambient conditions (0.1–100 µg/m<sup>3</sup>) while maintaining mass balance for more volatile co-products as well. Three versions of the EMEP model have been set up, introducing different aspects of the VBS approach in each version.

The new EC/OC inventory made available through the EUCAARI project and the VBS methods, are in use for the first time and hence require careful checking. The model still misses emissions from forest and agricultural fires, and does not include primary biological aerosol particles.

The intensive measurement periods have become an important addition to the EMEP monitoring programme, both with respect to the scientific development

and for capacity building; i.e. by extending the suite of measurement variables and measurement methods. A total of eighteen sites participated in the second intensive measurement period, and the final off-line analyses of the two latter campaigns are currently being undertaken and data processing is in progress. Such an amount of high quality data requires a substantial effort with respect to interpretation and reporting in the coming months and year. The first impression is that the measurements went quite smoothly. The methodology has been well harmonized and consistent, and standardized reporting protocols for new type of measurements are being developed. One preliminary finding is that wood burning emissions, as estimated from the samples content of levoglucosan, are a substantial contributor to particulate OC<sub>P</sub> levels at European rural background sites in winter.

### **Application of remote sensing data**

Chapter 3.1 describes ongoing work with modeling and use of remote sensing data for the assessment of air quality levels in Europe. Following a short overview of recent developments within the field of aerosol remote sensing, improvements of the calculations of aerosol optical depth (AOD) with the EMEP aerosol model are shown. AOD from the recent model version compares better with MODIS AOD than the earlier model version and the negative bias is reduced. The correlation between modelled and MODIS AOD is better for 2004 data, but unchanged for 2006 data. On average, model calculated AOD is between 33% and 45% lower than AOD from MODIS retrievals. The spatial correlation coefficients vary between 0.24 and 0.36 for the periods considered. The temporal correlation between calculated and MODIS AOD is even better than the correlation between calculated and measured PM for quite a few sites.

Furthermore, the EMEP model has been used to simulate pollution episodes associated with the agricultural and forest fires in Russia and Eastern Europe in spring 2006, showing good resemblance between the propagation patterns of AOD associated with fires as observed by MODIS and calculated with the model. However, the model tends to calculate up to a factor 2.5-3.5 lower AOD due to fire emissions than AOD from MODIS retrievals and sun photometer measurements, which can probably be explained by uncertainties in fire emission data.

The utilization of a particular satellite data product, so-called SYNAER, for monitoring of aerosols in Europe has been studied. The main advantage of this product is its ability to calculate, besides AOD, aerosol composition and concentrations of particulate matter. Compared to version v1.0, SYNAER v2.2 better resembles monthly averaged PM<sub>10</sub> data for several sites in Europe. For 2006, 22 out of 49 PM<sub>10</sub> and 17 out of 29 PM<sub>2.5</sub> sites show significant correlation between SYNAER and EMEP data. The majority of PM<sub>10</sub> data show an apparent negative bias, the PM<sub>2.5</sub> data show negative/positive biases, depending on the particular sites. The reason for the apparent bias and the good correlation at many sites versus the lack of correlation at other sites this is still under investigation.

### **Special events occurring during 2007**

Two distinct episodes of regional transport of particular matter are presented at the end of the report. One episode was due to wild fires in Greece during August,

while the other was caused by windblown dust from strong winds in Ukraine. Both episodes are evident from observations made at EMEP sites, and provide an excellent test for the modelling capabilities. The interpretation of the relative source strengths is however limited by the inadequate implementation of monitoring requirements.

## 1 Status of emissions, 2007

*By Katarina Merckova, Robert Wankmüller and Zbigniew Klimont*

### 1.1 PM emission reporting under LRTAP Convention

#### 1.1.1 Status of reporting

Parties to the *LRTAP Convention* submit air pollution emission data (SO<sub>x</sub>, NO<sub>x</sub>, NMVOCs, NH<sub>3</sub>, CO, HMs, POPs and PM) annually to the EMEP Centre on Emission Inventories and Projections (CEIP) and notify the LRTAP Convention secretariat thereof. Parties are requested to report emission inventory data using standard formats in accordance with the EMEP Reporting guidelines (UNECE, 2009). Parties should report sectoral PM emissions starting 2000 as a minimum (see also Appendix A). Emissions of SIA precursors are presented in EMEP status report 1 (EMEP, 2009) while the PM emission is discussed here.

42 Parties to the Convention (out of 51) submitted inventories before 31 May 2009. Only 33 Parties provided PM emissions, but compared to the year 2002, where only 27 Parties reported PM emissions, it is considered an improvement from 53% to 65% of Parties. Data as submitted by Parties can be accessed via the CEIP homepage at <http://www.ceip.at/emission-data-webdab/submissions-under-clrtap/2009-submissions/>. Completeness and consistency of reported emissions is analyzed in the EEA & CEIP technical report *Inventory review 2009*.

#### 1.1.2 PM emission trends<sup>1</sup>

The PM emissions trends vary quite considerably among the Parties to the CLRTAP. See examples in Figure 1.1. PM emissions in EU-27 region decreased; however, because of lacking data it is not possible to assess overall trend for the whole EMEP area. Since year 2000 PM<sub>10</sub> emissions have increased in 10 Parties and PM<sub>2.5</sub> emissions have increased in 8 Parties (out of 27 which reported PM in both 2000 and 2007). The biggest increase in PM emissions is reported by Croatia and Denmark. Between 2006 and 2007 emissions rose in 11 Parties, with the biggest increase being reported by Estonia and Romania (Table 1.1, Table 1.2).

---

<sup>1</sup> The trend tables contain only data as reported by Parties, no expert estimates are included.

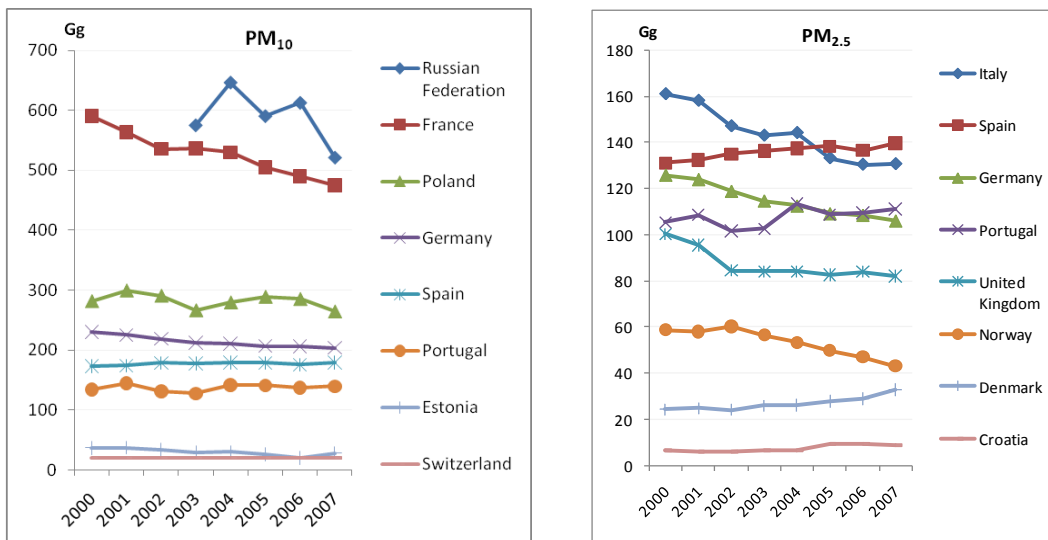


Figure 1.1: Examples of PM 2000-2007 emission trends within EMEP area PM<sub>10</sub> (left) and PM<sub>2.5</sub> (right).

Table 1.1: PM<sub>10</sub> emission trends (2000-2007) as reported by Parties.

Country / PM10 [Gg]	2000	2001	2002	2003	2004	2005	2006	2007	Change 2006- 07	Change 2000- 07
Albania										
Armenia										
Austria	43	44	44	45	45	44	45	43	-4%	-1%
Azerbaijan										
Belarus					48	36	40	39	-2%	
Belgium	48	45	44	44	42	38	37	34	-8%	-28%
Bosnia and Herzegovina										
Bulgaria								44		
Canada	5 083	5 182	5 156	5 282	5 369	5 646	5 828	5 952	2%	17%
Croatia	8.2	7.4	7.4	8.6	8.5	8.8	12	12	-3%	46%
Cyprus	3.5	3.6	3.7	4.0	4.0	4.1	4.0	4.2	4%	19%
Czech Republic		43	0.1	51	47	34	35	35	-1%	
Denmark	35	36	35	36	36	38	40	43	9%	22%
Estonia	37	37	33	30	30	26	20	28	43%	-23%
European Community	2 197	2 199	2 105	2 073	2 080	2 042	1 999	1 952	-2%	-11%
Finland	47	54	55	55	57	51	55	48	-12%	2%
France	590	564	535	536	530	505	490	475	-3%	-20%
Georgia										
Germany	230	225	219	213	211	207	206	204	-1%	-11%
Greece										
Hungary	47	43	44	48	47	52	48	36	-26%	-24%
Iceland										
Ireland	17	17	16	15	15	16	15	14	-6%	-17%
Italy	192	191	179	175	177	165	162	163	0%	-15%
Kazakhstan										
Kyrgyzstan										
Latvia	13	14	14	14	15	15	15	15	-1%	15%
Liechtenstein		0								
Lithuania					11	11	11	12	4%	
Luxembourg										
Malta	1.6	1.3	1.9	2.0	2.0	2.2	1.2	1.3	3%	-17%
Monaco										
Montenegro										
Netherlands	44	42	41	39	38	37	37	36	-2%	-17%
Norway	65	64	67	63	59	56	54	50	-6%	-22%
Poland	282	300	291	267	280	289	285	265	-7%	-6%
Portugal	134	145	131	127	142	141	137	139	2%	4%
Republic of Moldova	5	3	5	6	11	8	8		-100%	-100%
Romania						47	46	64	37%	
Russian Federation			0.6	576	647	591	613	522	-15%	
Serbia										
Slovakia	40	41	36	34	39	45	38	34	-12%	-15%
Slovenia	8	8	8	8	8	8	8	7	-7%	-12%
Spain	173	174	179	178	179	179	176	179	2%	3%
Sweden	43	43	43	43	44	44	44	44	1%	4%
Switzerland	20	20	20	20	20	20	20	19	0%	-5%
TFY Republic of Macedonia										
Turkey										
Ukraine			2.9		119	131				
United Kingdom	170	162	139	139	138	135	137	135	-1%	-20%
United States of America		21 266	19 346	19 335	19 322	19 310	17 533	15 762	-10%	

**Notes:** Blank cell indicates that no data were reported to EMEP

Cells highlighted red indicate increased emissions in given period

Emissions in row Russian Federation corresponds only "Russian Federation - EMEP domain"

Table 1.2: PM<sub>2.5</sub> emission trends (2000 - 2007) as reported by Parties.

Country / PM <sub>2.5</sub> [Gg]	2000	2001	2002	2003	2004	2005	2006	2007	Change 2006- 07	Change 2000- 07
Albania										
Armenia										
Austria	23	24	24	25	24	24	24	23	-5%	-2%
Azerbaijan										
Belarus					36	25	28	27	-2%	
Belgium	33	30	29	29	28	25	25	23	-7%	-30%
Bosnia and Herzegovina										
Bulgaria								21		
Canada	1 043	1 064	1 057	935	951	1 096	1 123	1 134	1%	9%
Croatia	6.5	5.7	5.8	6.8	6.7	9.1	9.2	8.8	-4%	35%
Cyprus	2.3	2.3	2.3	2.5	2.5	2.6	2.5	2.6	3%	13%
Czech Republic				38	35	21	22	21	-2%	
Denmark	24	25	24	26	26	28	29	33	13%	35%
Estonia	21	23	23	21	22	20	15	20	33%	-4%
European Community	1 445	1 426	1 365	1 349	1 358	1 329	1 296	1 266	-2%	-12%
Finland	37	38	39	38	38	34	35	34	-2%	-6%
France	402	380	355	356	349	331	317	303	-5%	-25%
Georgia										
Germany	126	124	119	115	113	109	109	106	-2%	-16%
Greece										
Hungary	26	24	25	27	27	31	29	21	-27%	-17%
Iceland										
Ireland	11	11	11	10	10	11	10	10	-5%	-16%
Italy	161	158	147	143	144	133	130	131	0%	-19%
Kazakhstan										
Kyrgyzstan										
Latvia	11	12	12	13	13	13	13	13	1%	18%
Liechtenstein										
Lithuania					8.8	8.7	8.9	10	7%	
Luxembourg										
Malta	1.0	0.5	1.3	1.3	1.3	1.5	0.5	0.5	1%	-47%
Monaco										
Montenegro										
Netherlands	25	24	23	23	21	21	20	19	-4%	-24%
Norway	59	58	60	56	53	50	47	43	-8%	-27%
Poland	135	142	142	142	134	138	136	128	-6%	-5%
Portugal	105	108	102	102	113	109	109	111	1%	6%
Republic of Moldova	2.1	1.6	1.5	2.7	5.8	6.2	7.2		-100%	-100%
Romania								31		
Russian Federation			0.4	341	383	350	409	348	-15%	
Serbia										
Slovakia	33	33	30	27	34	40	34	29	-14%	-10%
Slovenia	6	6	6	6	6	6	6	5	-6%	-17%
Spain	131	132	135	136	137	138	136	140	2%	7%
Sweden	31	31	31	31	31	32	31	32	2%	3%
Switzerland	9.1	8.9	8.7	8.6	8.6	8.6	8.4	8.3	-2%	-9%
TFY Republic of Macedonia										
Turkey										
Ukraine			0.01		15	125				
United Kingdom	100	95	84	84	84	83	84	82	-2%	-18%
United States of America		6 154	5 059	5 048	5 036	5 022	4 981	4 944	-1%	

**Notes:** Blank cell indicates no data have been reported to EMEP

Cells highlighted red indicates increased emissions in given period

Emissions in row Russian Federation corresponds only "Russian Federation - EMEP domain"

### 1.1.3 PM key categories

A key category is one that has significant influence on a country's total inventory in terms of absolute level of emissions<sup>2</sup>. The share of the top ten **key categories for Western and Eastern Europe** depicted in Figure 1.2 and Figure 1.3 contains emissions of sources that are within the 80% threshold:

1 A 1 a	Public Electricity and Heat Production
1 A 2 f i	Stationary Combustion in Manufacturing Industries and Construction - Other
1 A 3 b i	Road Transportation – Passenger Cars
1 A 3 b ii	Road Transportation – Light duty vehicles
1 A 3 b iii	Road Transportation – Heavy duty vehicles
1 A 3 b iv	Road Transport:, Automobile tyre and brake wear
1 A 4 b i	Residential – Stationary combustion
1 A 4 c ii	Agriculture/Forestry/Fishing - Off-road Vehicles and Other Machinery
1 B 2 a i	Exploration Production, Transport
2 A 7 d	Other Mineral products
2 A 7 a	Quarrying and mining of minerals other than coal
2 C 1	Iron and Steel Production
7 A	Other

Numbering of categories corresponds to EMEP nomenclature for reporting NFR08 (UNECE, 2009). If the total number of key categories for a particular pollutant was more than 11, emissions were summed up in 'Other key sources'. 'Other sources' contain the remaining (non-key) categories.

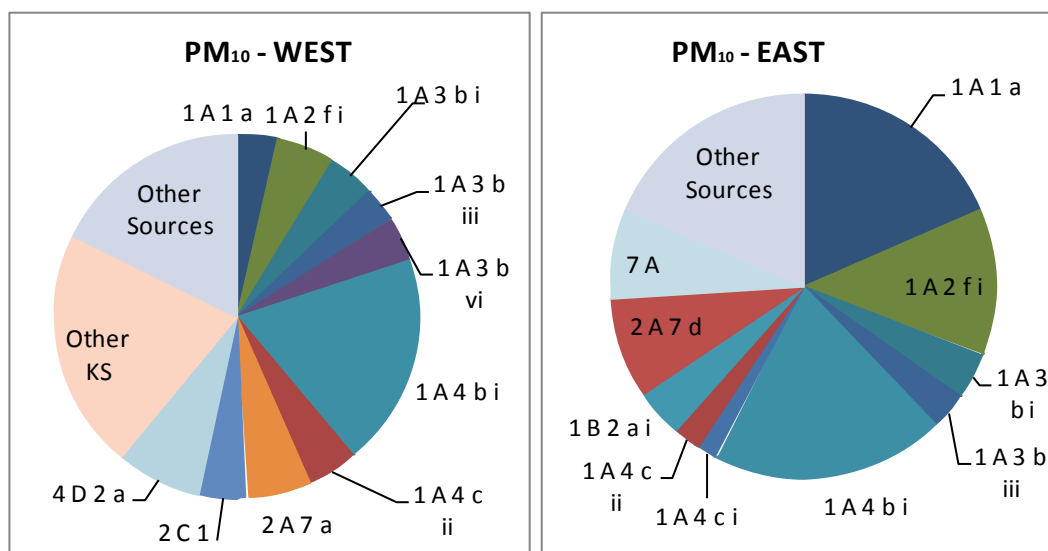


Figure 1.2: Key Category Analysis results of PM<sub>10</sub> 2007 emissions – comparison of Eastern and Western Europe (Numbering of categories corresponds to Nomenclature for reporting (NFR08)).

<sup>2</sup> For this year's KCA the threshold for identifying the key categories is 80%<sup>2</sup>, following the revised EMEP/EEA Air Pollutant Emission Inventory Guidebook (EEA/EMEP, 2009)

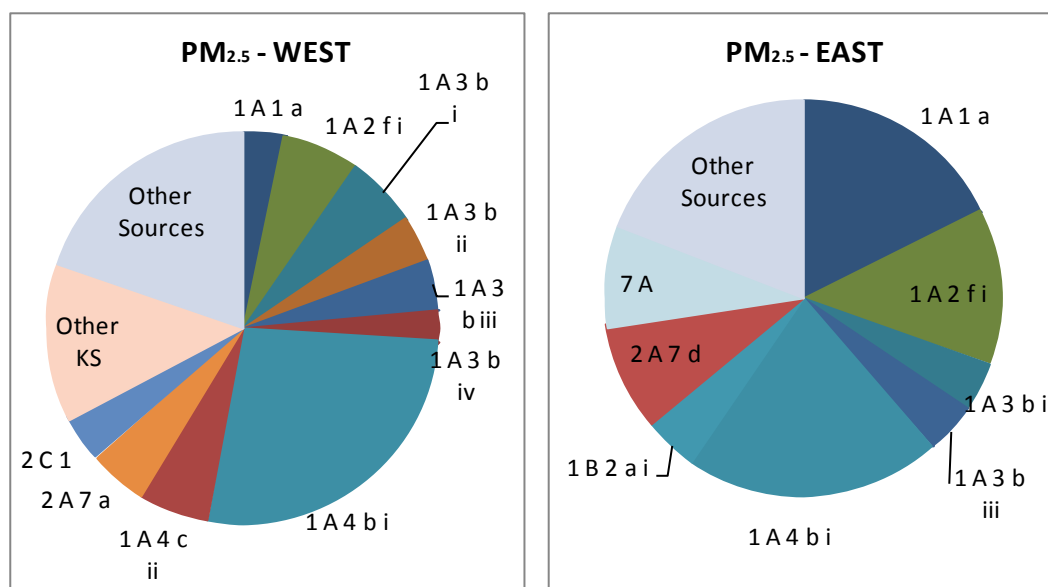


Figure 1.3: Key Category Analysis of  $PM_{2.5}$  emissions – comparison of Eastern and Western Europe.  
(Numbering of categories corresponds to NFR08).

The distribution of key categories identified for Eastern<sup>3</sup> and Western<sup>4</sup> Europe is different and the total number of identified key categories is higher in Western Europe for both  $PM_{10}$  and  $PM_{2.5}$  pollutants. Most of the emission categories identified as being the key source for both - Western and Eastern Europe - occur in combustion processes. The results of the Key Category Analysis (KCA) Figure 1.2 and Figure 1.3 show that:

- The most significant key source for  $PM_{10}$  and  $PM_{2.5}$  is *1A4bi Residential: Stationary combustion* in both Eastern and Western Europe contributing by about 20 % to  $PM_{10}$  emissions in the EMEP domain and almost 27 % to  $PM_{2.5}$  emission in Western Europe.
- In Eastern Europe followed by *1A1a Public Electricity and Heat Production* (19% to  $PM_{10}$ , 18 %  $PM_{2.5}$ ) and *1A2fi Stationary Combustion in Manufacturing Industries and Construction-Other* (13 %  $PM_{2.5}$ ). Whereas in Western Europe the share of *1A1a* on  $PM_{10}$  respectively on  $PM_{2.5}$  emissions is less than 4 % and share of *1A2fi* only 4.9 % ( $PM_{10}$ ) resp 6.3 % ( $PM_{2.5}$ ).
- Road Transport (*1A3bi Road Transportation - Passenger cars*, *1A3ii Road Transportation – Light duty vehicles* and *1A3biii Road Transportation – Heavy duty vehicles*, *Road Transportation: 1A3biv Automobile tyre and brake*

<sup>3</sup> Eastern European countries as referred to in the EMEP database = Albania, Armenia, Azerbaijan, Bosnia & Herzegovina, Bulgaria, Belarus, Cyprus, Czech Republic, Estonia, Georgia, Croatia, Hungary, Kyrgyzstan, Kazakhstan, Lithuania, Latvia, Republic of Moldova, Montenegro, Macedonia, Poland, Romania, Serbia, Russian Federation, Slovenia, Slovakia, Turkey, Ukraine.

<sup>4</sup> Western European countries as referred to in the EMEP database = Austria, Belgium, Switzerland, Germany, Denmark, Spain, Finland, France, United Kingdom, Greece, Ireland, Iceland, Italy, Liechtenstein, Luxemburg, Malta, Monaco, the Netherlands, Norway, Portugal, Sweden.

*wear*) contributes significantly to PM emissions in both Western and Eastern<sup>5</sup> Europe – PM<sub>10</sub> by 7.2 % and 7% and PM<sub>2.5</sub> by 16.5% and 8.3% .

It has to be noted that the share of PM key categories in individual countries differs from the distributions observed for Eastern and Western Europe. As expected *Road Transport* was detected as significant source of PM<sub>10</sub> and PM<sub>2.5</sub> emissions almost in all countries with the highest reported share in Canada (55% and 48% of national total emissions); the lowest *Road Transport* contribution was reported by Estonia (around 4%). Other common significant sources in many Parties are *Residential Heating*, which makes up for the highest share of PM<sub>10</sub> emissions in Norway (70%) and Cyprus (55%), and *Electricity and Heat Production* (e.g. in Malta 75%). The differences in key categories contribution do not necessarily indicate an underlying error, differences may also stem from different national circumstances. For detailed key category analysis results for 2006 for individual Parties please refer to the EEA & CEIP technical report Inventory review 2008, Appendix 7 (Mareckova & all, 2008).

#### **1.1.4 Emission data used for modelling**

Completeness of sectoral PM emissions needs improvement (an overview of PM sectoral emissions reporting is given in Appendix A). More or less complete data are available for Europe, except for some Balkan countries. No PM emissions were reported by the EECCA countries, Turkey and for the “Russian Federation extended EMEP domain”. To make submitted emission data usable for modellers missing information (not reported by Parties) have to be completed. Three basic methods have been used:

- a) Linear extrapolation of the last five years’ emissions (three years as a minimum).
- b) Copy of previous year’s emissions (data from 2006, 2005, 2003 or 2000) in case of missing trends.
- c) Other data sources (expert estimates, model results, etc..) if no reported data for a particular country are available

Shipping emissions for year 2007 have been estimated as linear interpolation between data from 2006 and ENTEC estimates for 2010.

The gap-filled and gridded data can be accessed via the CEIP homepage at <http://www.ceip.at/emission-data-webdab/emissions-used-in-emep-models/>. On the CEIP homepage, gridded data can also be visualized in Google Maps/Earth at <http://www.ceip.at/emission-data-webdab/emissions-in-google-maps/>. Figure 1.4 shows the differences between reported PM and gap-filled emission data on national total level:

<sup>5</sup>Source categories 1A3iii and 1A3biv does not appear among key categories in Eastern Europe.

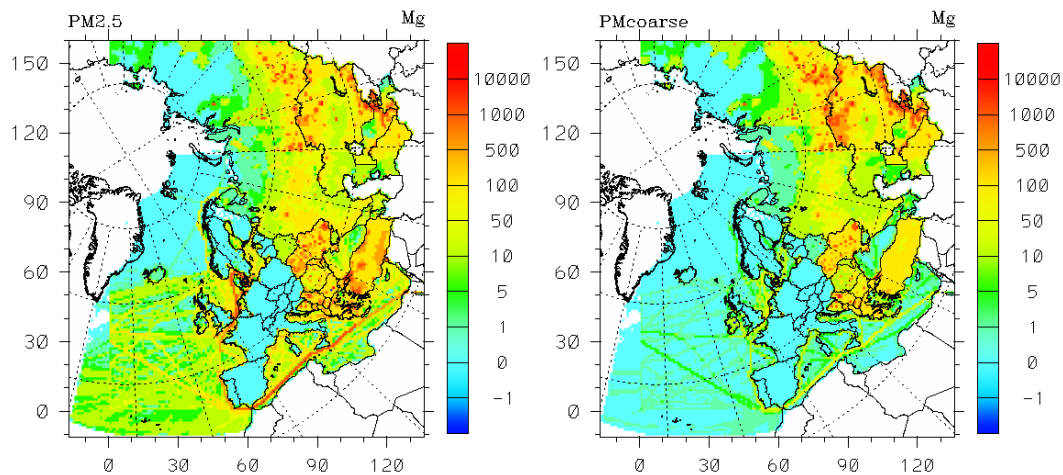


*Figure 1.4: Difference between reported PM emissions and emissions used in models in the extended EMEP grid for the 2007 inventory (Mg PM/grid).*

*Notes: Because of late submissions of corrected data from Bulgaria and Finland it was not possible to take into account the updated data in the model runs by MSC-W.*

*The extended EMEP domain<sup>6</sup> was considered in the gap-filling and gridding process for the first time. Because of not reported PM emissions from a number of countries in this area, MSC-W estimates from last year were used and gridded with current population data of this area, as provided by IIASA.*

*Light blue areas mean that either no gap-filling has taken place or the emission values in particular grids are slightly above zero (e.g. part of Russian Federation in the extended EMEP domain).*

## 1.2 Assessment of PM emissions using GAINS

Total European anthropogenic emissions of primary PM<sub>2.5</sub> have been estimated in GAINS model (<http://gains.iiasa.ac.at>) at 3.2 and 3 Tg for the year 2000 and 2005, respectively. The largest contribution originates from industrial and residential combustion, nearly 2 Tg (Figure 1.5) or about 60% of the total (Figure 1.6)<sup>7</sup>. Transport is the next biggest source with over 0.6 Tg of PM<sub>2.5</sub>. The contributions vary, however, for specific European regions (Figure 1.6) linked strongly to the economic development, fuel use structure, and level of emission abatement.

<sup>6</sup> The following areas in the extended domain were considered for gap-filling and gridding: Kyrgyzstan, Rest of Russian Federation in the extended EMEP domain, Rest of Kazakhstan in the extended EMEP domain, Uzbekistan in the former official EMEP domain, Turkmenistan in the former official EMEP domain, Rest of Uzbekistan in the extended EMEP domain, Rest of Turkmenistan in the extended EMEP domain, Caspian Sea, Tajikistan, Aral Lake in the former official EMEP domain, Rest of Aral Lake in the extended EMEP domain, Modified Remaining Asian Areas in the former official EMEP domain, Remaining Asian Areas in the extended EMEP domain, Arctic Ocean in the extended EMEP domain

<sup>7</sup> The presented values (also in the following charts referring to “all countries”) based on the GAINS model calculations do not include some of the EECCA (Eastern Europe, Caucasus and Central Asia) countries who are members of the UNECE, i.e., Armenia, Azerbaijan, Georgia, Kazakhstan, Kyrgyzstan, as well as Lichtenstein, Monaco, San Marino, Holy See, Canada and the US. For Russian Federation only emissions from the European part are included.

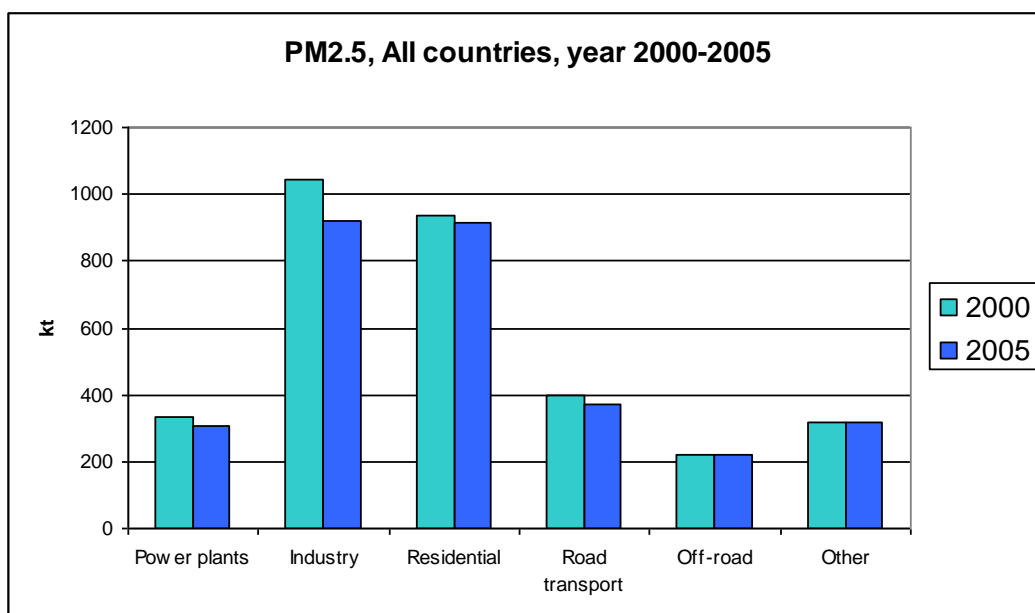


Figure 1.5: European  $PM_{2.5}$  emissions for key source sectors; Source: GAINS model calculation

While in the EU15 transport sector is a key contributor with over 30% share, in the other regions this sector represents about 10% of the total (Figure 1.6). Of course, the vehicle fleet in the EU15 is larger than that in most countries of the other regions but what is even more important is a large share of diesel vehicles that continued to grow in the last decade. Residential combustion is an important contributor in most countries with the highest share in the New Member States (NMS) of about 40% which is linked to the high consumption of solid fuels in this sector, a lot of it coal which has been largely eliminated in the EU15. The still relatively large contribution of the domestic sector even in the EU15 (about 25%) is related to the consumption of biomass fuels, specifically fuel wood. In the non-EU countries the majority of  $PM_{2.5}$  has been estimated to originate from industrial sources (>40%) which include industrial combustion in boilers and process emissions. The majority of these emissions come from non-EU FSU (Former Soviet Union) countries and Russian Federation where there are still many coal fired stokers in use and the level of PM abatement on smaller and older industrial boilers lags behind that of Western Europe. A relatively high share of power plant sector in the NMS (EU-12) is related to the high use of coal in some of these countries and/or not yet state-of-the-art abatement; most of the contribution in this sector (75%) originates from Bulgaria, Czech Republic, Poland, and Romania.

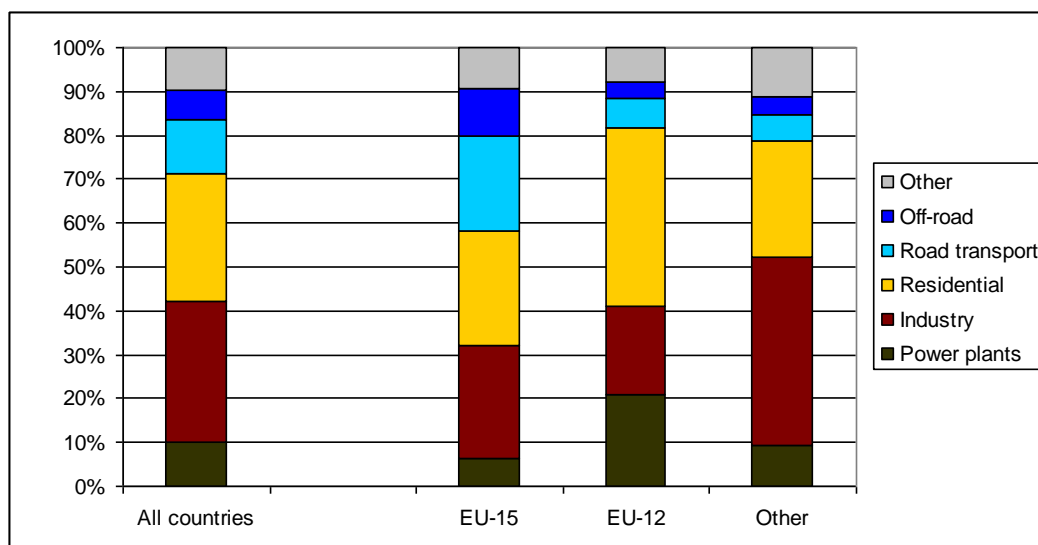


Figure 1.6: Sectoral contribution to PM<sub>2.5</sub> emissions for the year 2000 in the different European regions of the UNECE. Source: GAINS model calculations.

It is expected that the total European PM<sub>2.5</sub> emissions will decline in the coming decades by about 20% compared to the year 2005 (Figure 1.7). Most of the decline will take place in the EU countries, especially EU15 (reduction of about 40%), where more stringent legislation in transport, increasing role of new large scale combustion installations with state-of-the-art abatement, and reduced use of solid fuels in residential sector is expected to make key contributions to the reduction. For Russian Federation, Ukraine, and Turkey a significant growth of emission is expected provided no additional legislation is introduced in the considered period.

A comparison of national submissions to the CLRTAP (in 2009) and GAINS model estimates for the EU15 (by key aggregated sectors) is shown in Figure 1.8. At this level of aggregation there is relatively good agreement for specific sectors. Also the total estimate for 2000 and 2005 agrees very well, 1.21 and 1.08 Tg (CEIP) and 1.27 and 1.11 Tg (GAINS). GAINS estimates are somewhat higher but it has to be noted that Greece and Luxembourg did not submit their national numbers to CLRTAP (see also Figure 1.9).

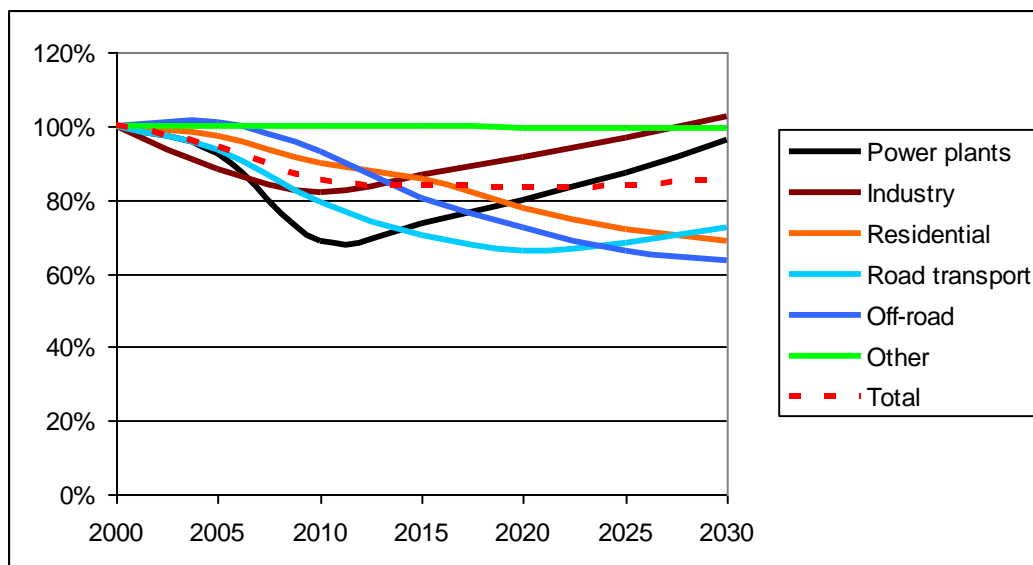


Figure 1.7: Expected evolution of European  $PM_{2.5}$  emissions by sector (changes compared to the year 2005=100%); Source: GAINS calculations based on the scenarios from Amann et al., 2008; Amann et al., 2004.

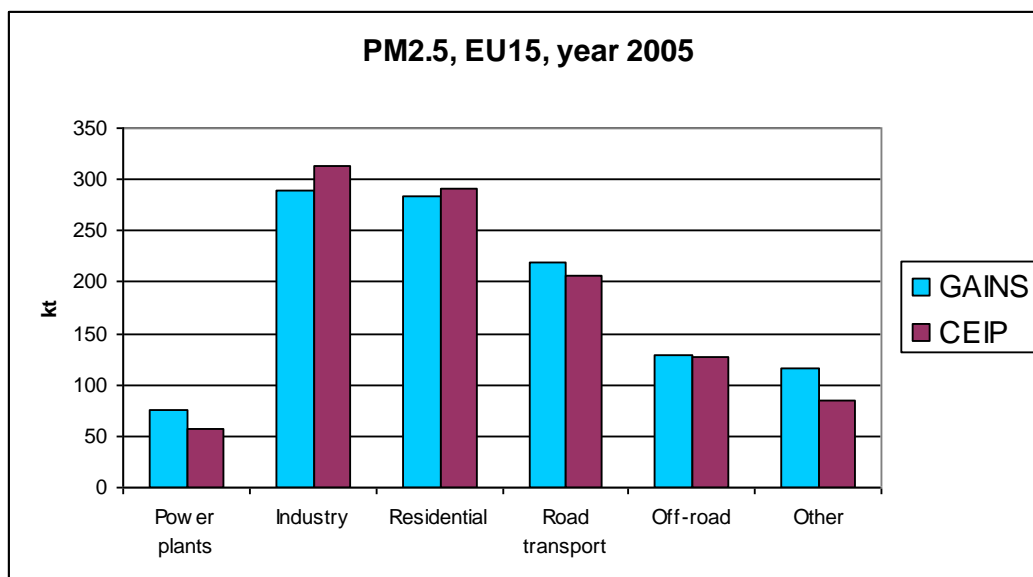


Figure 1.8: Comparison of recent national submissions to the CLRTAP Convention (CEIP) and GAINS model sectoral estimates of  $PM_{2.5}$  emissions for the year 2005 in the EU-15.

The comparison on a country level for the EU15 countries (Figure 1.9) shows obviously a larger variation in estimates for several countries indicating that GAINS potential overestimates emissions by about 20% for several countries while for a few countries a significant underestimation is shown, especially Finland and Portugal. In case of Finland, national experts indicated that the CLRTAP submitted values for residential sector rely still on older methodology and the new estimates are consistent with GAINS, on the other hand GAINS

underestimates for Finland emissions from peat mining and management. Analysis of other discrepancies is under way and will be completed in time for the revision of the Gothenburg Protocol. Furthermore a more detailed discussion of differences for specific sectors and countries as well as other pollutants is provided in a collaborative report from CEIP and CIAM (CEIP/CIAM in prep.).

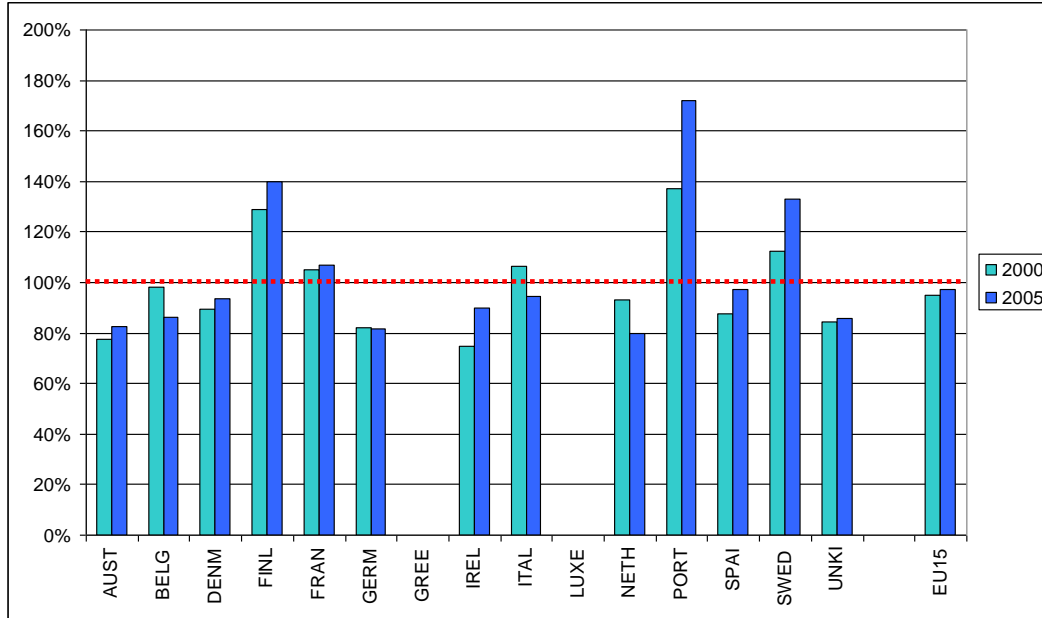


Figure 1.9: Comparison of the EU15 national submissions (in 2009) to GAINS (100%).

With respect to the comparison presented in Figure 1.9, it is important to remind that reporting of PM emissions, especially PM<sub>2.5</sub>, is a relatively recent process and the reported values tend to vary from year to year, changing also for the past years. An example of comparison made at the time of preparation of the review of the EU National Emission Ceiling Directive (Amann et al., 2006) (Figure 1.10) shows that several countries have not reported PM<sub>2.5</sub> at that time and that based upon the consultations with national experts RAINS model estimates for PM<sub>2.5</sub> shown a good agreement, typically within  $\pm 20\%$  of the RAINS model 2000 values. For countries like Finland, Portugal and Sweden where large differences are visible with a current round of submissions (Figure 1.9) the agreement was also well within  $\pm 20\%$  (Figure 1.10).

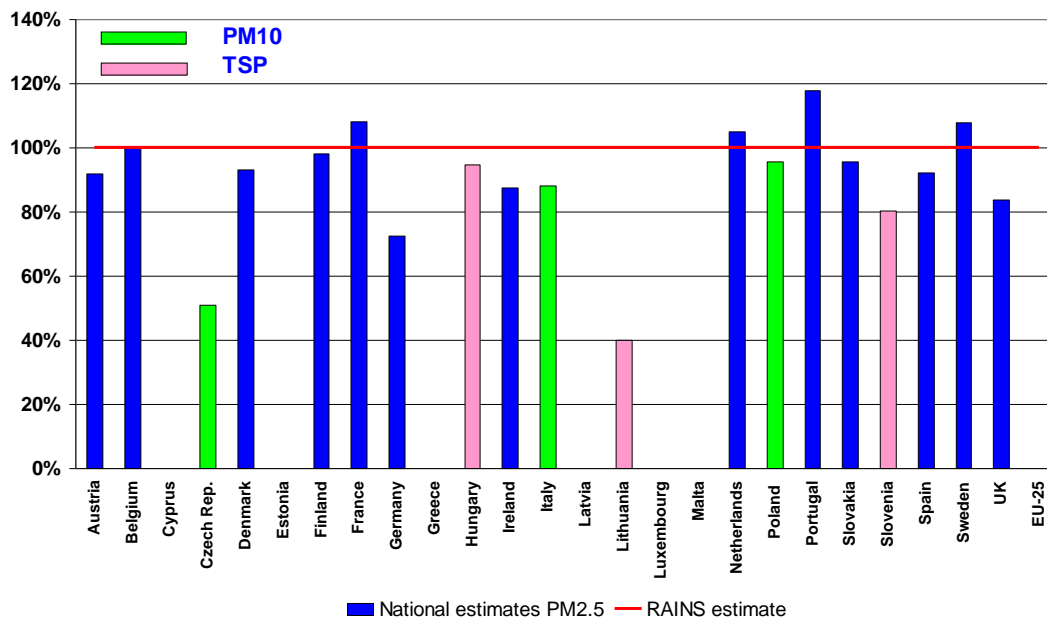


Figure 1.10: Comparison of national NEC submissions of 2000 emissions of PM in 2004 to RAINS estimates at the time (compatible with results presented in Amann et al., 2006).

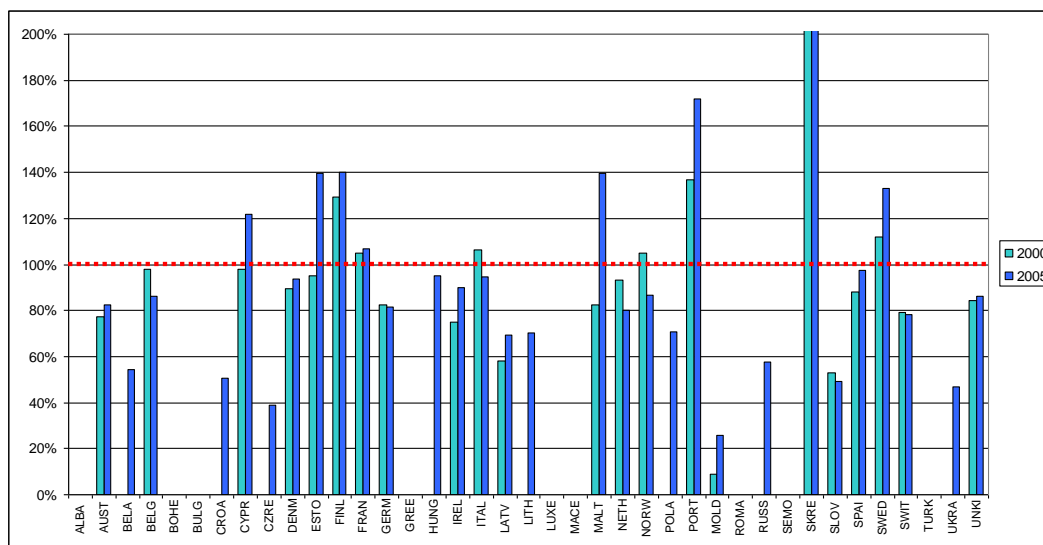


Figure 1.11: Comparison of the national submissions to the CLRTAP (in 2009) with GAINS model calculations for 2000 and 2005 (GAINS=100%).

Similar comparison for other regions is not possible since several countries have not reported emissions to the CLRTAP and so we present here just an overview for all countries (Figure 1.11). Some countries have reported emissions for 2005 but not for 2000. For some, there are very large differences to GAINS but it has to be also stressed that the calibration of the model for the year 2005 has not been yet completed; all of the current agreements and obligations refer to either to the year 2000 or previous years. Furthermore, in some submissions estimates for specific sector are not included, making a comparison difficult. In a few countries, rather surprising changes between 2000 and 2005, i.e., significant increase in emissions from residential sector, need some attention and explanation. It seems that there have been significant changes in the methodology used by national experts in estimating emissions of PM<sub>2.5</sub> since there are changes in the estimates for the past years when compared to the previous submissions, see Figure 1.10. The more detailed analysis is being performed under a different study (CEIP/CIAM, in prep.) and the agreement should improve in the near future and the remaining differences will be explained and documented.

### 1.3 Improved emission estimates of EC/OC

Total anthropogenic emissions of primary BC and OC in Europe<sup>8</sup> (excluding international shipping) have been estimated in GAINS model at about 0.6 and 0.75 Tg, respectively for the period 2000-2005. For both carbonaceous species the largest single contributing sector is residential combustion with share of 40 and 50% for BC and OC (Figure 1.12–Figure 1.13). For BC, road transport is nearly as important as residential combustion and combined with off-road transport makes a share of 50% (Figure 1.12–Figure 1.13). The importance of specific sectors varies however between the regions, especially between EU15 and the rest of Europe. In the EU15, transport emissions play a much more important role contributing more than twice as much as in other regions where residential combustion is the key sector (Figure 1.13).

The current assessment of BC and OC emissions shows somehow lower values than Kupiainen and Klimont (2007) estimates for 2000, especially for OC from residential combustion (Figure 1.12). Although there have been some updates of emission factors and other model parameters since, the main reason are updated activity data and control strategies for FSU countries and Russian Federation. In fact, there are large uncertainties in basic data needed for calculation of carbonaceous emissions in countries where reporting and other statistical data collection focuses on large industrial installations. This may possibly lead to missing developments for a number of smaller dispersed sources like residential combustion but also private transportation, especially with respect to the level of abatement of emission performance of technologies in use in these sectors. Beyond that, most of the emission factor information originates from either US and Western Europe or Asian measurements and finally the data on agricultural fires are of poor quality (emission estimates from the latter source are included in sector “Other” in Figure 1.13).

---

<sup>8</sup> The domain excludes some EECCA countries, see definition in section 1.2.

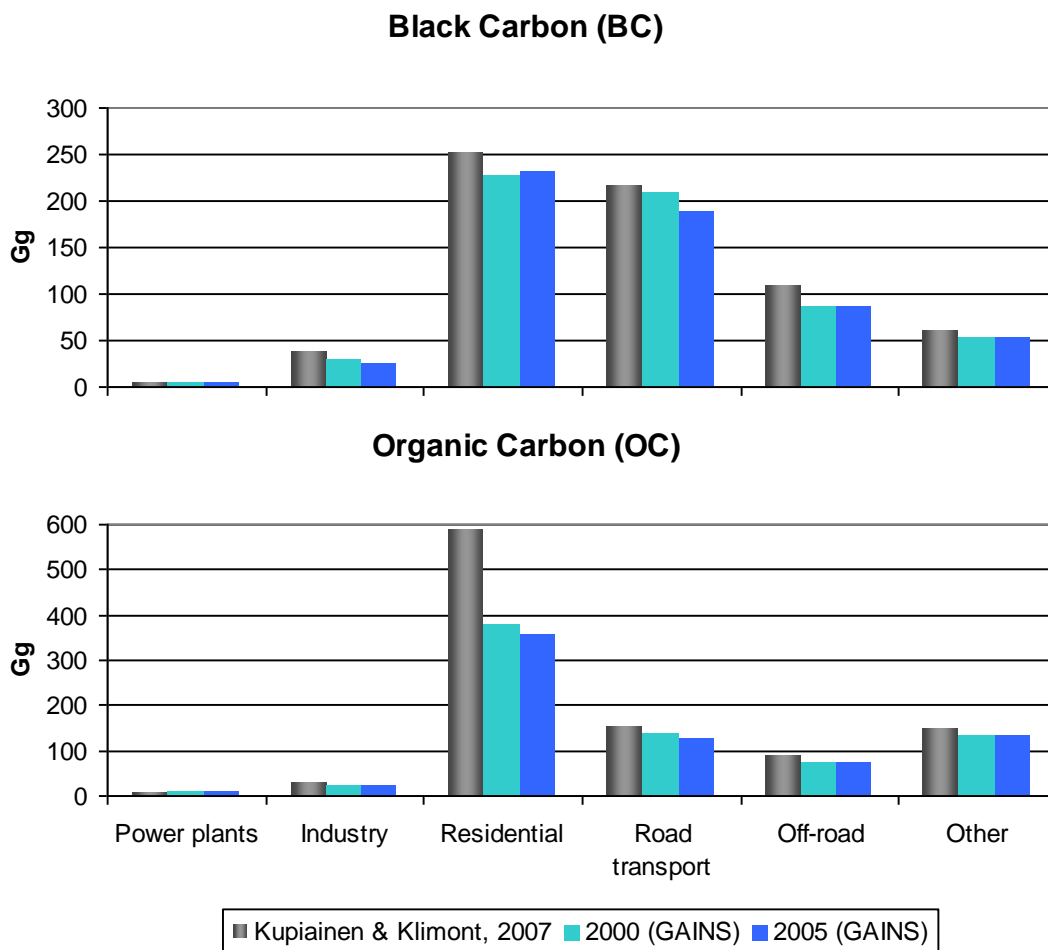


Figure 1.12: Sectoral emissions of BC and OC in Europe for 2000 and 2005.

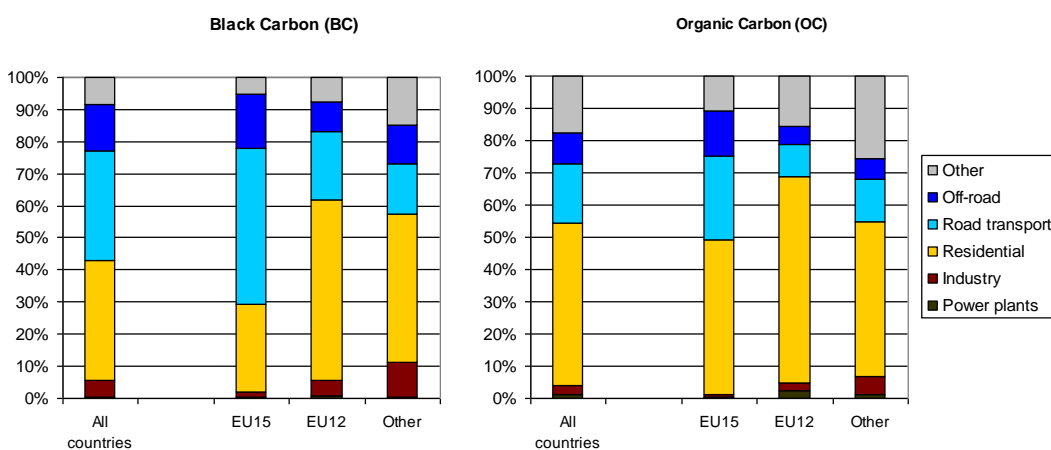


Figure 1.13: Share of key source sectors in total BC and OC emissions in 2000 for different regions; Source: GAINS model calculation

A recent report from Clean Air Task Force (Pettus, 2009) discusses in more detail contribution of BC emissions from agricultural burning to the arctic. The estimates provided there indicate, for example, that Russian contribution might be larger than previously believed, especially in the spring. The study estimate for Russia (March to May) is larger than the total calculated in GAINS for this source. The process of reviewing and interpreting the data is under way.

The other source which needs much more attention is flaring in on- and off-shore gas and oil production facilities and refineries. CIAM is reviewing the GAINS databases making use of the NOAA study (Elvidge *et al.*, 2007). While, estimates of the volume of gas flared for the North Sea in GAINS seem to be in accordance with the above study, there are some discrepancies for other countries that need to be resolved and might contribute to further revisions of the calculation with potentially important implications especially for the arctic. The NOAA study provides a more than decade time series and also gridded information that could be used by the modelling community to distribute the estimated emissions of various pollutant species.

A new set of spatially explicit 2005 BC and OC emissions for Europe has been recently prepared in collaboration between TNO and CIAM under EUCAARI project of the European Union (Denier van der Gon *et al.*, 2009) (see also chapter 2.4.2.3) The total emissions presented in this study are principally compatible with GAINS although they differ for some sectors and OC emissions, most notably residential wood combustion emissions are somewhat higher.

Total primary carbonaceous particles represent about 42% of primary emissions of PM<sub>2.5</sub> in Europe (Figure 1.14). For all sectors but transport BC/OC ratio is <1 with an overall BC/OC ratio of about 0.8; in Russia and few of the FSU countries, even for road transport the BC/OC ratio is <1 owing to larger share of gasoline vehicles. Sectoral shares of BC and OC in PM<sub>2.5</sub> vary greatly (Figure 1.14) but there is also significant variation between regions (low-high indicators in Figure 1.14 resulting primarily from different fuel structure, e.g., for road transport share of diesel makes a difference in BC and OC contributions – BC share high for diesel engines while the opposite is true for OC. For residential sector, the large variation for OC share is justified by varying importance of biomass vs. other fuels (coal, gas and liquid fuels) in domestic sector. In fact, the variation would be even larger if single countries rather than aggregated regions would be considered in the analysis presented in Figure 1.14 indicating the need for direct estimation of BC and OC emissions rather than reliance on general share of BC and OC in PM<sub>2.5</sub>.

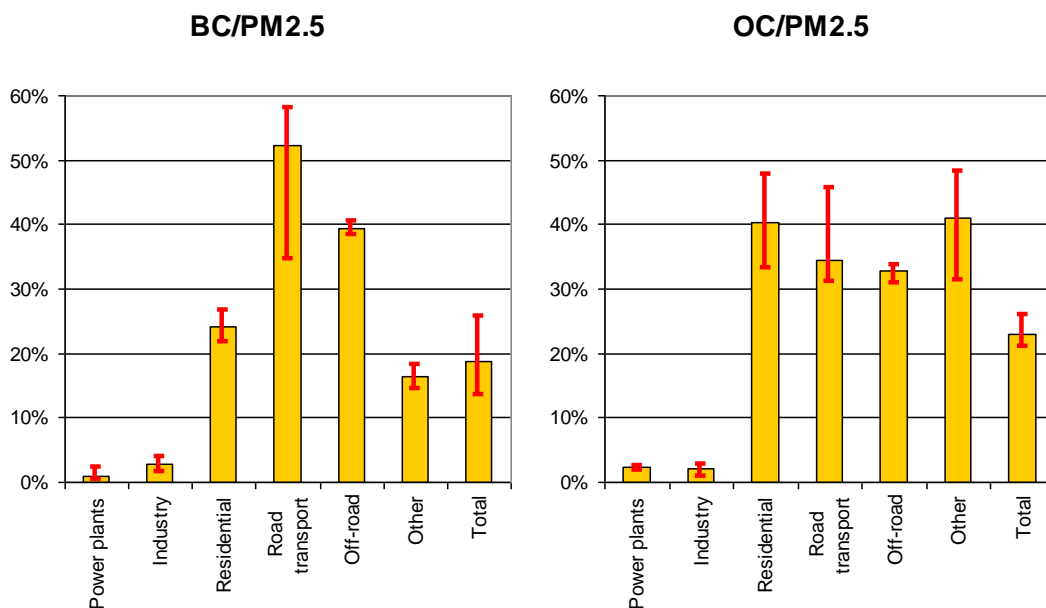


Figure 1.14: Share of BC and OC emissions in PM<sub>2.5</sub> (year 2000) for all countries and variation in the selected regions (low-high).

Future emissions of BC and OC are expected to decline (Figure 1.15) by about 25% mostly due to already implemented and envisaged policies in transport sector as well as structure of fuel use in domestic sector (less solid fuels). Figure 1.15 shows still a rather pessimistic picture as it assumes rather conservative air pollution policies in FSU and EECCA countries resulting in increase of emission in these regions mostly due to rapid motorization. If EU laws would be followed, significant cuts in emissions would be possible and the overall European reduction would be larger. For the EU15, it is estimated that BC and OC emissions from transport will decline by nearly 80% by 2030 leading to the overall reduction by 60%.

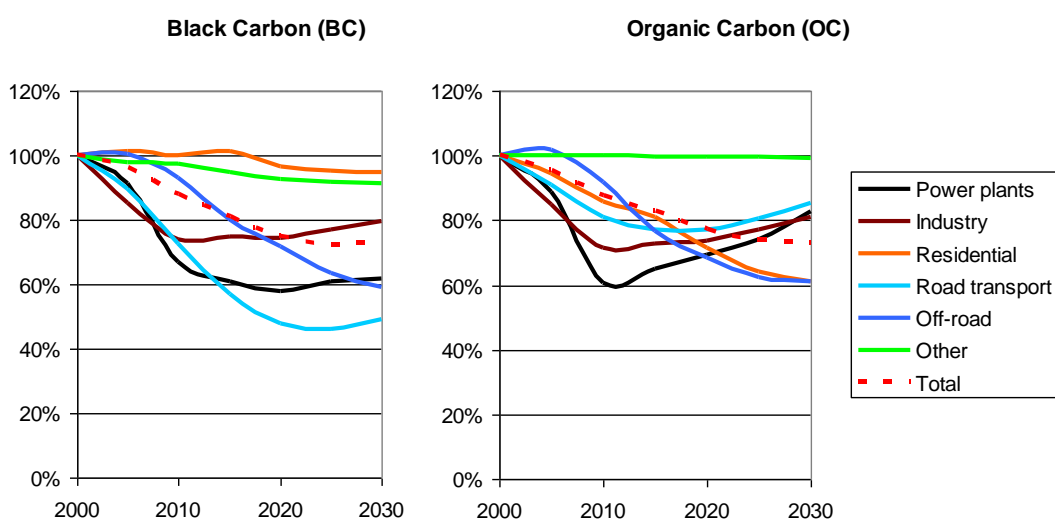


Figure 1.15: Projections of European BC and OC emissions; Source: Klimont and Kupiainen (2009, in prep.).

## 2 Measurement and model assessment of particulate matter in Europe, 2007

### 2.1 Particulate matter mass concentrations

*by Svetlana Tsyro, Karl Espen Yttri and Wenche Aas*

#### 2.1.1 Introduction

The assessment of concentration levels of regional background particulate matter (PM<sub>10</sub> and PM<sub>2.5</sub>) based on EMEP model calculations and EMEP monitoring data has been made for the year of 2007. For the first time, calculated PM concentrations are presented for the EMEP extended area, including the EECCA countries. The calculated regional background PM<sub>10</sub> and PM<sub>2.5</sub> concentrations are compared to the WHO Air quality guidelines. Finally, an assessment of the inorganic constituents and the carbonaceous fractions of PM are made.

#### 2.1.2 The EMEP model and runs setup

The description of the Unified EMEP model can be found in EMEP (2003), EMEP (2004b) and EMEP (2005a). The calculations presented here have been performed with an extended version of the model, which allows for description of the chemical composition of primary PM and which includes natural sea salt and dust particles (Tsyro, 2008), in addition to the secondary inorganic constituents.

The important change this year is that the calculations have been performed with a more recent version of the EMEP model (version rv3.1) compared to the model version rv2.7.10 used for last year's reporting (EMEP, 2008a). In the rv3.1 version, a revised scheme for night-time formation of nitric acid was used as documented in EMEP Report 1/2008 (EMEP, 2008b). The changes resulted in an appreciable decrease in the concentrations of nitrate and ammonium compounds. Evaluation results of the model performance for PM<sub>10</sub> and PM<sub>2.5</sub> and main aerosol components with EMEP observations in 2007 are provided in this chapter.

Another important change this year is the use of a new meteorological driver. The meteorological data for 2007 used in the model simulations was produced with the HIRLAM model, which is an up-to-date version compared the PARLAM-PS model used until recently. HIRLAM was run on a spherical rotated coordinate system, using a grid resolution of 0.2 x 0.2 °. The meteorological fields were interpolated to the EMEP 50x50 km<sup>2</sup> grid in a polar-stereographic projection. The first test runs with HIRLAM meteorology and the evaluation of results was presented in last year's report (EMEP, 2008b). In general, air concentrations calculated with HIRLAM meteorology had a tendency to be lower than those calculated with PARLAM meteorology. The reason for that is to be further investigated.

The national emissions of SO<sub>x</sub>, NO<sub>x</sub>, NH<sub>3</sub>, PM<sub>10</sub> and PM<sub>2.5</sub> for the year 2007 were prepared by EMEP/CEIP and gridded at MSC-W. Rather large differences between 2006 and 2007 emissions were reported for a number of countries, including all pollutants. Both significant emission increases and decreases (in excess of 30%) are reported (see EMEP Report 1/2009 (EMEP, 2009) and

Chapter 1.1 in this report). The largest differences are observed for EECCA countries in the EMEP extended area, for the Russian Federation, Ukraine, Romania, Bulgaria, Hungary, Croatia, Italy, the UK, Germany and Portugal.

The chemical speciation of primary PM<sub>10</sub> and PM<sub>2.5</sub> emissions was based on the estimates of BC/OC emissions in 2000 in Europe by Kupiainen and Klimont (2007). A discussion of these emission estimates can be found in Chapter 1.5.

### **2.1.3 Status of particulate matter mass observations**

The observed annual mean concentrations of PM<sub>10</sub>, PM<sub>2.5</sub>, and PM<sub>1</sub> for 2007 are presented in Hjellbrekke and Fjæraa (2009).

For 2007, mass concentrations of PM are reported for 52 sites (50 for PM<sub>10</sub> and 26 for PM<sub>2.5</sub>), which are 3 more than for 2006 (3 more for PM<sub>10</sub> and 1 more for PM<sub>2.5</sub>). For the sites GB0048 (Auchencorth Moss), FR0009 (Revin), and FR0013 (Peyrusse Vieille), 2007 was the first time mass concentrations of PM have been reported to EMEP. One site (SK0005) was closed down from 2006 to 2007. 18 countries reported mass concentrations to EMEP for 2007, which is one more compared to the previous year. The inclusion of the two French sites (FR0009 and FR0013) makes an important extension to a part of Western Europe, which previously has not reported PM levels to EMEP. Nevertheless, large parts of the EMEP domain are still not covered by the monitoring network, hence it is once more timely to emphasize this critical issue, which is particularly pronounced for Eastern Europe.

The lowest concentrations of PM<sub>10</sub> and PM<sub>2.5</sub> were observed in the northern and north-western parts of Europe, i.e. the Scandinavian Peninsula, Northern Ireland and Scotland, and for high altitude sites (> 900 m asl) on the European mainland. The spatial pattern seen for PM<sub>10</sub> and PM<sub>2.5</sub> in 2007 corresponds to that reported for previous years, and reflects both population density and major anthropogenic sources. The lowest annual mean concentration of PM<sub>10</sub> was observed at the Jungfrauoch (CH01) (3.2 µg m<sup>-3</sup>) site situated in the Swiss Alps, whereas the highest was recorded at the Italian site Montelibretti (IT01) (31.5 µg m<sup>-3</sup>). For PM<sub>2.5</sub> the lowest annual mean was reported for Birkenes (NO01) (3.3 µg m<sup>-3</sup>) and the highest for Ispra (IT04) (25.7 µg m<sup>-3</sup>).

The majority (78%) of the sites which reported levels of PM<sub>10</sub> both for 2006 and 2007 experienced lower annual mean concentrations in 2007 compared to the previous year. Nearly 40% of the sites experienced a decrease by 15% or more. The most substantial decreases are not constrained to one particular geographical region. 67% of the sites which reported annual mean concentrations of PM<sub>2.5</sub> both for 2006 and 2007 experienced lower annual mean concentrations in 2007 compared to 2006. For the majority of these sites the decrease was above 10%, i.e. 17% on average. The decrease in PM<sub>10</sub> experienced by the majority of the sites going from 2006 to 2007 appears to be attributed mostly to PM<sub>2.5</sub>.

The annual mean concentration of PM<sub>1</sub> was reported for five sites in 2007, which equals that of 2006. Thus, the annual mean concentrations of PM<sub>1</sub> are reported for four countries. The highest annual mean was reported for the Austrian site Illmitz (AT02) (11.4 µg m<sup>-3</sup>), which is four times higher than that observed at the

Birkenes site (NO01) ( $2.7 \mu\text{g m}^{-3}$ ), reporting the lowest annual mean. A decrease ranging from 22-27% was reported for the four sites when compared to the previous year.

#### 2.1.4 Spatial distribution of $\text{PM}_{10}$ and $\text{PM}_{2.5}$

Annual mean concentration fields of regional background  $\text{PM}_{10}$  and  $\text{PM}_{2.5}$  in 2007 have been obtained by combining EMEP model calculation results and EMEP measurements (Figure 2.1). Calculated  $\text{PM}_{10}$  and  $\text{PM}_{2.5}$  include primary PM and secondary inorganic aerosols (SIA) from anthropogenic emissions, natural aerosols of sea-salt and windblown dust and particulate water. Note that model calculated PM presented in this chapter does not include secondary organic aerosols (SOA). A status of SOA modelling is presented in Chapter 2.4.2. Figure 2.2 shows the combined map of annual mean concentrations of  $\text{PM}_{10}$  and  $\text{PM}_{2.5}$  in 2007. Supplementary maps of calculated and observed annual mean concentrations of  $\text{PM}_{10}$  and  $\text{PM}_{2.5}$  at EMEP sites, and the interpolated differences (bias) are presented in Appendix B.

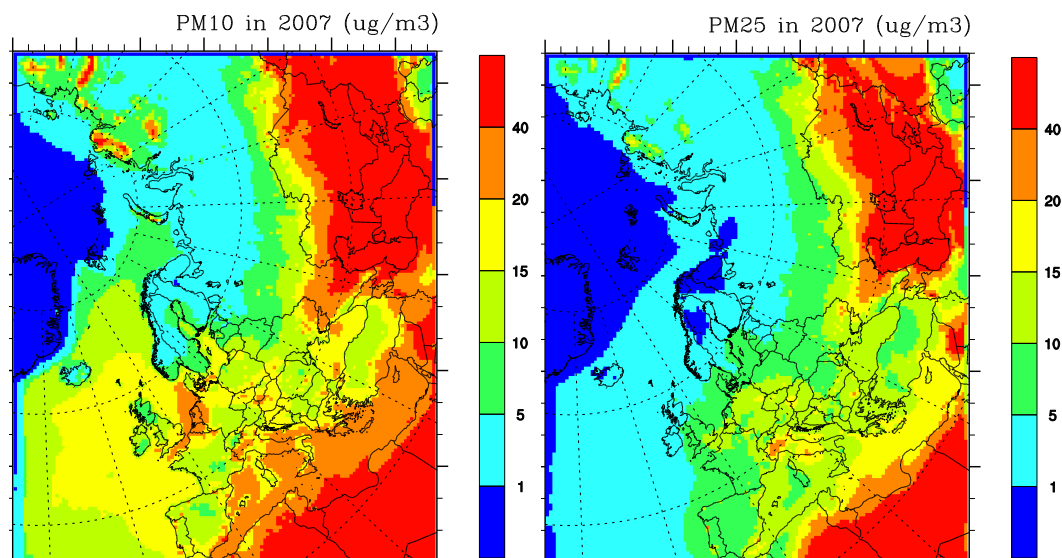


Figure 2.1: Annual mean concentrations of  $\text{PM}_{10}$  (left) and  $\text{PM}_{2.5}$  (right) in 2007, constructed based on EMEP model calculations and EMEP observational data.

Figure 2.2 clearly demonstrates the predominant role of secondary aerosols in  $\text{PM}_{10}$ , and that the relative importance of primary PM increases significantly in areas influenced by large emissions from traffic and residential heating; i.e. close to major urban areas.

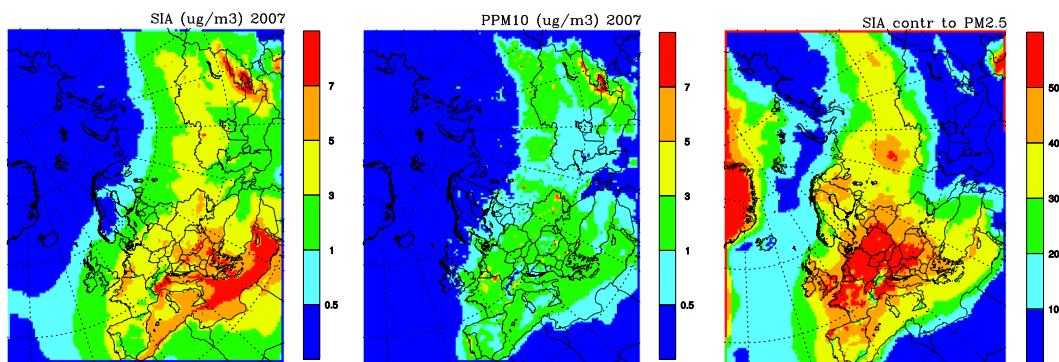


Figure 2.2: Annual mean concentrations of SIA ( $PM_{10}$ ) (left), primary  $PM_{10}$  (middle), and relative contribution (in %) of SIA to  $PM_{2.5}$  (right) in 2007, calculated with the EMEP model.

### 2.1.5 Temporal trends in $PM_{10}$ and $PM_{2.5}$

14 of the sites reporting concentrations of  $PM_{10}$  for 2007 have time series extending more than five years. The longest time series, going back to 1997, are reported for the four Swiss sites and one British. Six sites reporting concentrations of  $PM_{2.5}$  for 2007 have time series that extend five years. Both for  $PM_{10}$  and  $PM_{2.5}$  none of these sites show any stepwise year-by-year reduction or increase in the concentration. Large inter annual variations are observed of which the peak in 2003 is the most pronounced (Figure 2.3).  $PM$  levels for 2007 are low for both size fractions at most sites compared to previous years. The reason for this decrease appears to be mixed, being affected both by meteorological variability and a rather broad decrease in emissions of primary  $PM$  and secondary  $PM$  precursors.

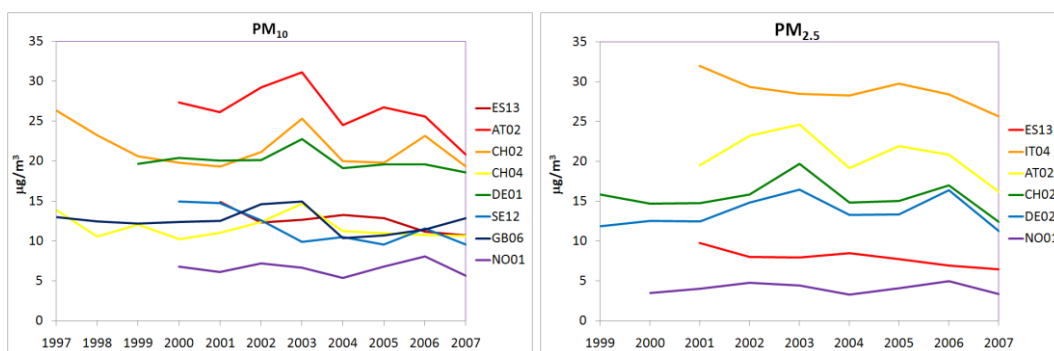


Figure 2.3: Time series of  $PM_{10}$  and  $PM_{2.5}$  at selected EMEP sites.

### 2.1.6 Differences in model results, 2007 vs. 2006

There are quite substantial differences (exceeding 30 %) between model results for  $PM_{10}$  and  $PM_{2.5}$  obtained for 2007 compared to the calculations performed for previous years (e.g. those presented in Report 4/2008). Partly, this is a consequence of the use of the revised scheme for night-time formation of nitric acid. The scheme update resulted in the decrease of  $NO_3^-$  concentrations by 10-40%, and a decrease of  $NH_4^+$  concentrations by 10-30% over all Europe, with

the largest concentration changes observed for central Europe. As a consequence, concentrations of  $PM_{10}$  and  $PM_{2.5}$  decreased as well and in particular for central Europe. In addition, the new meteorological driver (HIRLAM model) used for the 2007 calculations contributed to the observed differences.

Meteorological variability and the new meteorological driver used to prepare the data for 2007 have likely affected the differences seen for PM when comparing 2006 and 2007. The analysis of the effect of the inter-annual meteorological variability on PM concentrations, based on the use of the same meteorological driver, is included in Report 1/2009. In brief, the analyses show that central Europe, large parts of southern and south-eastern Europe, and Scandinavia experienced more precipitation in 2007 than for 2006, while it was drier in Spain, northern France, the UK and most of Russia and Central Asia compared to 2006. The ambient temperature was higher in central- and south-eastern Europe and for the EECCA area, while lower in the west and north of Europe in 2007 compared to 2006. A particularly warm and wet winter was observed for most of Europe in 2007, causing lower  $PM_{10}$  and  $PM_{2.5}$  concentrations, which is reflected both with respect to observations and model results. Particularly low PM levels occurred in January at a number of EMEP sites (e.g. in Germany, Poland and Switzerland).

The change of the meteorological driver was found to have a larger effect on the model results than the different meteorological situation experience in 2007 compared to 2006. The changes in the meteorological data when using HIRLAM instead of PARLAM-PS, typically overrides the inter-annual variability of precipitation and surface stress fields (which determine aerosol removal by wet and dry deposition) and seems to be equally important as the inter-annual variability for surface temperature between 2006 and 2007. When calculations are based on HIRLAM, calculated concentrations of  $PM_{10}$  are 20-40 % less for Europe than when applying PARLAM-PS, whereas the corresponding reduction for  $PM_{2.5}$  is 20-75%.

There were considerable changes in the PM emission data for 2007 compared to that of 2006 (see chapter 1.1.2 and EMEP Report 1/2009 (EMEP, 2009)). Both substantial increases and decreases of gaseous PM precursors and primary PM were reported. Further, emissions for the EECCA countries were re-gridded for 2007, causing significant changes in their spatial distribution. The combined effect of the various emission changes on PM was a decrease of  $PM_{10}$  and  $PM_{2.5}$  concentrations by up to 30% for most of Europe and an increase of  $PM_{10}$  and  $PM_{2.5}$  by up to 30% for the northern most part of Scandinavia and Central Asia.

The model calculated concentrations of anthropogenic  $PM_{10}$  and  $PM_{2.5}$  were 5-30% lower for 2007 compared to 2006 for most of the EMEP area, except from Spain, France, northern Italy, northern Scandinavia, and in the extended areas of EMEP. Besides,  $PM_{10}$  and  $PM_{2.5}$  levels were higher in 2007 in the eastern Mediterranean, Eastern Europe and along the western border of Russia due to enhanced concentrations of natural mineral dust (these areas experienced relatively dry and warm weather in 2007).

In general, the model calculated concentrations of anthropogenic  $PM_{10}$  and  $PM_{2.5}$  that were 5-30% lower in 2007 than in 2006 for most of the EMEP area except

from Spain, France, northern Italy, the northernmost part of Scandinavia, and in the extended areas of EMEP. The areas where the concentrations of PM<sub>10</sub> and PM<sub>2.5</sub> were found to be higher in 2007 included the eastern part of the Mediterranean region, Eastern Europe and the areas along the western border of Russia. This was mainly attributed to enhanced concentrations of natural mineral dust and were the same regions experiencing relatively dry and warm weather in 2007.

### 2.1.7 Particulate matter size distributions

Table 2.1 and Figure 2.4 show the annual mean observed and model calculated PM<sub>2.5</sub>-to-PM<sub>10</sub> ratio at EMEP sites reporting both variables for 2007. In Figure 2.4, the sites are ranked from left to right according to decreasing PM<sub>2.5</sub>-to-PM<sub>10</sub> ratio.

*Table 2.1: Observed and model calculated annual mean PM<sub>2.5</sub>-to-PM<sub>10</sub> ratios and observed PM<sub>1</sub>-to-PM<sub>10</sub> and observed PM<sub>1</sub>-to-PM<sub>2.5</sub> ratios at EMEP sites in 2007.*

		Site	PM <sub>2.5</sub> /PM <sub>10</sub>		PM <sub>1</sub> /PM <sub>10</sub>	PM <sub>1</sub> /PM <sub>2.5</sub>
			Obs	Mod	Obs	Obs
Northern Europe	Norway <sup>1)</sup>	NO01	0.59	0.68	0.45	0.74
	Sweden	SE12	0.71	0.68		
Central/Western Europe	Austria	AT02	0.77	0.84	0.57	0.74
	Switzerland	CH02	0.62	0.81	0.49	0.79
		CH05	0.76	0.75	0.55	0.76
	Czech Rep. <sup>2)</sup>	CZ03	0.90	0.84		
	Germany	DE02	0.68	0.78	0.38	0.55
		DE03	0.79	0.85		
DE44		0.80	0.77			
Great Britain	GB36	0.54	0.63			
	GB48	0.70	0.56			
Southern Europe	Spain	ES07	0.58	0.58		
		ES08	0.56	0.47		
		ES10	0.55	0.59		
		ES11	0.54	0.72		
		ES12	0.64	0.74		
		ES13	0.62	0.73		
		ES14	0.71	0.73		
	ES16	0.65	0.66			
Italy	IT01	0.71	0.69			
South-Eastern Europe	Slovenia	SI08	0.65	0.81		
	Cyprus	CY02	0.53	0.68		
Average			0.66	0.71	0.50	0.72

1) Not estimated with concurrent days for model run and measurements (1+6 days sampling) 2) Only 50% data coverage (measurement every 2<sup>nd</sup> day).

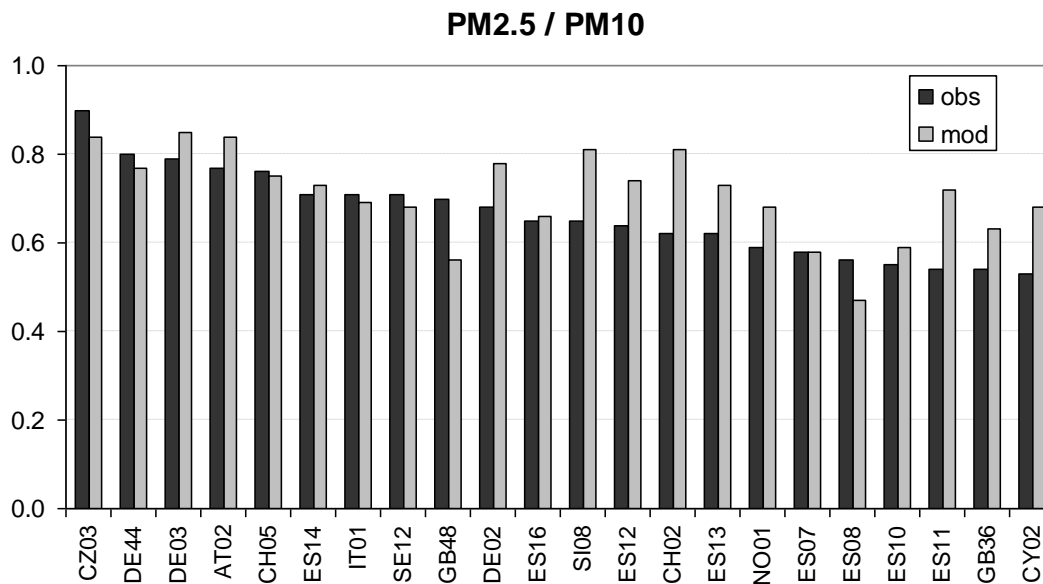


Figure 2.4: Observed and model calculated annual mean  $PM_{2.5}$ -to- $PM_{10}$  ratio at EMEP sites in 2007. The sites are ranked from left to right according to decreasing observed  $PM_{2.5}$ -to- $PM_{10}$  ratio.

The average  $PM_{2.5}$ -to- $PM_{10}$  ratio for the sites listed in Table 2.1 is 0.66 when calculated based on observations and 0.71 when obtained by the model. The observed fine fraction of  $PM_{10}$  ranges from 0.53 at Ayia Marina (CY02) to 0.9 at Košnice (CZ03). The observations show that  $PM_{2.5}$  typically account for a larger fraction of  $PM_{10}$  in central Europe, reflecting the strong influence of anthropogenic sources. For the southern most sites, e.g. the Spanish sites and the Cypriote site, the fine fraction is less dominant, as these are more affected by eroded dust from semi-arid regions on the Iberian Peninsula and by Saharan dust. Some sites are well-known to be influenced by marine aerosols (sea-salt), which could lower the  $PM_{2.5}$ -to- $PM_{10}$  ratio substantially, e.g. as seen for the  $PM_{2.5}$ -to- $PM_{10}$  ratio at Birkenes (NO01).

The model predicts larger fractions of fine particles (i.e.  $PM_{2.5}$ ) in  $PM_{10}$  mass compared with measurements for 11 of 20 stations. Partly, this can be associated with uncertainties in the emissions of coarse PM, especially from fugitive industrial and agricultural sources. Re-suspended road dust, which is one of the important sources of coarse particles, was not included in the calculations. With respect to natural sources, there are considerable uncertainties in modeling of windblown dust from semi-arid areas, arable lands and other erosive surfaces. Also, biogenic aerosols which may contribute significantly to the coarse aerosol mass were not accounted for in the model results.

Table 2.2: Observed and calculated  $PM_{2.5}$  to  $PM_{10}$  ratios at EMEP sites in 2007.

	Obs	Mod
Year	0.69	0.73
winter (jan-feb)	0.79	0.68
spring	0.65	0.77
summer	0.65	0.74
autumn	0.70	0.71

The observations show that the contribution of fine particles to  $PM_{10}$  is less in spring and summer (65% on average), increasing to 70 % in autumn and to 79% in winter. The relatively smaller fine fraction in  $PM_{10}$  observed in spring and summer is largely due to the increase of the coarse PM fraction. This seasonal variation of the  $PM_{2.5}$ -to- $PM_{10}$  ratio reflects the relative contribution of anthropogenic (typically smaller) particles in the cold season and natural (predominantly coarse) particles in the warm seasons. The model does not manage to reproduce the observed seasonal variation, calculating larger contribution of fine PM in spring/summer and smaller in autumn/winter. Calculated  $PM_{2.5}$  concentrations show higher mean levels in spring and summer than in autumn and winter. Note that the model underestimates  $PM_{2.5}$  and SIA greater in the cold seasons, as seen in Table 2.4 below). On the other hand, model calculated coarse PM has rather small seasonal variation.

$PM_1$  is the major fraction of  $PM_{10}$  on an annual basis for the five sites reporting concurrent measurements of  $PM_{10}$ ,  $PM_{2.5}$  and  $PM_1$ , constituting between 38–57% of  $PM_{10}$  (Figure 2.5). The relative contribution is somewhat higher for the three most southerly sites (AT02, CH02, and CH05) (54% on average) compared to the two northern ones (DE02 and NO01) (42% on average). The  $PM_{2.5-1}$  fraction varies between 13% at CH02 to a substantial 30% at DE02, nicely underlining the spatial variability in the saddle point between the fine and the coarse fraction of  $PM_{10}$  and that  $PM_{2.5}$  is not a good proxy for the fine PM fraction at several rural background sites in Europe.

The relative contribution of the coarse fraction ( $PM_{10-2.5}$ ) to  $PM_{10}$  ranged between 24-40%. At DE02 and NO01, the relative contribution of  $PM_{10-2.5}$  was almost equally large as that of  $PM_1$ .

When comparing the relative contribution of the various size fractions to  $PM_{10}$  for the days with the 5% highest  $PM_{10}$  concentrations with that of the annual mean, there is no consistency in  $PM_1$  being higher when the  $PM_{10}$  concentration is high, but  $PM_{2.5}$  is always higher. Consequently, the coarse fraction of  $PM_{10}$  turns out to be less important when the  $PM_{10}$  concentration is high.

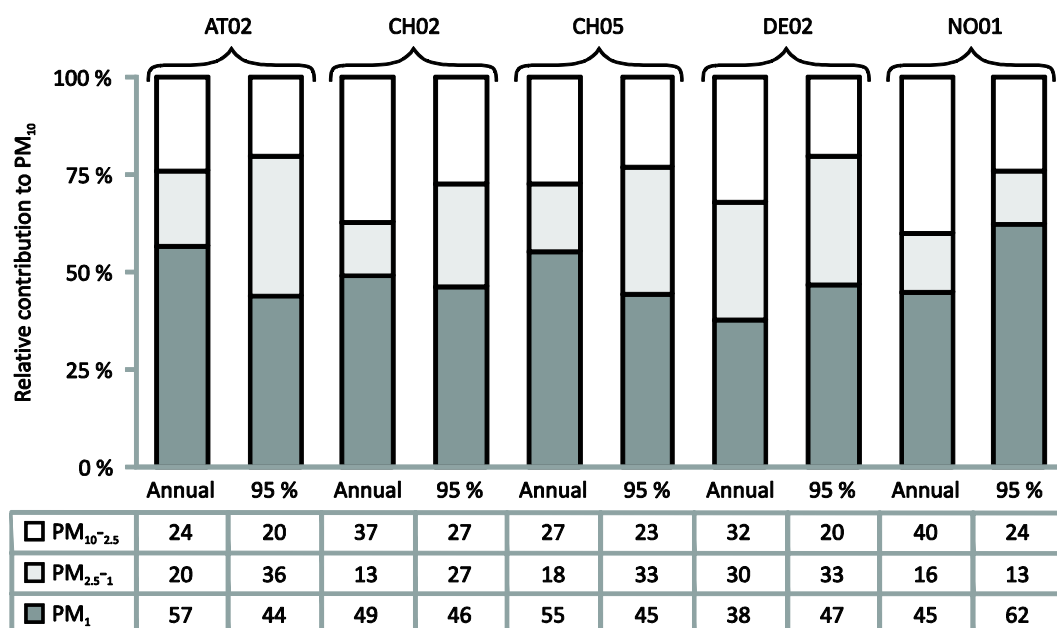


Figure 2.5: Relative contribution of PM<sub>1</sub>, PM<sub>2.5-1</sub> and PM<sub>10-2.5</sub> to PM<sub>10</sub> at the sites Illmitz (AT02), Payerne (CH02), Rigi (CH05), Langenbrügge (DE02) and Birkenes (NO01) for the year 2007 and for the 5-percent highest concentrations of PM<sub>10</sub> in 2007.

## 2.2 Exceedances of WHO AQGs by regional background PM mass

by Svetlana Tsyro, Karl Espen Yttri and Wenche Aas

In the following, model calculated regional background concentrations of PM<sub>10</sub> and PM<sub>2.5</sub> for 2007 are compared to EU limit values and World Health Organization (WHO) Air Quality Guidelines (AQGs).

The EU limit values for PM<sub>10</sub> (Council Directive 1999/30/EC) are: 40 µg m<sup>-3</sup> for the annual mean and 50 µg m<sup>-3</sup> for daily PM<sub>10</sub> (not to be exceeded more than 35 times pr calendar year).

The WHO AQGs (WHO, 2005) are:  
for PM<sub>10</sub>: 20 µg m<sup>-3</sup> annual; 50 µg m<sup>-3</sup> 24-hour (99<sup>th</sup> percentile or 3 days per year)  
for PM<sub>2.5</sub>: 10 µg m<sup>-3</sup> annual; 25 µg m<sup>-3</sup> 24-hour (99<sup>th</sup> percentile or 3 days per year).

Model calculated annual mean regional background concentrations of PM<sub>10</sub> in 2007 were below the EU limit value of 40 µg m<sup>-3</sup> in most of Europe, with the exception of the East Asian countries (Figure 2.1). However, the calculated annual mean PM<sub>10</sub> exceeded the WHO recommended AQG of 20 µg m<sup>-3</sup> pr year in several polluted areas, among others in the Benelux countries, the Po Valley, Slovakia, and also in a number of grid cells associated with large cities or other greater emission sources. PM<sub>10</sub> concentrations were also in excess of 20 µg m<sup>-3</sup> in the southern parts of Mediterranean countries and in the Caucasus and in the Central Asian countries due the influence of desert dust from Africa. The regional background annual mean PM<sub>2.5</sub> concentrations were above the WHO

recommended value of  $10 \mu\text{g}/\text{m}^3$  in the same areas and also in several countries in central Europe.

Figure 2.6 and Figure 2.7 show the number of days with model calculated  $\text{PM}_{10}$  exceeding  $50 \mu\text{g m}^{-3}$  and  $\text{PM}_{2.5}$  exceeding  $25 \mu\text{g m}^{-3}$  in 2007, respectively. The left maps in both figures are for total PM, while the right maps are for PM from anthropogenic sources only. In most of Europe, there were less than 35 days (EU requirement) when regional background  $\text{PM}_{10}$  exceeded  $50 \mu\text{g m}^{-3}$ . However in a rather extensive area, except from parts of central Europe, Scandinavia and the north of Russia,  $\text{PM}_{10}$  exceedance of  $50 \mu\text{g m}^{-3}$  occurred more than 3 days, which is the maximum number of days recommended by the WHO. Furthermore, the WHO AQG for  $\text{PM}_{2.5}$  was exceeded by regional background concentrations in more than 3 days in most of the European countries, except northern Europe and northern Russia. Figure 2.6 and Figure 2.7 illustrate the significant contribution from natural dust to the exceedances of  $\text{PM}_{10}$  and  $\text{PM}_{2.5}$  limit values and AQGs.

Model calculated and observed number of days with  $\text{PM}_{10}$  and  $\text{PM}_{2.5}$  exceeding the WHO AQGs in 2007 has been compared. The results are provided in Table 2.3. In addition to the total number of exceedance days, the number of common days is shown, i.e. the days for which observed PM exceedances were also predicted by the model.

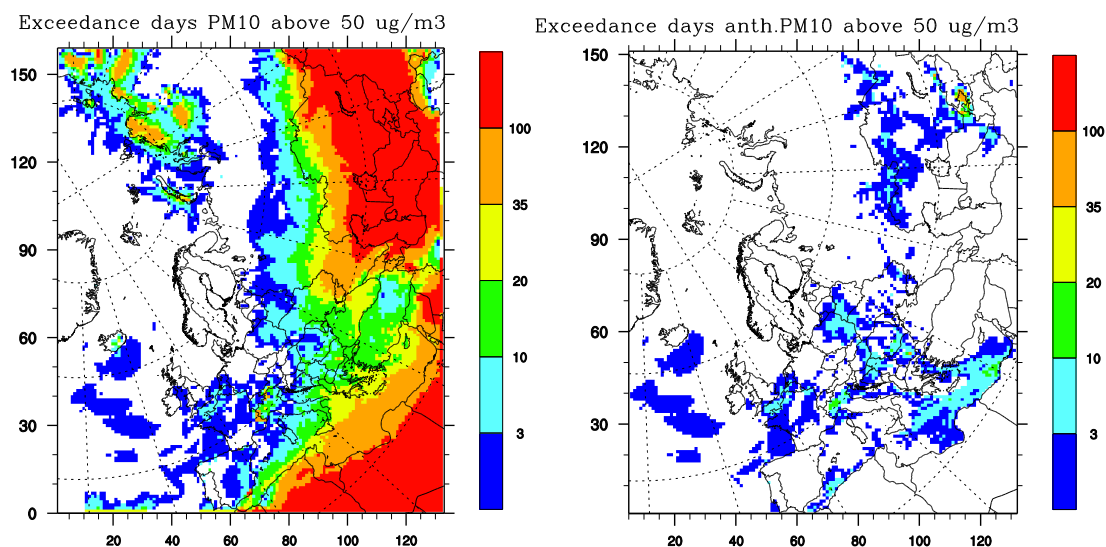


Figure 2.6: Calculated number of days with  $\text{PM}_{10}$  exceeding  $50 \mu\text{g m}^{-3}$  in 2007: for total  $\text{PM}_{10}$  (left) and for anthropogenic  $\text{PM}_{10}$  (right). Note: EU Directive requires not more than 35 days, while WHO recommendation is not more than 3 days with exceedance.

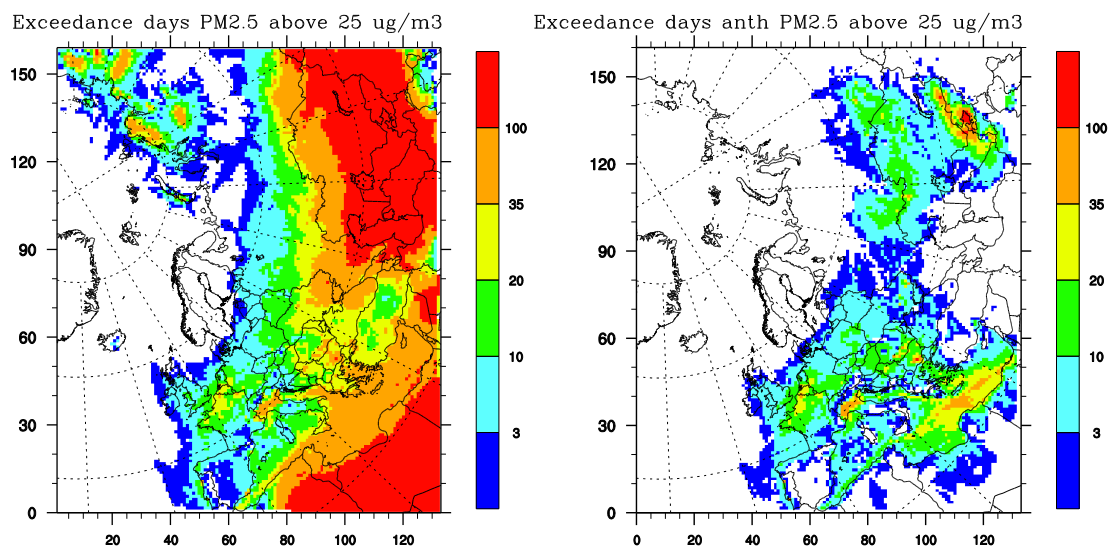


Figure 2.7: Calculated number of days with PM<sub>2.5</sub> exceeding the WHO AQG of 25 µg m<sup>-3</sup> in 2007: for total PM<sub>2.5</sub> (left) and for anthropogenic PM<sub>2.5</sub> (right). Note: WHO recommendation is not more than 3 days with exceedances.

For most sites, the model under-predicts the number of exceedance days, although with some exceptions. Typically, the discrepancy between modelled and observed number of exceedance days is larger for the sites with the highest observed number of such days (e.g. IT01, IT04, NL07, NL09, AT02, DE02). For most of these sites, the model also tends to underestimate the average PM levels to a greater extent (see model comparison with observations below). As seen from the Table 2.3, the days predicted by the model to be exceedance days do not always coincide with the observed exceedance days. The “Hit ratio” in Table 2.3 shows the percentage of observed exceedance days correctly predicted by the model. The hit ratios vary a lot (from 0 to 100%) between the sites. In general, the hit ratios of exceedance days are better for PM<sub>2.5</sub> than for PM<sub>10</sub>, with the mean values being 19% and 5% respectively.

Table 2.3: Number of days and common days where PM exceeds the WHO AQGs ( $50 \mu\text{g m}^{-3}$  for  $\text{PM}_{10}$  and  $25 \mu\text{g m}^{-3}$  for  $\text{PM}_{2.5}$ ) at EMEP stations according to model calculations and observations.

	PM <sub>10</sub>				PM <sub>2.5</sub>			
	Obs	Model	Common	Hit ratio	Obs	Model	Common	Hit ratio
AT02	21	0		0	66	7	6	9
AT05	0	2						
AT48	2	1		0				
CH01	1	3		0				
CH02	8	2	1	13	47	6	4	9
CH03	6	1	1	17				
CH04	1	2		0				
CH05	3	2	1	33	8	8	5	63
CY02	34	40	16	47				
CZ01	2	0		0				
CZ03	2	0		0	20	6	3	15
DE01	5	0		0				
DE02	4	0		0	27	5	2	7
DE03	3	0		0	6	7	3	50
DE07	0	0						
DE08	1	0		0				
DE09	4	0		0				
DE44	10	0		0	71	11	11	15
DK05	9	0		0				
ES07	13	4	2	15	8	3		0
ES08	1	7		0	17	9	3	18
ES09	0	1						
ES10	2	0		0	4	5	2	50
ES11	5	0		0	1	1		0
ES12	3	3		0	2	3		0
ES13	2	0		0	1	2		0
ES14	1	2		0	15	9	1	7
ES15	0	2						
ES16	1	0		0	2	3	2	100
FR09	9	1	1	11				
FR13	0	2						
FR13	0	2						
IT01	31	4		0	111	6	6	5
IT04					121	44	21	17
NL07	19	2		0				
NL09	14	0		0				
PL05	10	2	2	20				
SE11	0	0			3	0		
SE12	0	0						0
SE35	0	0						
SI08	1	0		0	8	3		0
GB06	0	0						
GB36	9	1	1	11	10	10	6	60
GB43	2	0		0				
GB48	0	0			7	4	3	43

Hit ratio (%) shows the percentage of observed exceedance days correctly predicted by the model (common\_days/obs\_days x100%).

## 2.3 Contribution of secondary inorganic species to PM mass

by Svetlana Tsyro, Karl Espen Yttri and Wenche Aas

### 2.3.1 Introduction

Speciation of particulate matter has historically been focused on the secondary inorganic constituent (SIA) which are known to have a long range transport potential; i.e. sulphate, ammonium and nitrate. Therefore, the majority of the EMEP Parties have these component included in their measurement programme. The carbonaceous content of PM on the other hand is reported for four sites only, and also the modelling of carbonaceous matter has relatively recently been included in the standard EMEP model, although primary emissions only so far. Modelling of secondary organic aerosol (SOA) is still very much a matter of ongoing research and is subject to continuous development. Also base cations, sea salt ions and mineral dust are part of the monitoring programme, but only a few countries are reporting data. This is particularly true for mineral dust and only campaign data are available for silicon and aluminium, which are the most critical parameters for apportioning the mineral dust content. This chapter presents an assessment of the contribution of SIA to PM mass.

### 2.3.2 Measurements and modelling of secondary inorganic aerosol (SIA)

Concurrent measurement of sulphate and PM<sub>10</sub> is performed at a total of 26 sites. At the majority of these sites, SO<sub>4</sub><sup>2-</sup> is collected using a sampler with an undefined cut-off, whereas at a few sites a sampler with a PM<sub>10</sub> inlet is applied. The sampling conditions are similar for nitrate and ammonium, but these variables are collected at somewhat fewer sites; i.e. 23 for NO<sub>3</sub><sup>-</sup> and 15 for NH<sub>4</sub><sup>+</sup>. However, this doesn't reflect the total picture of the number of sites performing reactive nitrogen measurements, as there are almost 50 sites measuring nitrate as the sum of NO<sub>3</sub><sup>-</sup> and HNO<sub>3</sub> and more than 40 measuring ammonium as the sum of NH<sub>4</sub><sup>+</sup> and NH<sub>3</sub>. For details see the EMEP/CCC data report (Hjellbrekke and Fjæraa, 2009). It should be noted that only IT01 and Netherlands measure NO<sub>3</sub><sup>-</sup> and NH<sub>4</sub><sup>+</sup> using the recommended denuder method. The method used at the other sites may give positive artefact due to absorption of NH<sub>3</sub> or HNO<sub>3</sub> or negative artefact due to evaporation of NH<sub>4</sub>NO<sub>3</sub>.

There are only three sites with a full year of chemical speciation in the fine fraction. To be able reflect on the European spatial resolution of SIA contribution to PM<sub>2.5</sub>, it necessary to look at the model results. As seen in Figure 2.8, the contribution is relatively high, mostly ranging between 30-55%, and the highest levels are seen for central Europe. This is consistent with the three EMEP sites in Germany and Italy showing 30-50% contribution of SIA to the PM<sub>2.5</sub>, i.e. SIA constitute 40% of PM<sub>2.5</sub> at DE44, 50% at IT04, and 31 % IT01 (Hjellbrekke and Fjæraa, 2009).

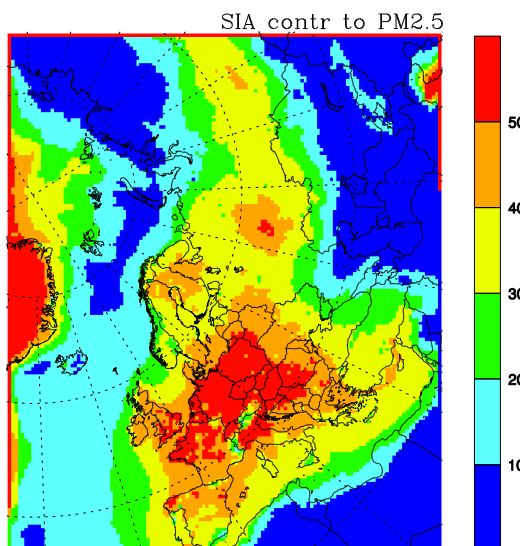


Figure 2.8: Model calculated relative contribution of SIA to  $PM_{2.5}$  in 2007.  
Unit: %.

The number of sites doing concurrent measurements of SIA and  $PM_{10}$  makes it possible to create kriged maps with annual average contribution ratios, which can be compared with modelled results (see Figure 2.9, Figure 2.10 and Figure 2.11). The modelled data show in general somewhat higher relative contribution than that based on observations and also greater variations. This is partly due to the underestimation of the mass concentration of PM by the model, although also SIA is underestimated by the model (see also Chapter 2.3.3). Furthermore, the measurement sites are not located in the most polluted areas. This is particularly true for sulphur, where the highest calculated levels are seen in the southeast of Europe.

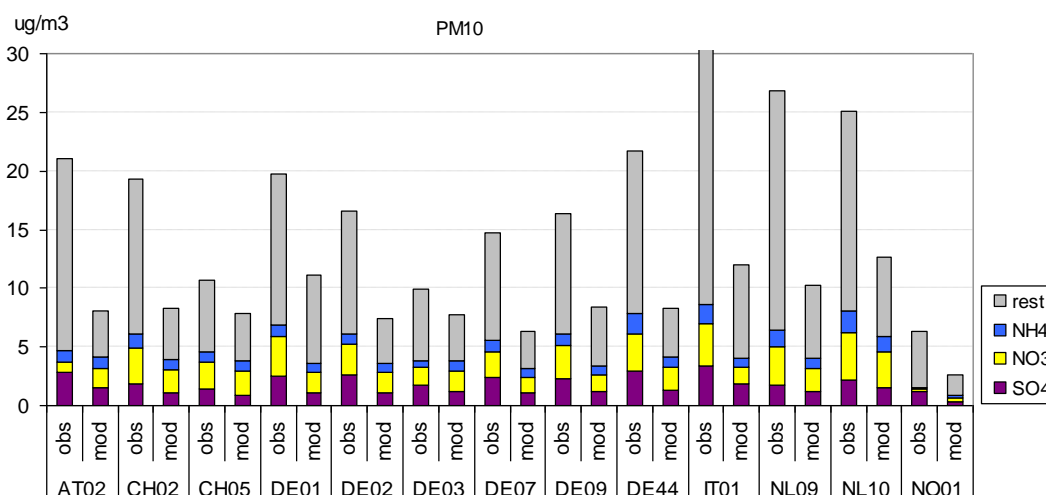


Figure 2.9: Comparison between calculated and observed  $PM_{10}$  and its SIA ( $SO_4^{2-}$ ,  $NO_3^-$  and  $NH_4^+$ ) content at the EMEP sites with SIA observations in 2007.

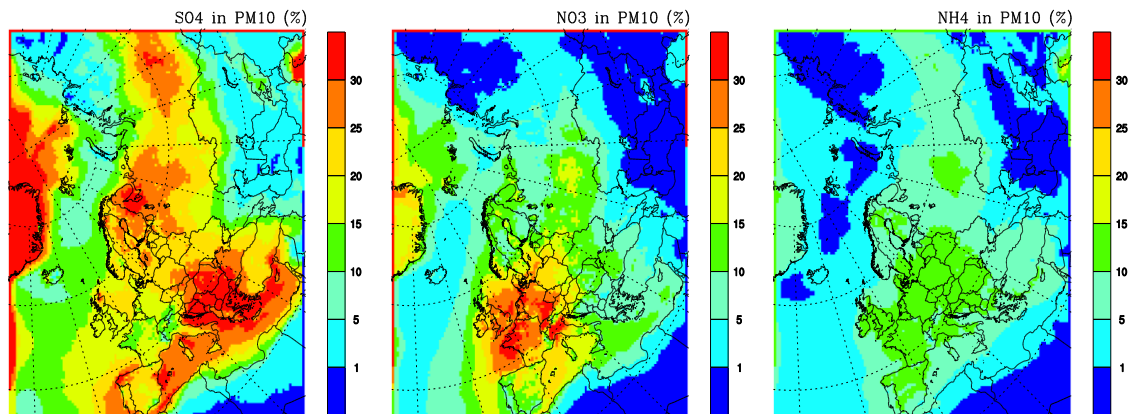


Figure 2.10: Model calculated relative contribution of  $\text{SO}_4^{2-}$ ,  $\text{NO}_3^-$  and  $\text{NH}_4^+$  to  $\text{PM}_{10}$  in 2007. Unit: %.

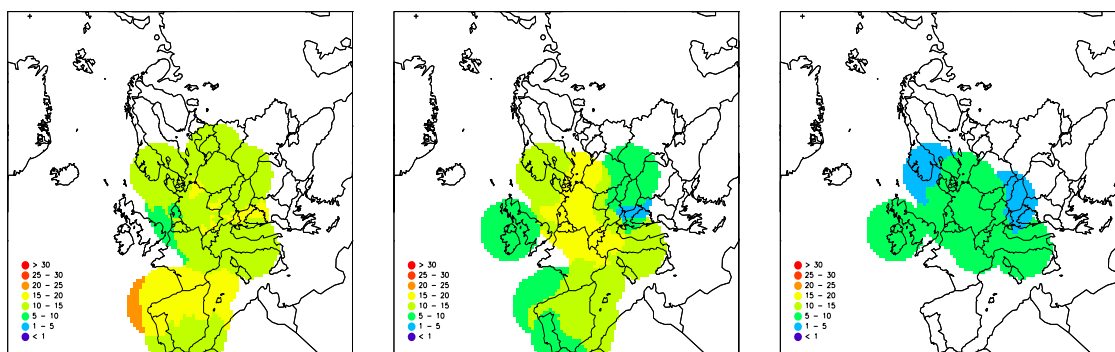


Figure 2.11: Kriged maps of observed relative contribution of  $\text{SO}_4^{2-}$ ,  $\text{NO}_3^-$  and  $\text{NH}_4^+$  to  $\text{PM}_{10}$  in 2007. Unit: %.

The relative contribution of  $\text{SO}_4^{2-}$  to  $\text{PM}_{10}$  and  $\text{NO}_3^-$  to  $\text{PM}_{10}$  based on the data reported for 2007 are quite similar;  $14\pm 4\%$  for  $\text{SO}_4^{2-}$  and  $13\pm 4\%$  for  $\text{NO}_3^-$ . However, the spatial distributions are quite different. For  $\text{SO}_4^{2-}$  the highest contributions are seen in the southeast of Europe, at the northern coast of Spain and at the Kola Peninsula in the northeast of Russia. This pattern is also reflected in the  $\text{SO}_2$  emissions in Europe (EMEP, 2009). The relatively high level of  $\text{SO}_4^{2-}$  at the coastline of Spain is partly reflecting ship emissions, contribution from sea salt sulphur, and a relatively low  $\text{PM}_{10}$  concentration, while in southeast Europe there are large industrial sources dominating in addition to ship emissions in the Mediterranean Sea. For nitrate the highest relative contribution is seen in central Europe, which is due to the large contribution of  $\text{NO}_x$  emissions from traffic sources. This is enhanced by the widespread use of diesel cars in central and Western Europe compared to other parts of the continent. For ammonium the relative contribution to  $\text{PM}_{10}$  based on observations was  $6\pm 1\%$ . The spatial pattern is similar for both model and observations with the highest contribution seen for central Europe.

Time series of the relative contribution of the individual SIA constituents to  $\text{PM}_{10}$  were examined for those sites reporting such data for a period of five years or

more (Figure 2.12). For these six sites, the relative contribution of  $\text{SO}_4^{2-}$  was found to be rather consistent, except for a few years (e.g. 2003). Several of the sites reported a decrease in the concentration of  $\text{PM}_{10}$  for 2007 compared to the previous year, but for some of these sites the decrease in SIA was even more pronounced, i.e. at DE07 and NO01, resulting in a decreasing ratio.

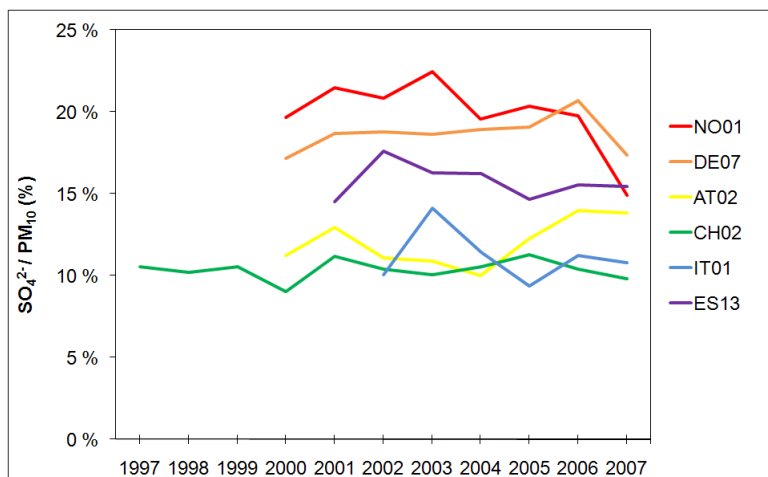


Figure 2.12: Trends in observed relative contribution of  $\text{SO}_4^{2-}$  to  $\text{PM}_{10}$ . Unit: %.

### 2.3.3 Evaluation of the model performance for PM mass and SIA

To evaluate the ability of the EMEP model to reproduce observations of PM, the calculated concentrations of  $\text{PM}_{10}$ ,  $\text{PM}_{2.5}$  and the main aerosol constituents have been compared to observed concentrations at EMEP sites for 2007.

A comparison of the model's performance on the annual and seasonal basis is provided in Table 2.4. Significant changes are observed for most PM constituents compared to that reported for previous years. These changes are due to the update of the  $\text{HNO}_3$  night-time formation scheme and the use of HIRLAM meteorological data (see chapter 2.1.6). These updates resulted in a significant decrease of  $\text{NO}_3^-$  and  $\text{NH}_4^+$  concentrations so that on average the model currently underestimates  $\text{NO}_3^-$  by 28% and  $\text{NH}_4^+$  by 30%, while for previous years these variables have been overestimated. Calculated  $\text{SO}_4^{2-}$  concentrations were found to be decreased as well and the model's negative bias increased to -34%. As a result, SIA is currently underestimated by 34% by the model.

The model underestimation of SIA contributes to the model's negative bias for  $\text{PM}_{10}$ , and particularly for  $\text{PM}_{2.5}$ , which is larger than what has been reported for previous years.  $\text{PM}_{10}$  is currently underestimated by 43%, while  $\text{PM}_{2.5}$  by 41%. As the relative contribution of SIA to PM varies across Europe, the recent updates of the model affected the calculated PM to a various extent. Therefore, the changes have caused a somewhat different regional distribution of calculated  $\text{PM}_{10}$  and  $\text{PM}_{2.5}$  over Europe compared to previous years. The annual mean spatial correlation between calculated and measured  $\text{PM}_{10}$  and  $\text{PM}_{2.5}$  is somewhat lower than that seen in the earlier reports, the correlation coefficient being 0.60 for  $\text{PM}_{10}$  and 0.70 for  $\text{PM}_{2.5}$ . On the other hand, the tempo-spatial correlation coefficients,

which characterize the correlation between daily  $PM_{10}$  and  $PM_{2.5}$  from model results and observations for all EMEP sites, are about the same (for  $PM_{10}$  and SIA) or better (for  $PM_{2.5}$ ).

The model performance seems to be better for the warm season compared to the cold season when compared to observations. In spring and summer, the model underestimation is less and the spatial correlation with observations is better for  $PM_{10}$ ,  $PM_{2.5}$  and SIA. For instance,  $PM_{2.5}$  is underestimated by 38% in spring and by 29% in summer, while in autumn and winter the underestimation increases to 57% and 61%, respectively. For sea salt ( $Na^+$ ), the model bias is relatively small for all seasons (slightly larger in winter, though). The spatial correlation with observations range between 0.76 and 0.82 for winter, spring and fall, while it is reduced to 0.56 for summer.

Table 2.4 provide comparison statistics between model-calculated and observed daily  $PM_{10}$  and  $PM_{2.5}$  for the EMEP stations. The average bias for all sites model bias is -44% for  $PM_{10}$  and -41% for  $PM_{2.5}$  and temporal correlation between model results and observations is 0.59 for both components. Note that for Swedish and British sites, hourly  $PM_{10}$  and  $PM_{2.5}$  concentrations measured with TEOM were averaged to 24-hourly concentrations.

Figure 2.13 shows model bias and temporal correlation between calculated and measured concentrations of  $PM_{10}$ ,  $PM_{2.5}$ , and SIA at sites performing concurrent measurements of these variables in 2007. At four German sites (DE01, DE02, DE07 and DE09), the model underestimation of SIA by 25% to 38% can to a large degree explain the negative bias for PM. For AT02, DE03 and NL09, the underestimation of  $PM_{10}$  and  $PM_{2.5}$  is considerably larger than what can be attributed to SIA. Correlation between model and observations is somewhat better for SIA than for  $PM_{10}$ . Correlation for  $PM_{2.5}$  is considerably better than for  $PM_{10}$  at most of the sites, particularly at the Spanish sites.

Figure 2.14 shows model bias and temporal correlation between calculated and measured SIA and its components, namely  $SO_4^{2-}$ ,  $NO_3^-$  and  $NH_4^+$ , for the sites performing such measurements. At most of the sites, SIA is underestimated as  $SO_4^{2-}$ ,  $NO_3^-$  and  $NH_4^+$  all are underestimated by the model. At a few sites (e.g. AT02, DE03, LV10, LV16, PL03), calculated SIA is quite close to the observed value due to the error compensation between its components, typically as a result of  $NO_3^-$  overestimation. The correlation coefficients range largely between 0.4 and 0.7, being poorest for the Latvian sites, for the sites in the north of Norway, and even negative at PL03.

Finally, Figure 2.9 compares calculated and measured chemical composition of  $PM_{10}$ , as consisting of  $SO_4^{2-}$ ,  $NO_3^-$ ,  $NH_4^+$  and the “rest” for 13 EMEP sites where co-located measurements of these constituents were performed in 2007.

Table 2.4: Annual and seasonal comparison statistics between EMEP model calculated and EMEP measured concentrations of  $PM_{10}$ ,  $PM_{2.5}$ , SIA,  $SO_4^{2-}$ ,  $NO_3^-$ ,  $NH_4^+$  and  $Na^+$  for 2007

Period	N sites	Obs ( $\mu\text{g}/\text{m}^3$ )	Mod ( $\mu\text{g}/\text{m}^3$ )	Bias,%	RMSE	R
<b><math>PM_{10}</math></b>						
Yearly mean	40	16.32	9.23	-43	8.67	0.60
Daily mean	44	16.26	9.14	-44	12.19	0.56
JanFeb	44	14.31	7.06	-51	11.68	0.55
spring	44	18.32	11.04	-40	12.81	0.60
summer	44	15.82	8.92	-44	11.47	0.50
autumn	43	15.75	8.67	-45	11.66	0.55
<b><math>PM_{2.5}</math></b>						
Yearly mean	21	11.55	6.82	-41	6.18	0.70
Daily mean	24	11.27	6.70	-41	9.62	0.50
JanFeb	23	11.26	4.81	-57	12.38	0.49
spring	23	11.88	8.51	-28	8.19	0.62
summer	24	10.36	6.64	-36	6.73	0.54
autumn	23	10.99	6.18	-44	9.61	0.43
<b>SIA</b>						
Yearly mean	25	4.66	3.08	-34	2.28	0.78
Daily mean	26	4.57	2.96	-35	4.11	0.65
JanFeb	25	4.17	2.14	-49	4.38	0.51
spring	24	5.41	3.64	-33	4.40	0.70
summer	25	3.74	2.54	-32	2.94	0.65
autumn	25	4.32	2.47	-43	4.07	0.62
<b><math>SO_4^{2-}</math></b>						
Yearly mean	54	1.85	1.04	-44	1.05	0.69
Daily mean	63	1.86	1.05	-44	1.64	0.57
JanFeb	63	1.53	0.61	-61	1.62	0.44
spring	62	2.02	1.26	-38	1.56	0.60
summer	62	1.91	1.37	-29	1.40	0.62
autumn	62	1.78	0.77	-57	1.70	0.60
<b><math>NO_3^-</math></b>						
Yearly mean	27	1.66	1.20	-28	0.87	0.83
Daily mean	28	1.60	1.15	-28	2.06	0.60
JanFeb	28	1.55	0.99	-36	2.06	0.49
spring	27	2.10	1.44	-31	2.33	0.68
summer	27	1.03	0.53	-49	1.25	0.53
autumn	27	1.51	1.09	-27	1.90	0.58
<b><math>NH_4^+</math></b>						
Yearly mean	33	0.90	0.63	-30	0.43	0.77
Daily mean	33	0.88	0.60	-31	0.90	0.65
JanFeb	32	0.74	0.43	-41	0.88	0.53
spring	32	1.09	0.78	-29	1.06	0.68
summer	33	0.72	0.53	-26	0.64	0.60
autumn	33	0.81	0.48	-41	0.88	0.63
<b>Na</b>						
Yearly mean	7	0.80	0.92	15	0.27	0.93
Daily mean	7	0.78	0.90	14	0.80	0.75
JanFeb	7	1.08	1.37	27	1.07	0.79
spring	7	0.81	0.93	14	0.75	0.76
summer	7	0.55	0.47	-13	0.78	0.56
autumn	7	0.81	0.95	18	0.67	0.82

Here, Ns – the number of stations, Obs – the measured mean, Mod – the calculated mean, Bias is calculated as  $\frac{\sum(\text{Mod}-\text{Obs})}{\text{Obs}} \times 100\%$ , RMSE – the Root mean Square Error =  $[\frac{1}{N_s} \sum (\text{Mod}-\text{Obs})^2]^{1/2}$ , R – the tempo-spatial correlation coefficient between modelled and measured daily concentrations and spatial correlation for seasonal mean concentrations.

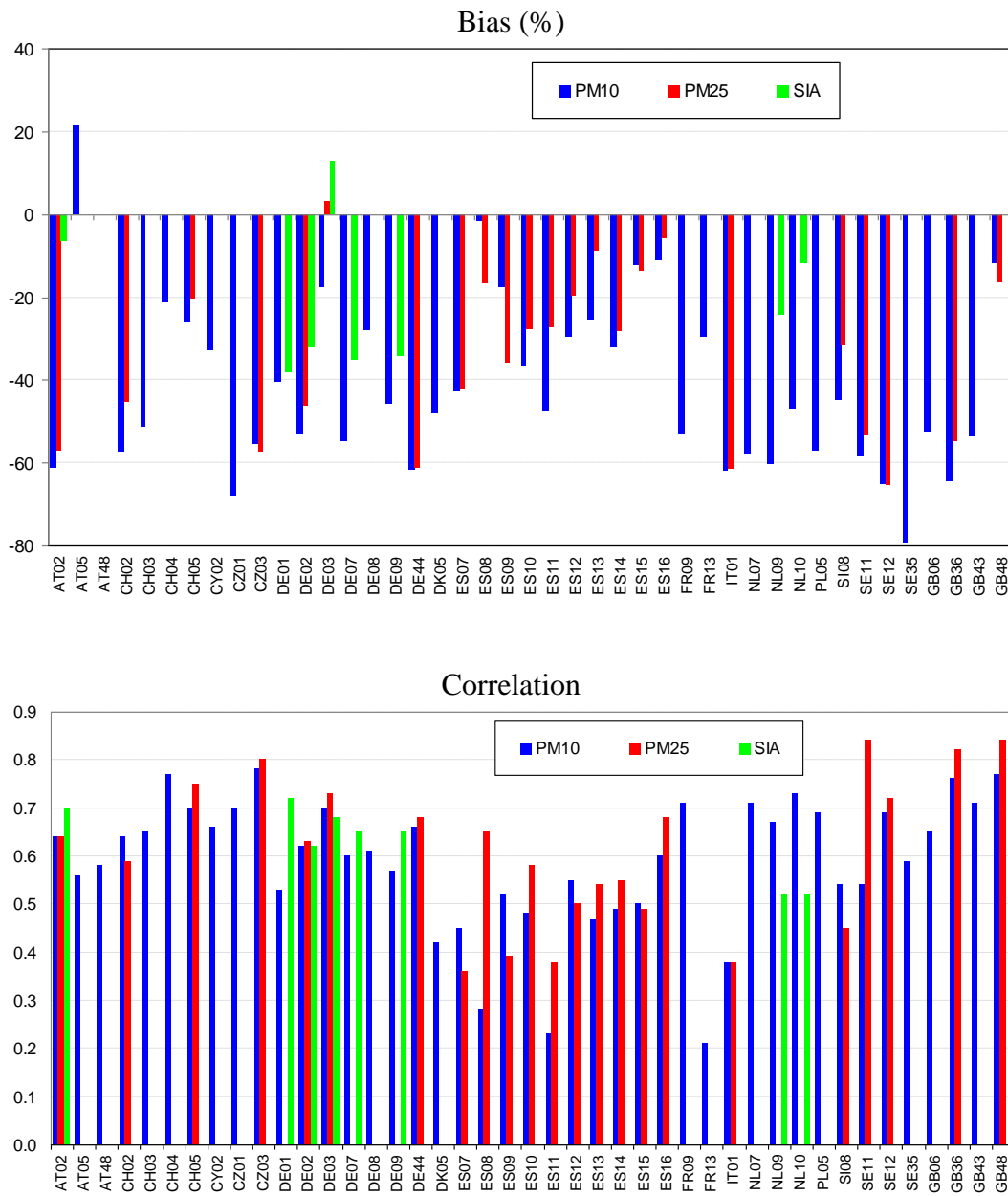


Figure 2.13: Bias and temporal correlation for model calculated  $PM_{10}$ ,  $PM_{2.5}$  and SIA compared to observations at EMEP sites in 2007.

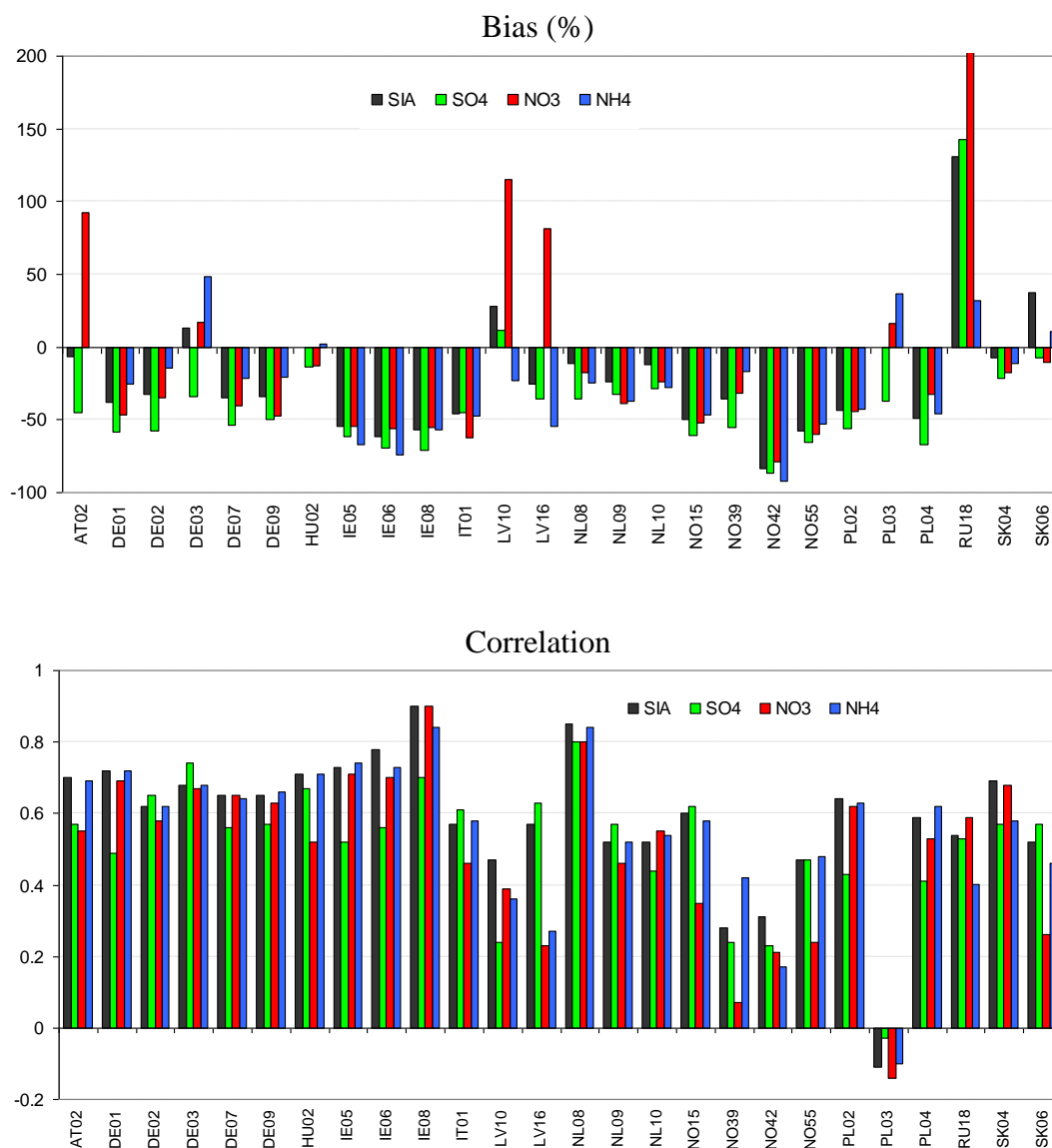


Figure 2.14: Bias and temporal correlation for model calculated SIA and its components  $\text{SO}_4^{2-}$ ,  $\text{NO}_3^-$  and  $\text{NH}_4^+$  compared to observations at EMEP sites in 2007. Here, only the sites with co-located and concurrent measurements of  $\text{SO}_4^{2-}$ ,  $\text{NO}_3^-$  and  $\text{NH}_4^+$  are included.

## 2.4 Elemental and Organic Carbon

### 2.4.1 Status of sampling and measurement, and quality of observation data

By Karl Espen Yttri and Wenche Aas

There is a lack of comparable EC/OC data in Europe, which makes it difficult to address the spatial and temporal variation of these variables on the regional scale. This situation did not improve from 2006 to 2007. Currently there are only two datasets available that can be used to obtain such information, namely that of the EMEP EC/OC campaign (Yttri et al., 2007), and the CARBOSOL project (Pio et al., 2007). Data from these two campaigns have been used by Simpson et al. (2007) to validate the performance of the EMEP model with respect to OC and

TC. However, more recent measurements are needed to get an overview of the current situation, and to validate the progress made with respect to the model development.

A substantial increase in the number of countries and sites reporting levels of EC and OC are expected in the coming years. This can be explained by the importance of such measurements, and because of the ongoing development of the unified protocol for sampling and measurement of the ambient aerosol content of EC and OC within EUSAAR. An effort to establish a large and harmonized dataset which goes beyond the ordinary EC/OC/TC measurements when addressing the carbonaceous content of the rural background aerosol has been made in the two most recent intensive EMEP measurement campaigns. A brief introduction and some preliminary results from this effort are presented in Chapter 2.5 of this report.

Four countries reported measurements of EC and OC for 2007, which is one more than for 2006. The sites performing such measurements are Birkenes (NO01) in Norway, Melpitz (DE44) in Germany, Ispra (IT04) in Italy, and Montseny (ES17) in Spain. A brief overview of the data reported for these sites are described in the following subchapters. Information concerning sampling period and size fractions for the actual sites are listed in (Table 2.5).

*Table 2.5: Sites reporting EC and OC to the EMEP database, including size fractions and sampling period.*

Site (Country)	EC	OC	PM <sub>1</sub>	PM <sub>2.5</sub>	PM <sub>10</sub>	Period
<b>Birkenes (Norway)</b>	x	x		x	X	2001, 2002, 2003, 2004, 2005, 2006, 2007,
<b>Melpitz (Germany)</b>	x	x		x	X	2006, 2007
<b>Ispra (Italy)</b>	x	x		x		2002 <sup>1)</sup> , 2003 <sup>2)</sup> , 2004 <sup>2)</sup> , 2005 <sup>2)</sup> , 2006, 2007
<b>Montseny (Spain)</b>	x	x		x	x	2007

1. EMEP EC/OC campaign
2. Both PM<sub>2.5</sub> and PM<sub>10</sub>.

Table 2.6 lists the most crucial parameters concerning the quality of the EC/OC data. Similar sampling time and sampling frequency were only applied at two of the sites. Neither of the samplers operated according to a sampling technique that corrected for, or quantified, the negative artefacts, while the positive artefact was accounted for at Ispra.

Table 2.6: *Sampling equipment and analytical approach used at the sites reporting EC and OC to the EMEP database.*

Site (Country)	Sampling time/frequency	Filter face velocity	Sampling equipment	Analytical approach
<b>Birkenes (Norway)</b>	(6+1) days, weekly	54 cm s <sup>-1</sup>	Single filter (no correction)	Sunset TOT (quartz. par)
<b>Melpitz (Germany)</b>	24 hr, daily	54 cm s <sup>-1</sup>	Single filter (no correction)	VDI 2465 Part 2
<b>Ispra (Italy)</b>	24 hr, daily	20 cm s <sup>-1</sup>	Denuder (pos. artifact)	Sunset TOT/TOR (EUSAAR-2)
<b>Montseny (Spain)</b>	24 hours, irregular	54 cm s <sup>-1</sup>	Single filter (no correction)	Not provided

Thermal-optical analysis was used to quantify the samples content of EC and OC at Birkenes and Ispra, whereas the samples collected at Melpitz were analyzed using a non-optical system that do not account for charring of OC during analysis. According to Schmid et al. (2001) only methods that correct for charring during analysis, or that prevent charring to take place, should be recommended when it comes to splitting TC into EC and OC. Thus, any comparison of data from the four sites listed in Table 2.5 should be based on TC. Despite that the results are not likely comparable with respect to EC and OC, they still provide valuable information concerning seasonal variation, mass closure of PM, and time-trends at the respective sites.

The analytical protocol for quantification of the aerosol filter samples content of EC, OC and TC developed within EUSAAR for subsequent adaption by EMEP has been subject to modification throughout the duration of the project. A detailed description of its final version and performance has recently been submitted to a peer reviewed scientific journal for publication in order to ease it's availability for a wider scientific community.

#### **2.4.1.1 EC and OC levels at the Norwegian site Birkenes (NO01)**

The Birkenes atmospheric research station (58° 23'N, 8° 15'E, 190 m asl) is a joint supersite for EMEP and GAW and is situated approximately 20 km from the Skagerrak coast in the southern part of Norway. The site is often influenced by episodes of transboundary air pollution from continental Europe and has frequently been used to study long-range air pollution. The station is located in a boreal forest with mixed conifer and deciduous trees. The station has been operational since 1971.

Birkenes most likely have the longest continuous time series of EC, OC, and TC using thermal optical analysis in Europe, going back to 2001. Given its strategic position it is well suited to monitor the outflow of air pollutants from the European continent, and the time series of the carbonaceous content of PM<sub>10</sub> and PM<sub>2.5</sub> closely resemble that of the secondary inorganic constituents. This resemblance appears to be greater for TC in PM<sub>2.5</sub> than for PM<sub>10</sub>. This might be attributed to the significant signal of coarse mode (PM<sub>10-2.5</sub>) TC at Birkenes, which most likely is dominated by Primary biological aerosol particles (PBAP) and which have a more local than regional origin.

For the period 2001–2007, OC in PM<sub>10</sub> ranged from 0.8-1.2 µg m<sup>-3</sup>, whereas the corresponding range for OC in PM<sub>2.5</sub> was 0.6-1.0 µg m<sup>-3</sup> (Figure 2.15). For PM<sub>10-2.5</sub> the annual mean concentration of OC ranged from 0.1-0.3 µg m<sup>-3</sup>. The annual mean concentrations of EC ranged between 0.1-0.2 µg m<sup>-3</sup> for PM<sub>10</sub> and PM<sub>2.5</sub> for the period in question, whereas it did not exceed 0.05 µg m<sup>-3</sup> for PM<sub>10-2.5</sub>.

From 2006 to 2007 there was an almost 30% decrease in OC for both PM<sub>10</sub> and PM<sub>2.5</sub>, and a more than 20% reduction for OC in PM<sub>10-2.5</sub>. This appears to be within the natural variation as changes in the annual mean OC concentration ranging between 30-40% from one year to the next have been reported for this site previously. There were only minor changes for EC when compared to the previous year, and the levels are in general very low.

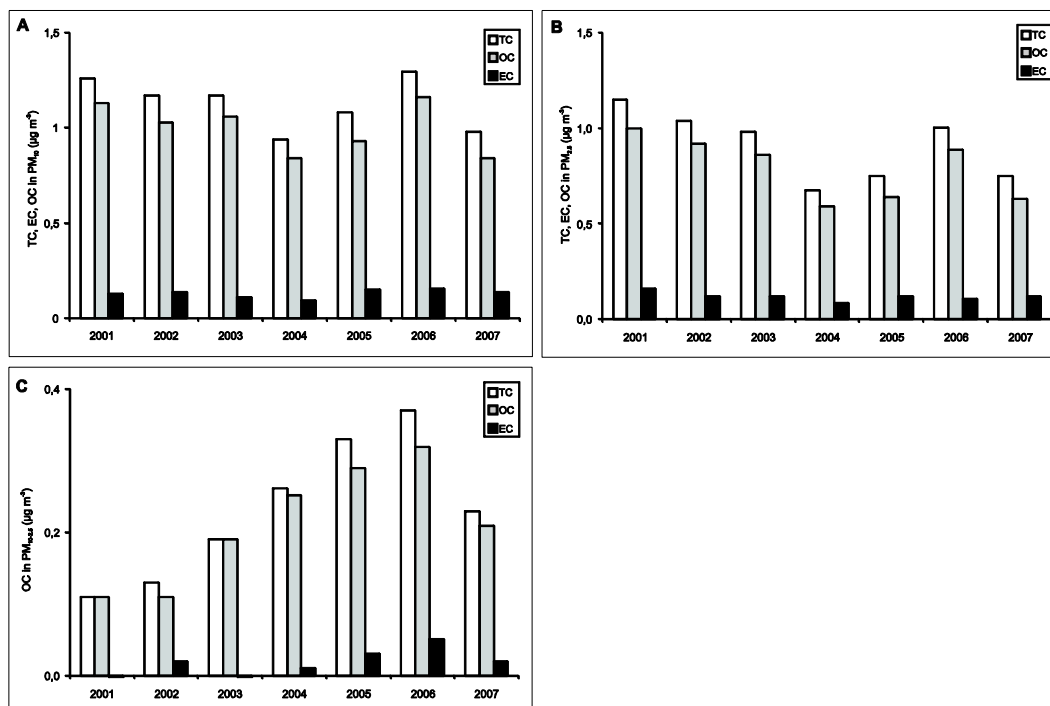


Figure 2.15: Annual mean concentrations of EC, OC and TC in PM<sub>10</sub> (A), PM<sub>2.5</sub> (B) and PM<sub>10-2.5</sub> (C) at the Norwegian site Birkenes.

The concentration of OC is always higher during summer compared to winter at Birkenes. This seasonal variation is seen both for PM<sub>10</sub> and PM<sub>2.5</sub>, but it is most pronounced for PM<sub>10</sub>, as a result of the increased levels of OC<sub>PM10-2.5</sub> in summer. For EC, the concentration tends to be higher in winter both for PM<sub>10</sub> and PM<sub>2.5</sub>, but it is not a consistent pattern.

OC is always the dominant fraction of TC at Birkenes, regardless of size fraction and typically account for 85-90% of the TC fraction in PM<sub>10</sub> on an annual basis, whereas the remaining 10-15% is attributed to EC. Only minor differences are seen for PM<sub>2.5</sub> compared to PM<sub>10</sub> with respect to the relative contribution of EC and OC to TC.

The majority of OC in  $PM_{10}$  can be attributed to the fine fraction; 76% in 2007. Fine OC makes a less contribution to OC in  $PM_{10}$  in summer and fall. This seems to be attributed to the impact of primary biological aerosol particles (PBAP) (Yttri et al., 2007), which mainly is found in the coarse fraction of  $PM_{10}$ . During summer, coarse OC may actually be the major fraction, accounting for more than 50% of OC in  $PM_{10}$  on a monthly basis.

For the period 2001–2007, the relative contribution of TCM-to- $PM_{10}$  [(TCM = Total carbonaceous matter (TCM = OC x 1.7 + EC x 1.1)] at Birkenes varied from 34% in 2001 to 26% in 2005/6 (Figure 2.16A). The relative contribution of TCM-to- $PM_{2.5}$  has the same temporal pattern as for TCM-to- $PM_{10}$ , accounting for 47% in 2001 and 32% in 2006. A slight increase in TCM to both  $PM_{10}$  and  $PM_{2.5}$  was observed for 2007 compared to 2006. The relative contribution of TCM to  $PM_{10-2.5}$  ranged from 9–21% for the actual period. While TCM-to- $PM_{10-2.5}$  increased substantially from 2001–2004, corresponding to the major increase in the  $OC_{PM_{10-2.5}}$  concentration shown in Figure 2.15C, the relative contribution have declined slightly again from 2004 and onwards. Compared to  $SO_4^{2-}$ ,  $NO_3^-$ ,  $NH_4^+$ , and sea salt, TCM accounts for the greatest contribution of mass to  $PM_{10}$  at Birkenes (Figure 2.16B). Interestingly, the contribution of TCM to  $PM_{10}$  equals that of the secondary inorganic constituents (SIA) for 2007, and while the relative contribution of TCM to  $PM_{10}$  appears to increase, SIA seems to have a downward tendency.

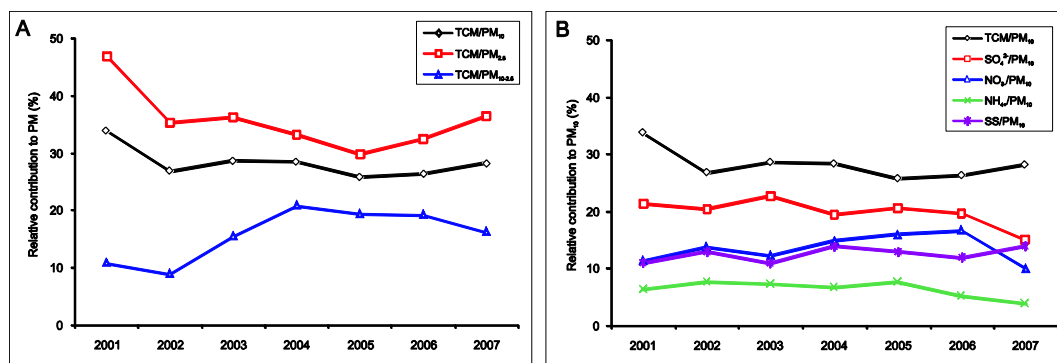


Figure 2.16: Relative contribution of TCM (Total Carbonaceous Matter) to  $PM_{10}$ ,  $PM_{2.5}$  and  $PM_{10-2.5}$  (A) and relative contribution of TCM,  $SO_4^{2-}$ ,  $NO_3^-$ ,  $NH_4^+$  and sea salt to  $PM_{10}$  (B).

#### 2.4.1.2 EC and OC levels at the Italian site Ispra (IT04)

The Italian site Ispra (IT04) (45° 49'N, 8° 38'E, 209 m asl) is situated in the Po Valley in the north-western part of Italy. The site is representative for the rural parts of the densely populated central Europe and has been operational since 1985.

PM constituents show quite high levels at Ispra, including the carbonaceous fraction of the aerosol; this is also the situation for 2007 with annual mean concentrations of EC, OC and TC being  $2.3 \mu\text{g m}^{-3}$ ,  $9.3 \mu\text{g m}^{-3}$  and  $11.6 \mu\text{g m}^{-3}$ , respectively. For TC this is a factor of 4-15 higher than for comparable data from the other three sites reporting TC concentrations for 2007.

Ispra has a time series of EC, OC, and TC in PM<sub>2.5</sub> using thermal optical analysis going back to 2003 (Figure 2.17). For the period 2003–2007, OC in PM<sub>2.5</sub> ranged from 6.8–10.1 µg m<sup>-3</sup>, whereas the corresponding range for EC was 1.3–2.5 µg m<sup>-3</sup>. From 2006 to 2007 there were only minor changes (< ±8%) in the annual mean concentration for any of the three carbonaceous fractions. For previous years, inter annual variations of 30% has been observed for TC.

At Ispra the carbonaceous content of PM<sub>2.5</sub> has a pronounced seasonal variation being substantial higher in winter compared to summer (see Figure 1.10 in last year's report); e.g. the monthly mean being 9 times higher in December (27 µg m<sup>-3</sup>) compared to August (3 µg m<sup>-3</sup>) 2007. It is interesting to note that the seasonal variation of the carbonaceous aerosol at Ispra is completely opposite of that reported for OC and TC at the Norwegian site Birkenes.

OC is always the dominant fraction of TC at Ispra, accounting for 80% of TC, whereas the remaining 20% is attributed to EC

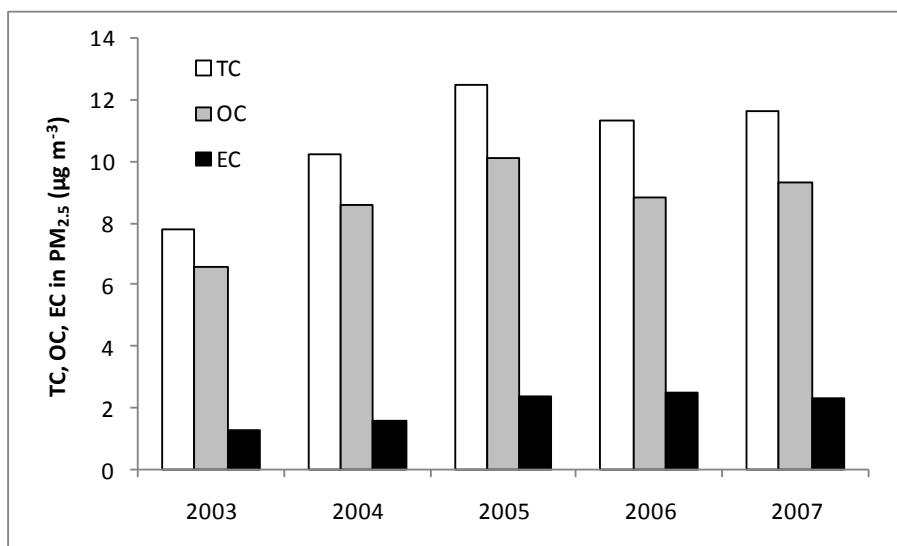


Figure 2.17: Annual mean concentrations of EC, OC and TC in PM<sub>2.5</sub> the Italian site Ispra.

For 2007 the annual mean concentration of TCM accounted for 56% of PM<sub>2.5</sub> (Figure 2.18). This is the highest relative contribution reported so far, but only with a short margin (54% in 2005). Thus, the importance of the carbonaceous fraction of the aerosol at Ispra is demonstrated once more. A conversion factor of 1.4 was used to convert OC to OM at Ispra, whereas a factor of 1.1 was used to account for hydrogen associated with EC (Kiss et al., 2002). The conversion factors for OC reported in literature range from 1.2–2.6, depending on the origin of the aerosols and to what extent they have been aged in the atmosphere (Turpin and Lim, 2001). Undoubtedly, the use of such a wide range of conversion factors might introduce a significant level of uncertainty to the TCM-to-PM estimates. Although a factor of 1.4 is considered rather conservative, there were quite few incidences where the mass closure based on SIA and TCM exceeded 100% of the PM<sub>2.5</sub> mass concentration (not included in Figure 2.18), which is rather difficult to explain, and that even without accounting for mineral dust.

From Figure 2.18 it is apparent that the relative contribution of carbonaceous matter to  $PM_{2.5}$  at Ispra is much higher than any of the single inorganic secondary constituents measured. The carbonaceous fraction is also higher than the sum of  $SO_4^{2-}$ ,  $NO_3^-$  and  $NH_4^+$  for all years considered (2003–2007).

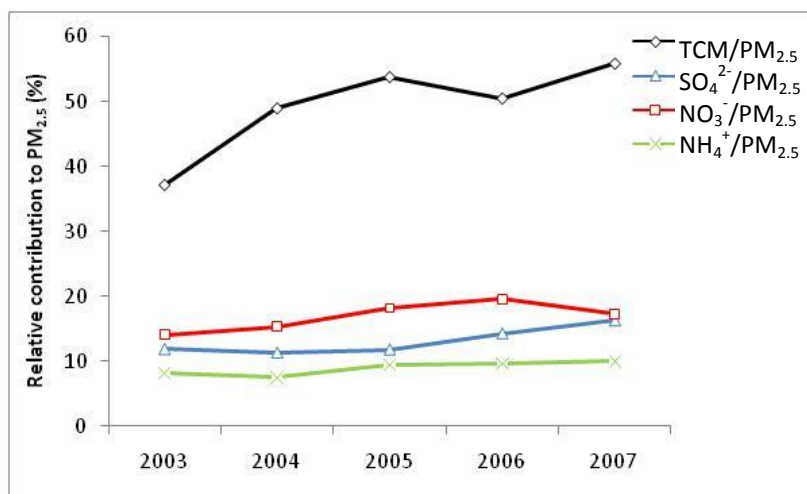


Figure 2.18: Relative contribution of TCM (Total Carbonaceous Matter) and major inorganic constituents to  $PM_{2.5}$  at Ispra for the period 2003–2007.

#### 2.4.1.3 EC and OC levels at the German site Melpitz (DE44)

2007 was the second year levels of EC, OC and TC has been reported for the German site Melpitz (51° 32' N, 12° 54' E, 87 m asl). As for the other three sites reporting EC/OC data for 2007, Melpitz is a supersite in the EUSAAR (European Supersites for Atmospheric Aerosol Research) network. The site is situated in an agricultural area and is surrounded by meadows for fodder production.

The annual mean concentration of EC, OC and TC for  $PM_{10}$ ,  $PM_{2.5}$  and  $PM_{10-2.5}$  at Melpitz are shown in (Table 2.7). There is a major decrease for all carbonaceous fractions in  $PM_{10}$  and  $PM_{2.5}$  at Melpitz going from 2006 to 2007. The most apparent reduction is seen for  $PM_{2.5}$ , where EC is reduced by more than 40%, OC by approximately 30% and TC by 35%. It is mainly the reductions seen for  $PM_{2.5}$ , which causes the reductions for  $PM_{10}$  as TC in  $PM_{10-2.5}$  experiences a 10% reduction only.

As can be seen from Table 2.7, OC was the major fraction of TC, however by quite a narrow margin. This can be explained by the analytical procedure used for quantification, i.e. the VDI protocol, which do not correct for charring of OC during analysis, hence artificial EC is generated during the analysis overestimating the true EC concentration in the sample. When compared to the three other sites listed in Table 2.6, the EC/TC ratio for Melpitz is actually 2-4 times higher. It should be emphasized that not the entire difference necessarily is attributed to the analytical issue but partly also reflect the various influence of EC at the different sites. Despite the erroneous feature of the VDI protocol, the results could still provide useful information concerning seasonal variation and

time trends. However, it could introduce substantial uncertainties in mass closure studies.

*Table 2.7: Annual mean concentrations of EC, OC, and TC in PM<sub>10</sub>, PM<sub>2.5</sub> and PM<sub>10-2.5</sub> at the German site Melpitz (DE44) for 2006 ( $\mu\text{g m}^{-3}$ ).*

Year	PM <sub>10</sub>			PM <sub>2.5</sub>			PM <sub>10-2.5</sub> <sup>1)</sup>		
	EC	OC	TC	EC	OC	TC	EC	OC	TC
2006	2.3	3.1	5.4	1.9	2.1	4.0	0.9	1.1	2.0
2007	1.6	2.7	4.3	1.1	1.5	2.6	0.6*	1.1*	1.8*

1) Annual mean concentrations of EC, OC and TC in PM<sub>10-2.5</sub> are based on concurrent 24 hour measurements of EC, OC and TC in PM<sub>10</sub> and PM<sub>2.5</sub> for which the difference between EC, OC and TC in PM<sub>10</sub> and PM<sub>2.5</sub> is > 0.

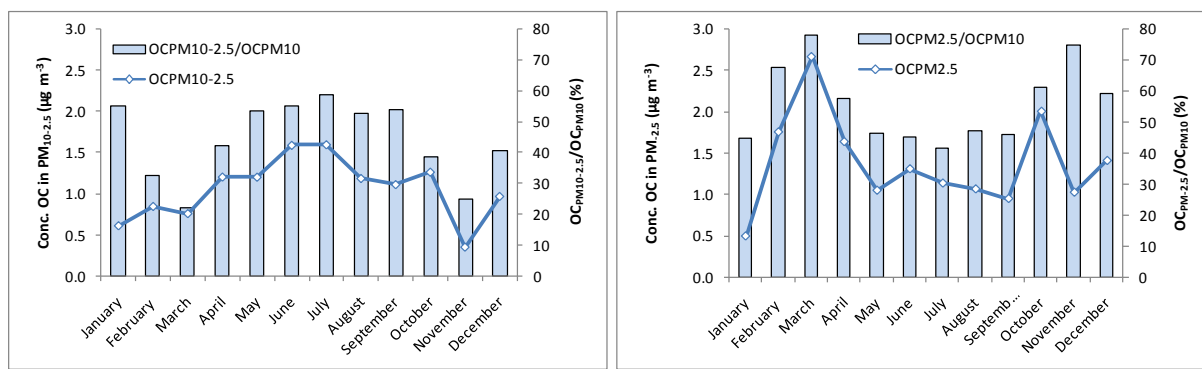


*Figure 2.19: Monthly mean concentration of OC in PM<sub>10-2.5</sub> (Left) and PM<sub>2.5</sub> (Right) at the German site Melpitz in 2007, illustrating the characteristic seasonal variation (Left axis). Relative contribution of OCPM<sub>10-2.5</sub>-to-OCPM<sub>10</sub> and OCPM<sub>2.5</sub>-to-OCPM<sub>10</sub>, increasing considerably during the vegetative season and the heating season, respectively (Right axis).*

The majority (60%) of the carbon content in PM<sub>10</sub>, here measured as TC, was associated with fine aerosols. This is expected as carbonaceous aerosols typically are derived from combustion or are the result of secondary formation in the atmosphere. Indeed, the seasonal variation of fine OC (Figure 2.19, right) show that its concentration peaks during the heating season, accounting for approximately 80% of OC in PM<sub>10</sub> in March. However, 60% on an annual basis would in general be considered a low fraction, and provides difficulties in explaining the origin of the 40% TC residing in the coarse fraction of PM<sub>10</sub>, which typically have been attributed to the ill defined group of primary biological aerosol particles (PBAP). A pronounced seasonal variation was observed for OC (and TC) in PM<sub>10-2.5</sub> for 2007 (see Figure 2.19, left), closely resembling the vegetative season, a feature which was not seen for 2006. This finding indicates the presence of PBAP, and closely resembles what has been reported for the Norwegian site Birkenes (Yttri et al., 2007). A bit surprising, EC in PM<sub>10-2.5</sub> at Melpitz show sign of a similar seasonal variation as coarse OC. This could indicate influence by another source or mechanisms than PBAB, but could equally

well be the results of the “thermal-only” analytical method failing to account for charring of OC and hence erroneously interpret OC as EC. Changing to a thermal-optical method would minimize this potential artefact and would help further interpretation of the sources of the carbonaceous aerosol at this site.

The relative contribution of TCM, that is the sum of organic matter (OM) and elemental matter (EM), to  $PM_{10}$  and  $PM_{2.5}$  is presented in Figure 2.20. For  $PM_{10}$ , 27% could be attributed to TCM, whereas the corresponding percentage for  $PM_{2.5}$  was 19%. As the analytical method (VDI) used leads to an erroneous separation of EC and OC, the relative contribution of TCM to  $PM_{10}$  and  $PM_{2.5}$  is underestimated. Thus, the difference between the relative contribution of the secondary inorganic constituents ( $SO_4^{2-}$ ,  $NO_3^-$ , and  $NH_4^+$ ) and TCM to  $PM_{10}$  and  $PM_{2.5}$  is somewhat less than what it should be. Figure 2.20 also shows the relative contribution of the speciated mass to  $PM_{10}$  and  $PM_{2.5}$  for 2006. With the exception of TCM in  $PM_{2.5}$ , experiencing a substantial reduction in the relative contribution from 27% in 2006 to 19% in 2007, there are no major changes observed.

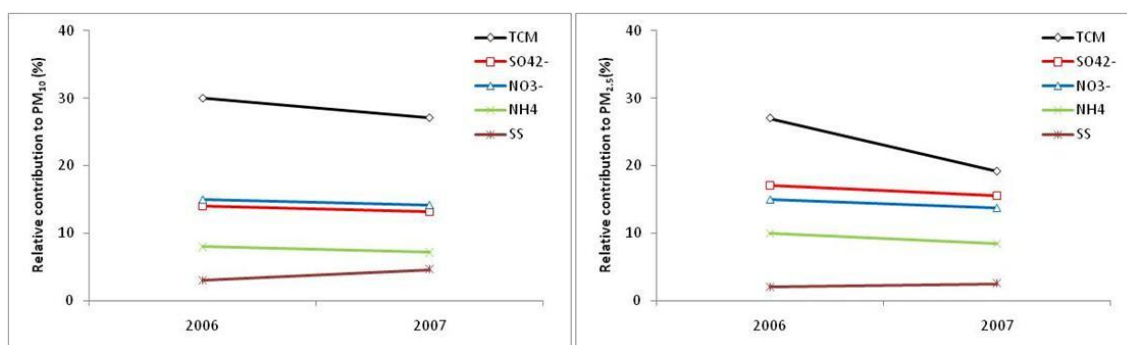


Figure 2.20: Relative contribution of TCM (Total Carbonaceous Matter = Organic matter (OM) + Elemental matter (EM)) and major inorganic constituents to  $PM_{10}$  (left) and  $PM_{2.5}$  (right) at Melpitz (DE44) for 2006 and 2007.

#### 2.4.1.4 EC and OC levels at the Spanish site Montseny (ES17)

Measurements of EC and OC at Montseny were performed on an irregular basis and are not well suited to establish annual mean concentrations or to study the seasonal variation, as the samples collected only cover 10% of the whole year.

The mean concentration of OC, EC and TC are identical for  $PM_{10}$  and  $PM_{2.5}$ , indicating that particulate carbonaceous material is associated entirely with the fine fraction of the aerosol. Hence, the correlation coefficient is high when correlating the carbonaceous material in the two size fractions, in particular for TC. The correlation between EC and OC is not particularly pronounced for either of the two size fractions, suggesting influence of various sources.

The mean concentration of TC ( $1.8 \mu\text{g m}^{-3}$ ), OC ( $1.6 \mu\text{g m}^{-3}$ ), and EC ( $0.2 \mu\text{g m}^{-3}$ ) in  $PM_{10}$  at Montseny are comparable to that reported for Scandinavian rural background sites by Yttri et al. (2007), thus the levels are amongst the lowest reported for Europe. The EC/TC ratios observed,  $11 \pm 3\%$  ( $PM_{10}$ ) and  $9 \pm 3\%$  ( $PM_{2.5}$ ), are just below that reported for the Scandinavian sites.

For Montseny there are no indication of a pronounced coarse fraction of OC as seen for the Birkenes (1.2.2) and Melpitz (1.2.4) sites. However, a more comprehensive dataset is needed for the Spanish site to conclude upon this.

#### **2.4.1.5 Concluding remarks**

There are large regional differences in the carbonaceous aerosol concentration, which call for a rapid increase in the number of sites performing measurement of this variable. Large inter-annual variations are reported for the carbonaceous aerosol, thus being one of several reasons for establishing continuous time series. The lack of a harmonized sampling- and analytical measurement protocol for the carbonaceous aerosol hampers any effort to establish a reliable picture of the regional distribution of the carbonaceous aerosol. Complementary analyses of e.g. organic tracers and  $^{14}\text{C}$ , along with AMS-measurements are necessary to reveal the sources of particulate carbonaceous matter. If we are not able to separate and understand the various anthropogenic and natural sources of the carbonaceous aerosol, effective abatement strategies for the anthropogenic part cannot be initiated.

#### **2.4.2 Improvements in modelling Secondary Organic Aerosols: Experiments with the VBS Approach**

*By David Simpson, Karl-Espen Yttri, Robert Bergström, Hugo Denier van der Gon, Svetlana Tsyro*

##### **2.4.2.1 Introduction**

The EMEP EC/OC model has previously been presented Simpson et al. (2007), in which two versions of a gas-particle scheme for secondary organic aerosol (SOA) were compared with measurements from the EMEP EC/OC campaign (Yttri et al., 2007) and the EU CARBOSOL project (Legrand and Puxbaum, 2007). The two schemes were Kam-2 from Andersson-Sköld and Simpson (2001), and a modification, Kam-2X. Additionally, we were able to compare the different components of total carbon (TC), e.g. the anthropogenic and biogenic secondary organic aerosols (ASOA, BSOA), against estimates of these compounds made by Gelencser et al. (2007). This study demonstrated that our scheme was able to predict observed levels of OC in Northern Europe quite well, but that we underestimated significantly in southern Europe. In wintertime, the underprediction was explained by problems with wood-burning emissions (possibly local). In summer the problems were shown to arise from an underprediction of the SOA components. This study also demonstrated that the model results were very sensitive to assumptions concerning the vapour pressure of the model compounds.

Problems should not be surprising. As discussed in e.g. Hallquist et al. (2009), the sources and formation mechanisms of SOA are still very uncertain, with many plausible pathways but still no reliable estimates of their relative importance. In such a situation one cannot expect a model to reliably capture measurements. Still, it is important to understand the extent to which models or parameterisations derived from smog-chambers can capture observed levels and variations in OC.

To this end, we have constructed a new version of the EMEP model, to use some of the recent ideas inherent in the so-called volatility-basis set (VBS) approach.

This chapter briefly illustrates some first results from the new model. Details will be presented in subsequent publications.

#### **2.4.2.2 *The volatility basis set (VBS) approach***

Donahue and co-workers (Donahue et al., 2006, 2009; Lane et al., 2008b; Pathak et al., 2007; Presto and Donahue, 2006, Robinson et al., 2007) have proposed the use of a volatility basis set (VBS) to help models cope with both the wide range of aerosol concentrations ( $C_{OA}$ ) in the atmosphere and the ongoing oxidation of semivolatile organics in both the gas and particle phases. The VBS consists of a group of lumped compounds with fixed saturation concentrations ( $C^*$ ,  $\mu\text{g}/\text{m}^3$ ), comprising up to 9 bins separated by one order of magnitude each in  $C^*$  at 300 K. Using the VBS, different SOA-forming reactions can be mapped onto the same set of bins over the range of organic aerosol mass concentration typical of ambient conditions ( $0.1\text{--}100 \mu\text{g}/\text{m}^3$ ) while maintaining mass balance for more volatile co-products as well. Aging reactions within the VBS can be added easily if the kinetics and volatility distribution of the products can be measured or estimated.

#### **2.4.2.3 *EC and OC emissions***

A new anthropogenic carbonaceous aerosol emission inventory for the year 2005 is made as part of the EUCAARI project (Kulmala et al., 2009) (see also Chapter 1.1). The emission inventory is based on previous particulate matter (PM) inventories, especially the PM module of the IIASA GAINS model (Klimont et al., 2002). Representative elemental carbon (EC) and organic carbon (OC) fractions are selected from the literature and applied to ~200 individual GAINS PM source categories and separated in  $< 1\mu\text{m}$ ,  $1\text{--}2.5 \mu\text{m}$  and  $2.5\text{--}10 \mu\text{m}$  size classes (Kupiainen and Klimont, 2004; 2007). The total EC and OC emission is constrained by the amount of PM emitted, which limits uncertainty. A review of activity data for residential wood combustion was made resulting in improved estimates. Another important feature of the new inventory is its improved spatial resolution of  $1/8^\circ \times 1/16^\circ$  lon-lat (or  $\sim 7 \times 7 \text{ km}$ ) compared to previous inventories. The emissions are gridded using especially prepared distribution maps. Particular attention has been given to the spatial distribution of transport emission and emission due to residential combustion. An example of the emission distribution pattern for  $\text{EC} < 1 \mu\text{m}$  is presented in Figure 2.21. In the case of  $\text{EC} < 1 \mu\text{m}$ , the emissions are dominated by transport and residential combustion (see also section 1.3) as can be seen by the highlighted urban centers, major road network and shipping tracks in Figure 2.21. Potentially, the higher resolution of the emission input will allow the model to predict sharper gradients, which should improve the model's capability to predict measured concentrations. Total carbonaceous aerosol emissions in  $\text{PM}_{2.5}$  are presented in Table 2.8. The results indicate that about half of the total  $\text{PM}_{2.5}$  emissions in Europe are carbonaceous aerosol, highlighting the importance of this fraction. Particle size distributions of EC and OC for mass show maxima in the range of 80 to 200 nm, thus being highly relevant for long range atmospheric transport. The emission inventory is described in more detail by Denier van der Gon et al. (2009).

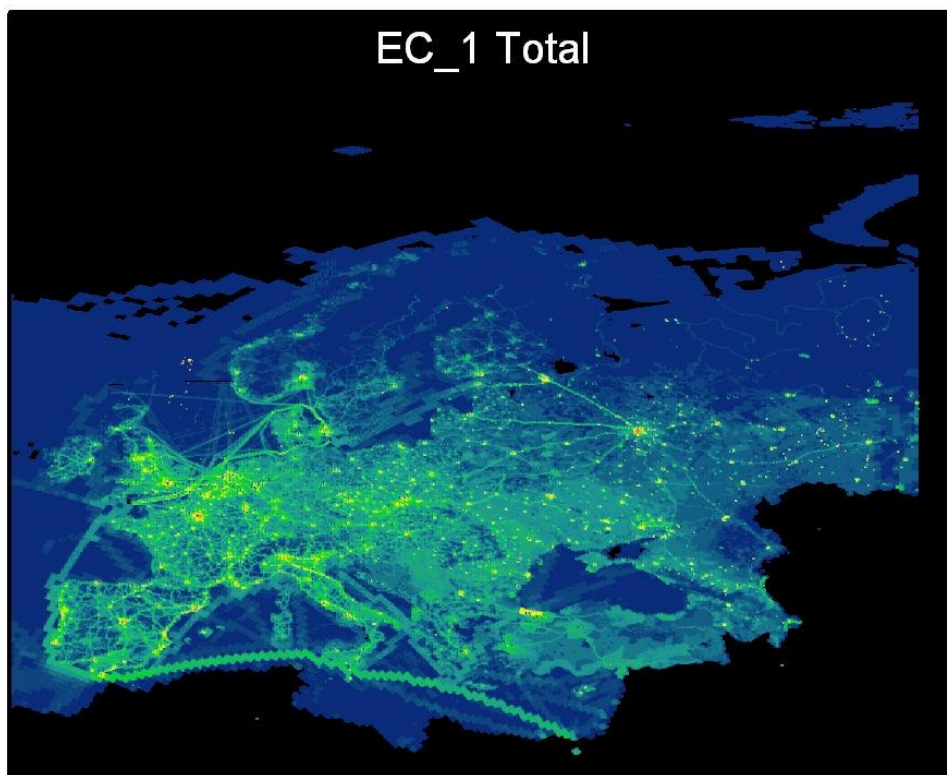


Figure 2.21: Emission intensity pattern of EC in  $PM_1$  over Europe (low to high: blue, green, yellow, orange); Source: Denier van der Gon et al., 2009.

Table 2.8: Estimated carbonaceous aerosol  $<2.5\mu m$  in UNECE Europe (ktonnes/yr) excluding international shipping.

EC $<1\mu m$	EC 1-2.5 $\mu m$	OC	Total OM <sup>a)</sup> $<2.5\mu m$	PM <sub>2.5</sub>
525	96	847	1722	3400

<sup>a)</sup> assuming Organic matter (OM) = EC + 1.3xOC

#### 2.4.2.4 EMEP-VBS OA models, and results

A number of papers have illustrated the use of VBS-based models in North America (Robinson et al., 2007; Lane et al., 2008a,b; Shrivastava et al., 2008) and we build upon this work here. Three versions of the EMEP model have been set up, introducing different aspects of the VBS approach in each version. The model versions are summarised in Table 2.9. For conciseness we will explain these versions in conjunction with a discussion of the results, shown in Figure 2.22. This figure shows the model predictions for OC, separated into components (e.g. BSOA, ASOA), as compared to the measured total from the rural site Hurdal, which lies ca. 50 km North of Oslo in southern Norway. As part of the Norwegian SORGA project, TC (split into OC, EC) was measured, at Hurdal, as well as 14C, levoglucosan, and some other tracers. A full source-apportionment of these data will be presented elsewhere (Yttri et al., article in preparation).

The first model version, VBS, uses the SOA scheme of Lane et al. (2008a), which includes SOA formation from aromatics, isoprene, and terpene species. Primary organic aerosol (POA) emissions are assumed non-volatile, taken directly from the EUCAARI emission data-set. Figure 2.22 shows that this basic-setup produces OC levels in fair agreement with the observations, but with a very high contribution of the primary fossil-fuel component.

The VBS-P (VBS+ partitioning emissions) model introduces two important changes to the treatment of emissions, following suggestions of Shrivastava et al. (2008):

- i. The emitted POA is assumed semi-volatile, and hence partitions. Essentially this allows a large fraction of the POA to evaporate.
- ii. We also assume that the POA emissions should be accompanied by emissions of low-vapour pressure (ie partitioning) gases, which are currently not captured in either the POA or the VOC inventories. Following Shrivastava et al. (2008) we assume that the total emissions of condensible material (including POA) amount to 2.5 times the POA inventory. We use the same partitioning coefficients as in Shrivastava et al. (2008) to calculate how much of this material is condensed at any moment.

*Table 2.9: Summary of EMEP VBS versions.*

Version	Emissions Partitioning?	Aging?
VBS	No	No
VBS-P	Yes	No
VBS-PA	Yes	Yes

Despite the extra emissions of condensible material in this VBS+P run, Figure 2.22 shows that the net effect is that much of the fossil-fuel associated evaporates, so that OA concentrations are much lower. This effect mimics that shown for N. America by Robinson et al. (2007). Finally, the VBS-PA run (VBS-P plus aging) introduces the concept of aging, similar to that done by Shrivastava et al. (2008). SOA compounds are allowed to react with OH, with each reaction resulting in a shift of the compound to the next lowest volatility bin. This aging reduces the volatility of the SOA mixture, and as seen in Figure 2.22 the effect is quite dramatic.

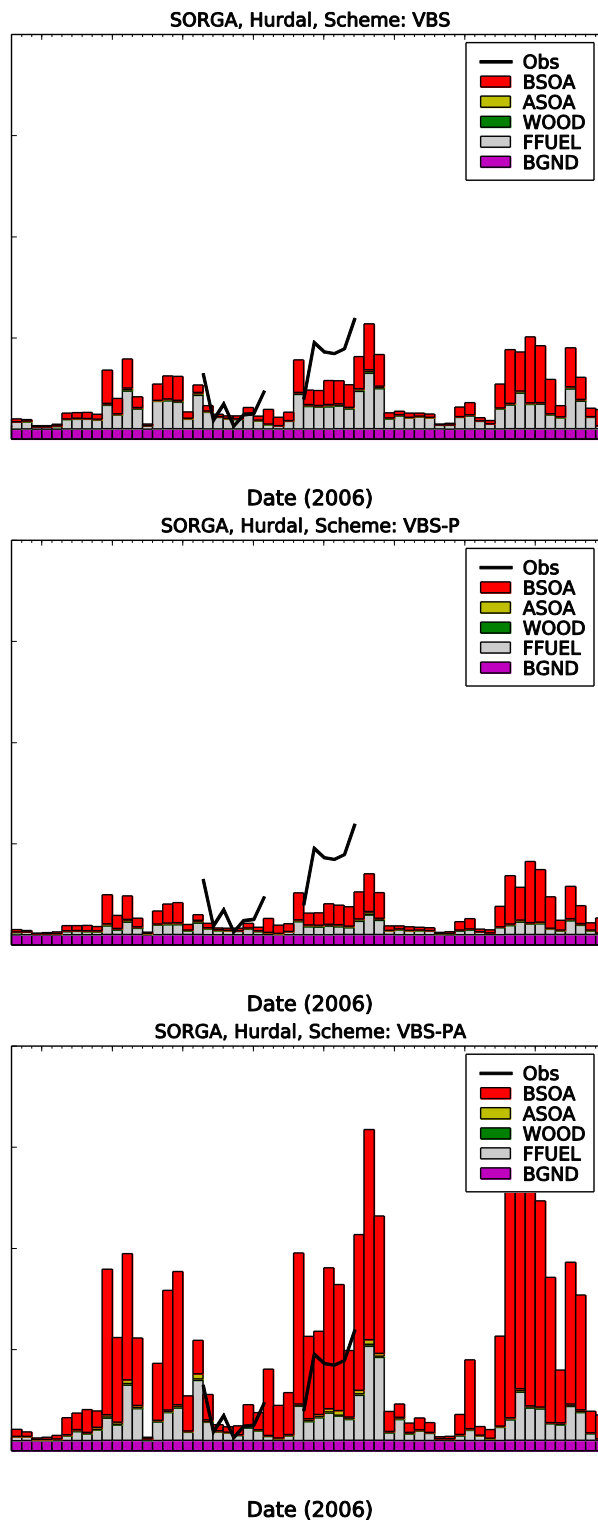


Figure 2.22: Results from EMEP model with three VBS-based SOA schemes (see text for details). Observed TC from the SORGA campaign is indicated with the black line. The modelled OC components are: ASOA, BSOA - anthropogenic and biogenic secondary organic aerosols; WOOD - OC from domestic/residential wood-burning; FFUEL - OC from fossil-fuel sources; and, BGND - background OC. Units are  $\mu\text{g(C)}/\text{m}^3$ .

#### 2.4.2.5 *Caveats, Conclusions and Future Work*

This chapter has just presented an overview of ongoing activities. All results are preliminary. The new EC/OC inventory, and the VBS methods, are in use for the first time and hence require careful checking. Moreover, since many improvements are made at the same time we also need to unravel which improvements prove critical and should be further pursued. The model still misses emissions from forest and agricultural fires, and does not include primary biological particles.

The main future plans involve work making use of new data arising from recent field experiments, which include sufficient measurements to allow source-apportionment of the aerosol. Major data-sets involve the recent EMEP intensives and data from the EU EUCAARI project (Kulmala et al., 2009). In addition, a revision of the 'Kam2(X)' gas/particle schemes is being undertaken, partly in cooperation with the EU EUROCHAMP project.

#### 2.4.2.6 *Acknowledgements*

This work presented here was funded by the EU EUCAARI project, Norwegian SORGA project, Swedish Clean Air Programme (SCARP), as well as by EMEP under UNECE.

### 2.5 **EMEP Intensive Measurement Periods**

*by Karl Espen Yttri and Wenche Aas*

The intensive measurement periods have become an important addition to the EMEP monitoring programme, both with respect to the scientific development and for capacity building; i.e. by extending the suite of measurement variables and measurement methods. The two first intensive measurement periods, conducted in June 2006 and January 2007, clearly pointed out the need for improvements for the intensive measurement periods to follow. In particular, improved harmonization of sampling and analytical methods was needed to obtain comparable datasets, e.g. by using centralized laboratories for selected variables. The quality of the reporting also needed improvement, as well as unambiguous information on data ownership. The second measurement period were conducted between 17 Sep. – 15 Oct. 2008 and 25 Feb. – 26 Mar. 2009. The measurement programme was extended compared to that of the first period both with respect to number of sites and measurement variables. The periods were chosen (i) to investigate the influence of different meteorological conditions during a time of the year where strong temperature gradients are experienced across Europe (beginning of autumn and beginning of spring), (ii) to include periods during which large parts of Europe experience high concentrations of nitrate, (iii) to maximise synergies between the EMEP intensive measurement periods and the intensive measurement year of the European Integrated Project EUCAARI (Kulmala et al., 2009). Furthermore, the measurements were coordinated with the EU funded project EUSAAR. The objectives and scope of the measurement were:

- Chemical speciation of particulate matter with respect to its inorganic, mineral and carbonaceous content with daily/weekly (EMEP) or hourly (EUCAARI) time resolution

- Gas/particle phase distribution of inorganic nitrogen constituents
- Aerosol size distribution (EUCAARI/EUSAAR)
- Separation of the carbonaceous aerosol into
  - primary vs. secondary
  - biogenic vs. anthropogenic
- Attempts to quantify the aerosol water content (EUCAARI)
- Attempts to quantify the OC/OM ratio (EUCAARI)
- Vertical profiles (coordinate with EARLINET)

A total of eighteen sites participated in the second intensive measurement period, but not all sites performed the full range of measurements (Figure 2.23). In the figure, speciation indicates which sites had chemical speciation including separation of the carbonaceous aerosols. AMS or IC intensive means two different methods for hourly time resolution. In addition, thirteen sites performed aerosol size distribution measurement, while nine addressed the aerosol water content. Information of which sites measured these two latter variables is not included in Figure 2.23, but they were in general the same as those performing hourly measurements using AMS and IC. The limitations of the dataset are mainly associated with the gas/particle phase distribution, only five sites with measurements of gas-phase precursor concentrations ( $\text{NH}_3$ ,  $\text{HNO}_3$ ,  $\text{SO}_2$ ). Furthermore, only three sites had simultaneous  $\text{NO}_3$  coarse and fine mode measurements. Only two sites (Ispra and Puy de Dôme) provided measurements of vertical profiles.

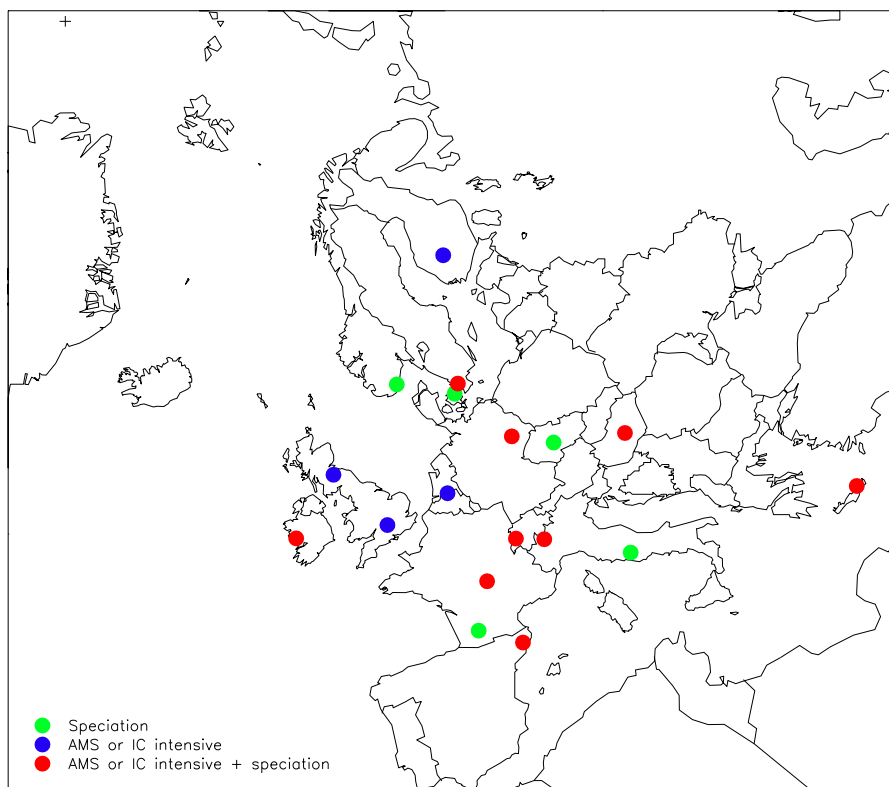


*Figure 2.23: Sites taking part in the combined EMEP, EUSAAR and EUCAARI intensive measurement period during fall 2008 and spring 2009 (AMS: Aerosol mass spectrometer; IC: Ion chromatograph).*

The final off-line analyses from the intensive measurement periods are currently being undertaken and data processing are in progress. Obviously, such an amount of high quality data requires a substantial effort with respect to interpretation and reporting in the coming months and year. The first impression is that the measurements went quite smoothly. The methodology has been well harmonized and consistent, and standardized reporting protocols for new type of measurements are being developed. The AMS dataset will actually be the largest dataset of synchronised measurements reported, which is also the case for the combined EC/OC, levoglucosan and  $^{14}\text{C}$  analysis. Given the amount of data from both the first and the second intensive measurement periods which is not yet published there will be a pause before the next one is initiated. This will also allow the conclusions from the works in progress to have an influence on our future priorities, and which will be a topic for discussion at the coming TFMM workshop.

Some preliminary results from the source apportionment study of the carbonaceous aerosol taking place during the EMEP intensive measurement period are shown in Figure 2.24. By the combined effort of  $^{14}\text{C}$ -, thermal-optical-, and organic tracer analyses, it is possible to apportion various sources contributing to the carbon content of the ambient aerosol.

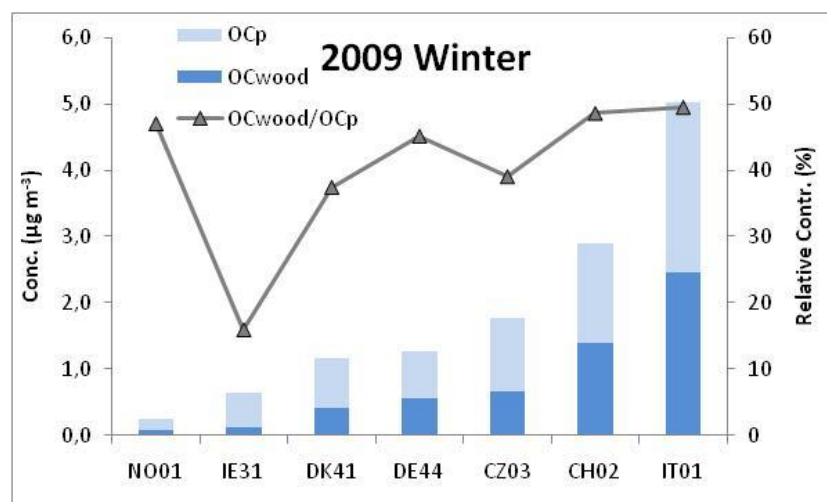


Figure 2.24: Concentrations of particulate OC ( $\text{OC}_p$ ) and OC from wood burning ( $\text{OC}_{\text{wood}}$ ), as estimated from the samples content of levoglucosan, for selected European rural background sites during the EMEP intensive measurement period in February-March 2009. The relative contribution of  $\text{OC}_{\text{wood}}$  to  $\text{OC}_p$  is also shown. (Preliminary results).

The present study benefits from centralized laboratories performing the analyses of  $^{14}\text{C}$  and the wood burning tracer levoglucosan and that harmonized sampling-(QBQ) and analytical protocol (EUSAAR-2) has been used to estimate the positive sampling artefact of OC and to quantify the filter samples content of EC, OC and TC.

The preliminary results from the February-March intensive measurement period (Figure 2.24) show that there is a substantial variation in the concentration of

particulate OC ( $OC_p$ ) amongst the various sites, ranging over one order of magnitude. The spatial variation corresponds to that reported for the EMEP EC/OC campaign conducted in 2002 and 2003 (Yttri et al., 2007). Although associated with a level of uncertainty the results indicate that wood burning emissions, as estimated from the samples content of levoglucosan, are a substantial contributor to  $OC_p$  levels at European rural background sites in winter.

When all chemical analyses are finalized, the data will be statistically treated using Latin hypercube (See Gelenscer et al., 2007) sampling to provide quantitative estimates of sources such as e.g. biogenic secondary organic aerosols (BSOA) and wood burning, which relative contribution to ambient PM is much debated. We are convinced that this data set will provide interesting results and that it will turn out to be highly valuable for validation of the ongoing SOA model development.

## 3 Aerosol optical properties and special events occurring during 2007

### 3.1 Remote sensing

*By Kerstin Stebel, Svetlana Tsyro, Aasmund Fahre Vik, Ann Mari Fjæraa, Mona Johnsrud, Thomas Holzer-Popp and Marion Schroedter-Homscheidt*

#### 3.1.1 Introduction

Since about 30 years, operational aerosol products have been generated from satellite sensors, like AVHRR onboard TIROS-N or TOMS onboard Nimbus-7, both launched in 1978. Quantities retrieved are aerosol index and aerosol optical depth (AOD). The Aerosol optical depth (AOD) is a quantitative measure of the extinction of solar radiation by aerosol scattering and absorption between the point of observation and the top of the atmosphere. It is a measure of the integrated columnar aerosol load and the single most important parameter for evaluating its impacts on the direct radiative forcing.

During the past few years the aerosol measurement capability of satellites has increased tremendously (see e.g. Kokhanovsky and de Leeuw, 2009 and references inside). Additional aerosol optical properties are now being retrieved including the Ångström coefficient (from AATSR, Veefkind et al., 1999), fine mode AOD from POLDER polarized multispectral measurements (Deuzè et al., 2001), the separation into fine and coarse mode aerosols (from MODIS, Levy et al., 2007), aerosol characterisation based on pre-defined aerosol types (using MISR, Kahn et al., 2005) and particle number concentrations (based on MERIS, von Hoyningen-Huene et al., 2003; Kokhanovsky et al., 2006). Several groups have furthermore made attempts to retrieve surface concentrations of PM<sub>2.5</sub> and PM<sub>10</sub> from satellite observations of AOD using empirical relations (e.g. Chu et al., 2003; Koelemeijer et al., 2006; Schaap et al., 2009; see also review by Hoff and Sundar (2009) and references inside). Koelemeijer et al. (2006) describe the correlation between AOD\* (= AOD divided by the boundary layer height and corrected for growth of aerosols with relative humidity) and PM<sub>10</sub> and PM<sub>2.5</sub>, using AIRBASE data from European rural and (sub) urban background stations. Nevertheless, correlations vary from site to site and season to season, therefore satellite AOD measurements can only be taken as a crude proxy for PM distributions over Europe. A more direct approach is based on the use of MERIS data utilized using Mie theory to derive PM<sub>10</sub> directly from measured spectral AOD (Kokhanovsky et al., 2006; von Hoyningen-Huene et al., 2008). Composition and size distribution of surface PM using the fractional column of AOD for different aerosol types retrieved from MISR have been retrieved by Liu et al (2007).

Another approach that has been used to extract aerosol properties (beyond AOD) is the SYNAER (SYNergetic Aerosol Retrieval product, Holzer-Popp et al., 2000, 2008) method. SYNAER data are provided through the ESA-GSE project PROMOTE II (see [www.gse-promote.org](http://www.gse-promote.org)). The SYNAER algorithm derives aerosol properties by exploiting complementary information from the Advanced Along Track Scanning Radiometer (AATSR) and the Scanning Imaging

Absorption Spectrometer for Atmospheric Cartography (SCIAMACHY), both onboard the European satellite ENVISAT (for more details see Holzer-Popp et al., 2009). Daily aerosol parameters on a  $60 \times 30 \text{ km}^2$  resolution are provided in near-real time (approximately 12 hours after acquisition) over Europe and Africa. Due to the limitations in instruments scan mode and swath width full cloud-free coverage at the equator is achieved only after 12 days. Beside AOD, aerosol composition (type of aerosols between continental, maritime, polluted, desert outbreak and biomass burning/heavily polluted air masses as mixtures of four basic aerosol components sulphate/nitrate, mineral dust, sea salt, soot) and near-surface PM concentrations ( $\text{PM}_{10}$ ,  $\text{PM}_{2.5}$  and  $\text{PM}_1$ ) are provided.

At present times, satellite data alone cannot fulfil the requirements for atmospheric composition monitoring, but ground-based stations and remote sensing instruments complement each other. Future monitoring requirements will most likely require operational use of satellite measurements. Ongoing algorithm development, the use of multiple satellite sensors (like combining aerosol height information derived from CALISPO with day- and night-time AOD retrieved from AIRS, for retrieval of aerosol dust information), upcoming satellite missions like the NASA Glory mission (to be launched in 2010, exploiting polarization and multi-angle information (see Mishchenko et al., 2007)) and dedicated space-based air-quality systems operating from geostationary (GEO) and low Earth orbit (LEO) respectively, will lead to further improvements and make remote sensing data more suitable for Air Quality purposes.

EMEP-CCC and MSC-W are seeking to incorporate space borne Earth Observation data in operational routines for assessment of air quality levels in Europe. A combined use of remote sensing and in-situ observations with modelling through data assimilation (“integrated monitoring”) might become best practice in the future.

### **3.1.2 Model calculations of AOD**

In the EMEP/CCC-Report 4/2008 results for Aerosol Optical Depth (AOD) calculated with the EMEP aerosol model was shown and compared with MODIS data for 2003 and 2004. Here, we present improved AOD calculations and comparison with MODIS Levels 2 data for 2004 and 2006 and sun photometer data for the year of 2006.

The AOD observation operator within the EMEP aerosol model has been revised. The changes made are:

- Improvement of lookup table for extinction efficiency due to using a better size resolution;
- Improvement of effective refractive index calculation for mixed aerosol using the Maxwell-Garnett (Maxwell-Garnett, 1904) and Bruggeman mixing rules (Bruggeman, 1935; Chýlek et al., 2000);
- Update of the absorption part of refractive index for mineral dust.

Model calculated AOD at  $0.55 \mu\text{m}$  has been compared with MODIS retrieved AOD from Aqua and Terra satellites. We use the daily averaged MODIS Level 2 product “Optical\_Depth\_Land\_And\_Ocean” (measurements along the satellite

track, with 10x10 km<sup>2</sup> resolution) at 0.55  $\mu\text{m}$ , which was aggregated in the EMEP grid with 50x50 km<sup>2</sup> resolution.

Table 3.1 shows that the comparison between MODIS data and AOD calculated with the most recent model version is better compared to the earlier model version. The negative bias is reduced. The correlation between calculated and MODIS AOD is better for data from 2004, while unchanged for 2006 data. On average, model calculated AOD is between 33 and 45% lower than AOD from MODIS retrievals. The spatial correlation coefficients over the model domain vary between 0.24 and 0.36 for the periods considered. Rather low spatial correlation between AOD from the model and MODIS data might be expected due to uncertainties in both model calculations and AOD retrievals (as discussed in Report 4/2008).

Table 3.2 shows the comparison statistics for AOD calculated with the revised and with the earlier version of observation operator with MODIS AOD for April-May 2006 for the model grid cells containing the EMEP measurement sites. The sites with PM<sub>2.5</sub> (or PM<sub>10</sub> given *in cursive*) observations have been selected. In addition, the comparison statistics between modelled and measured PM concentrations are provided. Grey shaded cells mark the sites where correlation between calculated and MODIS AOD is better than the correlation between calculated and measured particulate matter.

For most of the sites, a significantly better agreement has been achieved between calculated and MODIS AOD when using the revised observation operator. The revised model underestimation of AOD is significantly smaller for all sites and the temporal correlation between calculated and MODIS AOD is higher at most of the site (except CH02, ES10, ES14, FI17). The model underestimates AOD by between 0 and 67% for different sites compared to MODIS data. The temporal correlation between calculated and MODIS AOD is fairly good at most of the sites. It is even better than the correlation between calculated and measured PM<sub>2.5</sub> (or PM<sub>10</sub>) for quite a few sites (shaded grey in Table 3.2). However, it should be kept in mind that the data coverage for the considered period April-May 2006 is not necessarily the same for PM and AOD measurements. For most of the sites, fewer days with AOD data than with PM data were available. Therefore, the statistics for AOD and for PM may not always be comparable.

*Table 3.1: Bias and spatial correlation between MODIS AOD at 0.55  $\mu\text{m}$  and model AOD calculated with the revised (New) and the earlier (Old) version of the observation operator for the whole EMEP area.*

Period		New	Old
March-April 2004	Bias (%)	-33	-51
	R	0.24	0.11
July-August 2004	Bias (%)	-43	-54
	R	0.36	0.26
April-May 2006	Bias (%)	-45	-51
	R	0.34	0.34

*Table 3.2: Bias and correlation between MODIS AOD and model AOD calculated with the new and the old version of observation operator for grid cells representing some EMEP sites, where statistics for PM<sub>2.5</sub> (PM<sub>10</sub>) are also shown, for April-May 2006.*

Site	New		Old		PM <sub>2.5</sub> (PM <sub>10</sub> )	
	Bias (%)	R	Bias (%)	R	Bias (%)	R
AT02 Illmitz	-24	0.42	-34	0.22	-30	0.51
CH02 Payerne	-35	0.52	-50	0.53	-4	0.61
CZ03 Košetice	-29	0.51	-39	0.34	-48	0.54
DE01 Westerland	-28	0.45	-40	0.29	-15	0.52
DE02 Langenbrügge	-38	0.49	-50	0.27	-43	0.46
DE44 Melpitz	-49	0.74	-57	0.46	-45	0.73
ES08 Niembro	-11	0.69	-22	0.64	17	0.64
ES10 Cabo de Creus	-62	0.09	-66	0.19	-6	0.50
ES14 Els Torms	-57	0.39	-57	0.42	-4	0.52
ES16 O Saviñao	0	0.57	10	0.52	30	0.53
FI17 Virolahti	-59	0.64	-76	0.76	52	0.43
IE31 Mace Head	-43	0.59	-48	0.68	-59	0.49
IT01 Montelibretti	-32	0.43	-37	0.38	-20	0.33
IT04 Ispra	-50	0.67	-50	0.75	-18	0.24
NO01 Birkenes	-67	0.87	-75	0.80	-14	0.51
PL05 Diabla Gora	-45	0.43	-74	0.38	-55	0.47
SE11 Vavihill	-21	0.46	-42	0.30	-27	0.29
SI08 Masun	-14	0.39	-18	0.30	-20	0.37

### **3.1.3 Further testing of model AOD: Agricultural fires in spring 2006**

The EMEP model has been used to simulate pollution episodes associated with the agricultural and forest fires in Russia and Eastern Europe in spring 2006 (Stohl et al., 2007; Myhre et al., 2007). Monthly emissions of black and organic carbon have been taken from the Global Fire Emission Database (GFED2) at [www.ess.uci.edu/~jranders/](http://www.ess.uci.edu/~jranders/) (Giglio, L. et al., 2006). The monthly emissions have been distributed over the period from 15 April to 10 May based on the satellite information about the number of fires from Stohl et al. (2007). Figure 3.1 displays a series of maps, visualizing the evolution of AOD fields from MODIS retrievals and from model simulations over a two-week period (shown are daily maps for 27 and 29 April, 2, 6, 7 and 9 May 2006).

The model is doing a fairly good job reproducing the main features of AOD spatial distribution retrieved from MODIS measurements. There is quite a good resemblance between the propagation patterns of AOD associated with fires as observed by MODIS and calculated with the model. However, the model AOD due to fire emissions is generally lower than AOD from MODIS retrievals. This can possibly be explained by uncertainties in fire emission data, both in the amount of released smoke and particularly in the emission temporal variation and injection height. The uncertainty/bias of the satellite data may also be significant.

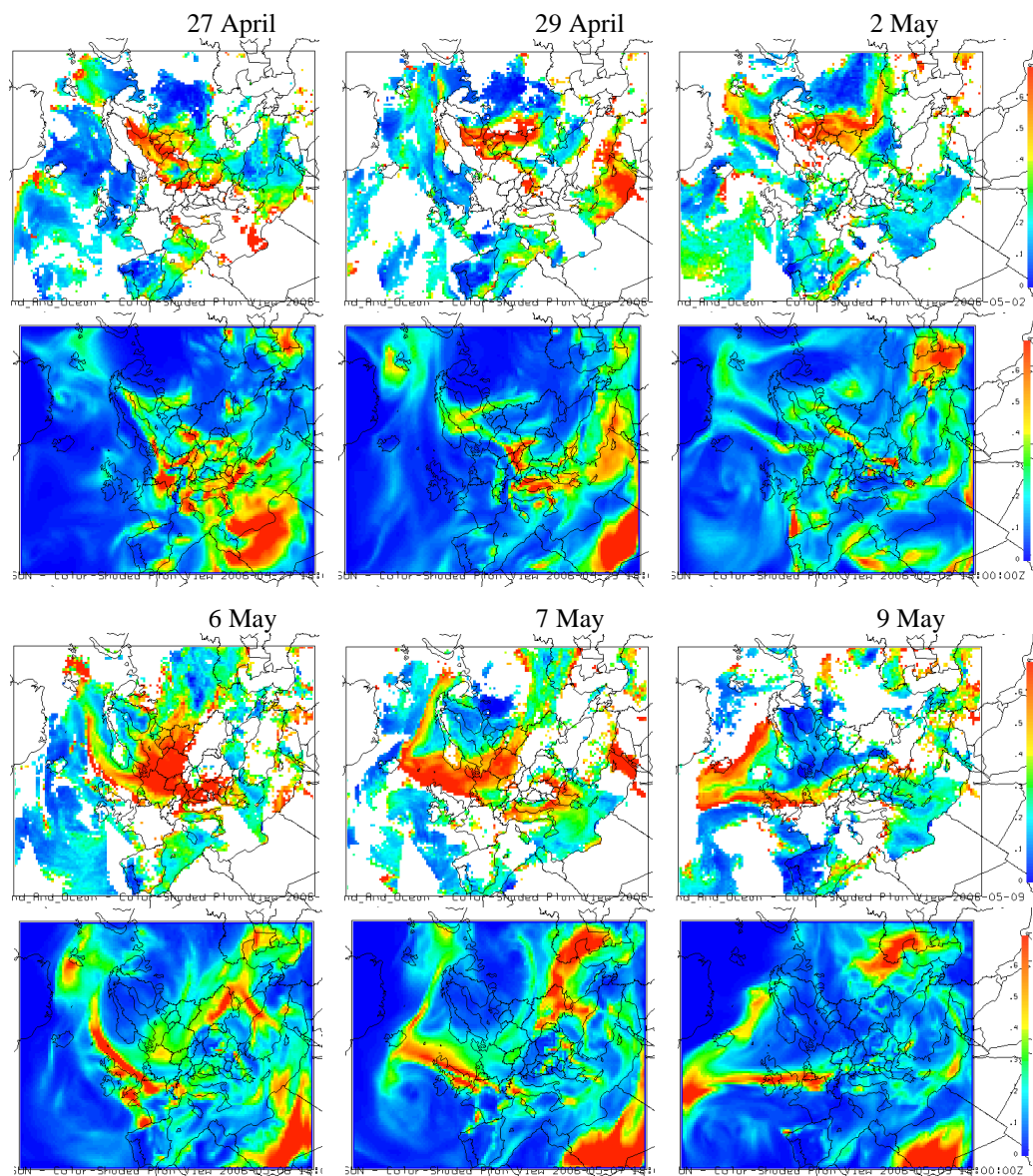


*Figure 3.1: Daily mean model calculated AOD (bottom panels) and MODIS AOD data (upper panels) at  $0.55 \mu\text{m}$  for the agricultural waste burning event in Eastern Europe in spring 2006.*

Model calculated AOD has been compared to MODIS data and AOD measured by sun photometers at several sites, which were affected by the pollution episodes associated with the agricultural and forest fires in spring 2006. Here, we show comparisons with sun-photometer measurements from the AERONET sites Minsk (Belarus) and Toravere (Estonia), and data from the GAW-PFR AOD site Sodankylä (Northern Finland) (see Myhre et al., 2007).

Figure 3.2 (left column) shows the time-series of hourly AOD calculated with the model and measured by sun photometers. Quite good correlation between modelled and measured AOD, with correlation coefficient being in a range of 0.42 to 0.87, indicates the model ability to capture pollution episodes. However, calculated AOD is significantly (by a factor 2.5-3.5) smaller than AOD measured

by sun photometers, and the underestimation is especially pronounced during the pollution episodes. This is probably because the fire emission data used in the simulations are too low. Figure 3.2 (right column) shows the time-series of modelled daily AOD compared with MODIS daily compiled AOD in the same model grid cells as for sun photometers. MODIS data coverage are quite good for Minsk and Toravere site locations, but poorer for Sodankylä for the period considered. In the model results, two calculations are displayed: with fire emissions being accounted for (red curve) and disregarded (blue curve). These results show the large enhancement of AOD values due to the fire smoke in several episodes between 24 April and 6 May.

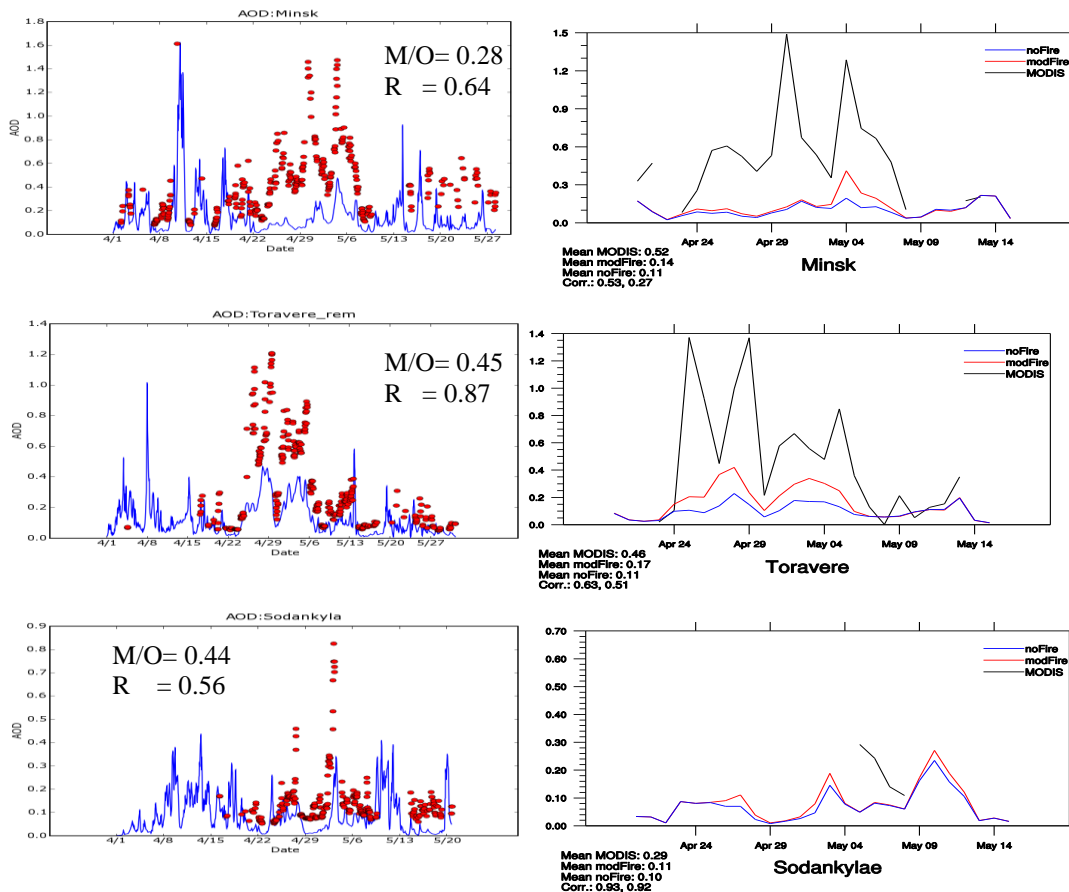


Figure 3.2: Time-series of: hourly modelled (blue) and sun photometer measured (red dots) AOD (left column) and daily modelled (red and blue) and MODIS (black) AOD for Minsk, Toravere and Sodankylä. Here,  $M$  – model,  $O$  – observations,  $R$  – correlation coefficient.

On average, the model underestimates MODIS AOD by a factor of 2.5-3.5, which is of the same order as the model underestimation of sun photometer AOD. The time-series show that the largest model underestimation of MODIS AOD occurs during the periods with enhanced AOD, i.e. when the site is affected by the fire pollution. Thus, there is a convincing indication that the emission estimates from fires are probably too low. The correlation between calculated and MODIS AOD is reasonably good, between 0.42 and 0.63, being slightly worse compared to sun photometers.

### 3.1.4 SYNAER measurements of Particulate Matter

SYNAER data have been provided through the ESA-GSE project PROMOTE II (see [www.gse-promote.org](http://www.gse-promote.org)). The improvements made for the version SYNAER/ENV v2.0 and first validation are documented in detail in Holzer-Popp et al. (2008). For more details on the data product see Holzer-Popp et al. (2009).

So far, we have evaluated several versions of the SYNAER data product (v0.9, v1.0, v1.8, v2.01, see e.g. EMEP/CCC-Report 4/2008 for evaluation of v2.01). Here, we show few examples from utilizing recent data (v2.2), which became available in May 2009. The data have been improved for high and low AOD and aerosol type selection.

In Figure 3.3 monthly averaged  $PM_{10}$  values from EMEP (left panel), SYNAER version 1.0 (middle panel) and SYNAER version 2.2 (right panel) for June 2006 are shown. One has to keep in mind that due to the low temporal coverage of the satellite sensors, the averages shown in 6.3 are not ‘real’ monthly averages, but more a collection of individual episodes. The data shown in Figure 3.3 clearly illustrate the improvements made between the early and the most recent data versions. For the latter, the number of retrieved pixels is higher and the qualitative comparison of the  $PM_{10}$  data seems much more satisfactory. The SYNAER v.2.2 data resemble typical patterns, e.g. the low PM values over Scandinavia while increased PM is seen in South England, Spain and Belgium/the Netherlands. The monthly mean concentrations of the SYNAER data are comparable to the in-situ observations. The main disadvantage of SYNAER is obviously the low spatial and temporal resolution and data coverage. A transfer of the SYNAER retrieval method to GOME-2/AVHRR on METOP and future geo-stationary missions will improve this shortcoming.

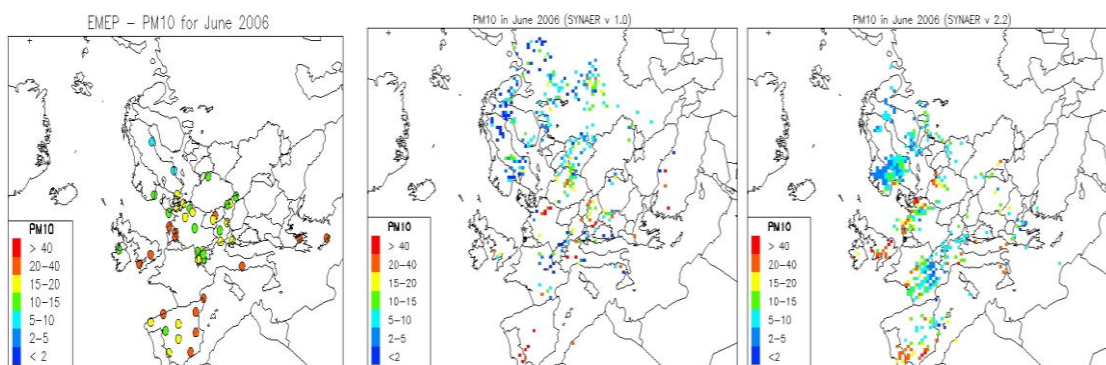


Figure 3.3: Monthly averaged  $PM_{10}$  values from EMEP (left panel), SYNAER  $PM_{10}$  version 1.0 (middle panel) and SYNAER version 2.2 (right panel) for June 2006 [in  $\mu\text{g m}^{-3}$ ]. SYNAER data are shown as averages when more than five centers of SYNAER pixels were found within a  $50 \times 50 \text{ km}^2$  EMEP grid-cell.

We use daily PM values from EMEP to compare with daily averaged co-located SYNAER data. The maximum allowed cloud-cover within the SYNAER pixel has been set to 35%. Only data with a spectral error below 0.02, AOD error below 0.14 (at 550 nm) and the land surface albedo below 25 (at 670 nm), have been

taken into account. As spatial co-location criteria, 1° spatial distance and data from the same day have been chosen. First validation results are summarized in Table 3.3.

*Table 3.3: First validation results of SYNAER vers.2.2 PM<sub>2.5</sub> and PM<sub>10</sub> using daily EMEP PM for comparison. As spatial co-location criteria, 1° spatial distance and data from the same day have been chosen.*

### PM<sub>10</sub>

significant (P < 0.05) and positive correlation at 22 from 49 stations

Station	R	Bias	N_SYNAER
ES0016R	0.79	-45	73
ES0017R	0.69	-19	11
FI0017R	0.68	-19	128
PL0005R	0.53	-26	166
GB0006R	0.53	51	41
DE0001R	0.51	-3	74
CH0004R	0.49	-56	96
NO0001R	0.47	-16	96
NL0009R	0.47	-23	91
GB0043R	0.43	44	64
SE0012R	0.41	-5	98
GB0036R	0.40	-6	126
CH0002R	0.39	-65	92
ES0012R	0.32	-23	200
AT0048R	0.29	-57	87
AT0002R	0.27	-51	135
SE0035R	0.27	-12	82
ES0013R	0.25	-4	149
SI0008R	0.21	-45	162
DE0008R	0.21	-28	119
ES0014R	0.19	-24	138
ES0011R	0.14	49	280

### PM<sub>2.5</sub>

significant (P < 0.05) and positive correlation at 17 from 29 stations

Station	R	Bias	N_SYNAER
ES0016R	0.773	-42.4	73
DE0007R	0.765	31	21
FI0017R	0.726	-35.1	73
SE0012R	0.46	-35.5	49
NO0001R	0.436	-3.7	96
GB0036R	0.435	33.7	126
IE0031R	0.42	47.4	51
ES0012R	0.354	-12.2	192
IT0004R	0.346	-19.8	139
CH0002R	0.333	-55.8	92
CH0004R	0.315	-46.6	96
AT0002R	0.314	-48.9	135
ES0011R	0.286	118.2	317
SE0011R	0.269	37	55
ES0014R	0.203	22.3	119
ES0010R	0.182	3.7	155
ES0007R	0.147	74	280

For several EMEP sites the data compare rather well (for PM<sub>10</sub> 22 out of 49 sites show significant correlation; for PM<sub>2.5</sub> correlations can be found for 17 out of 29 data sets), but there is a profound lack of correlation at other sites. The reason for the apparent bias and the correlation/lack of correlation is still under investigation. In general, the network wide correlation between SYNAER and EMEP PM seems to be better for PM<sub>2.5</sub> than PM<sub>10</sub>, with positive correlation at 68% for some of the sites. At a majority of EMEP sites SYNAER shows a negative bias for PM<sub>10</sub> while for PM<sub>2.5</sub> the bias is positive/negative for about half the sites each.

As examples for sites showing reasonable good agreements between SYNAER and ground-based observations, time-series of daily PM<sub>2.5</sub> values for Birkenes (NO01R) and O-Saviñoa (ES016R) are shown in Figure 3.4. EMEP data are shown in magenta, overlaid are the individual co-located satellite PM<sub>2.5</sub> (measured at the same day and within 1 degrees distance from the EMEP site) and the daily mean satellite PM<sub>2.5</sub> (in blue). It can be seen that co-located satellite overpasses mainly are from the summer months. SYNAER PM<sub>2.5</sub> values are slightly lower than ground-based PM<sub>2.5</sub> values. The correlation for the two sites shown in Figure 3.4 have been improved, compared to the results reported in EMEP/CCC-Report 4/2008, where data from version v2.01 within 2 degrees distance and

slightly different rejection criteria (e.g. cloud cover less than 0.2) have been used. For Birkenes (NO001) we calculate a  $PM_{10}$  correlation of 0.47 (prev. negative) and a bias of -16% (prev. +88%),  $PM_{2.5}$  correlation of 0.43 (prev. negative) and a bias of -3.7% (prev. +2%). For O-Saviñoa (ES016R), the actual  $PM_{10}$  correlation is 0.79 (prev. 0.25) and a bias of -16% (prev. 23%),  $PM_{2.5}$  correlation of 0.43 (prev. 0.18) and a bias of -42% (prev. -47%). Note that the same satellite raw data were used for SYNAER v2.01 and v2.2 in this comparison.

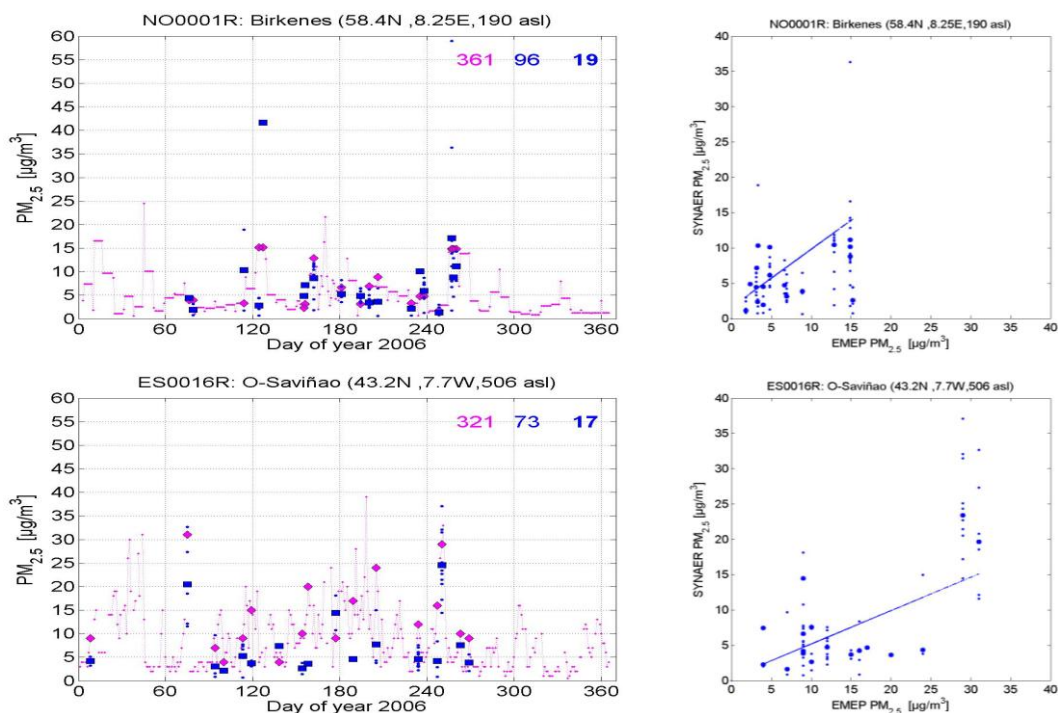


Figure 3.4: Left panel: Time-series of daily  $PM_{2.5}$  values for Birkenes (NO01) and O-Saviñoa (ES016R), in 2006 (in magenta). Overlaid are  $PM_{2.5}$  values measured at co-located SYNAER pixels (in blue). Daily mean satellite  $PM_{2.5}$  data are shown as larger bold blue symbols. The corresponding EMEP data are also marked in bold (magenta). The three numbers give the number of total EMEP data (magenta), the number of co-located SYNAER data and the number of days with co-locations (both in blue). Right panel: Correlation between data shown in left panel – numbers are presented in text above.

The results shown above are very promising, but also produce many new questions, like how does the station representativeness affect the correlation/bias and how representative is a satellite pixel for a region/site. The overall quality of the SYNAER PM products seems improved, but to fully understand the observed bias and correlation/lack of correlation at particular sites, further studies have to be performed. From a refinement of the 'validation' approach, e.g. using 1 hour averaged data from EMEP and several years of SYNAER data to estimate product stability we expect to get additional answers.

**Acknowledgements.** This work was supported by the Norwegian Space Centre/ESA through the project “AeroKval”, “SatLuft” and the ESA-GSE project PROMOTE. MODIS data are obtained courtesy from Langley Research Centre, NASA.

### 3.2 Special events in 2007

by Svetlana Tsyro and Wenche Aas

#### 3.2.1 Wild fires in Greece

Throughout the summer of 2007 there were a series of massive forest fires on the Greek mainland. The most severe episode started on August 2 and expanded rapidly till August 27, and was not extinguished until early September. A MODIS picture of this fire taken on the 26 of August can be seen in Figure 3.6. The fires mainly affected western and southern Peloponnese, but also influenced more distant parts of the Mediterranean region. Unfortunately, PM measurements at the Greek sites GR01 and GR02 were both out of operation (or data has not been reported) for major part of August and September 2007. No influence of the forest fires was observed at the Cypriote site, as the predominant wind direct during this period was westerly. Neither was there observed increased concentrations at the Italian sites, caused by the fire. In Spain on the other hand, there is a significant signal at all the east coast sites, as illustrated in Figure 3.6. The back trajectories (here illustrated for Viznar) suggest that the increased levels are influenced by the forest fires in Greece. However, the air masses influencing Viznar had also passed over Northern Africa, causing high levels of Saharan dust, making it difficult to distinguish between the relative source strength.

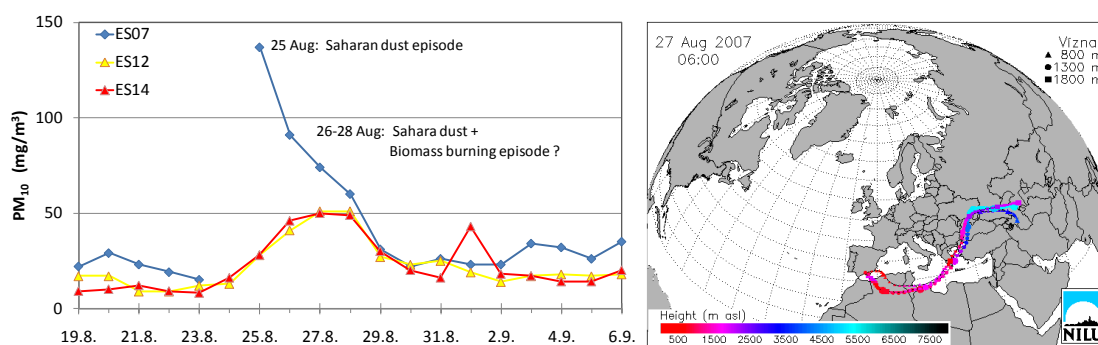


Figure 3.5: Concentrations of PM<sub>10</sub> at the three Spanish sites ES07, ES12 and ES14 during the period 19.08 – 06.09.2007, and back trajectory for 27 august for the Viznar (ES07) site.

When comparing the observed concentrations with that provided by the model, the model reproduces the temporal trend quite well (Figure 3.7). The model clearly demonstrates the influence of the mineral dust to the PM loading but since no data on fire emissions for 2007 were available the model cannot support the influence of the Greek forest fires suggested when combining the observed concentrations with the backward trajectories. Chemical speciation of the PM is not available, which otherwise could have contributed to distinguish between the various sources. The importance of including emissions from forest fires and agricultural biomass burning in the EMEP model calculations is nicely illustrated by this episode, and would greatly facilitate the analysis of observed PM pollution episodes, whether the source is known, unknown, or of mixed origin.



Figure 3.6: MODIS picture 26/8-2007.

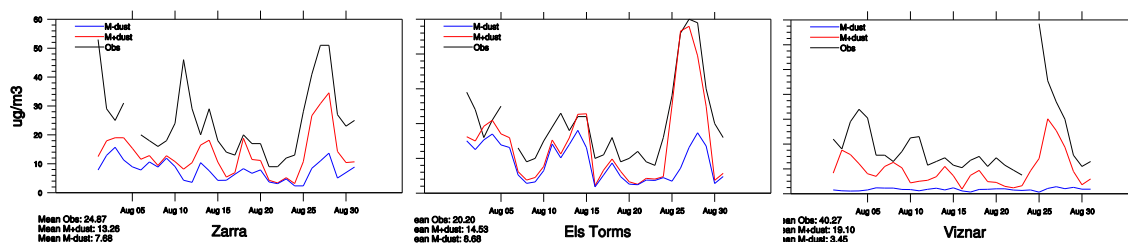


Figure 3.7:  $PM_{10}$  concentrations in august 2007 at Zarra (ES12), Els Torms (ES14) and Viznar (ES07). Observed concentrations are shown in black lines, modelled concentrations including mineral dust are the red lines, whereas the blue lines do not include mineral dust.

### 3.2.2 Dust episode in Ukraine observed across Europe

In the end of March 2007 a substantial dust plume was observed over central Europe (Birmili et al., 2008; Bessanget et al., 2008). The source of the plume was identified by satellite observation to be dust from southern Ukraine, where a severe dust storm broke out on the 23 March. In Germany, chemical speciation suggested that 75% of the daily mean concentration of  $PM_{10}$  could be attributed to mineral dust, whereas the corresponding percentage for the coarse fraction of  $PM_{10}$  ( $PM_{10-2.5}$ ) was 85% (Birmili et al, 2008). In the study presented by Birmili et al. (2008) the episode was identified in several central European countries including Slovakia, the Czech Republic, Poland, and Germany. The episode was further identified in UK (AEA, 2008), where high  $PM_{10}$  concentrations were observed at several of the rural as well as the urban sites. Twenty one of the sites in UK Automatic Urban and Rural monitoring network (AURN) had a record high pollution level. AEA (2008) identified the cause to likely have been agricultural fires in the Ukraine and western Russia. Calculations of erosion dust emissions in

Ukraine and its contribution to the enhanced PM<sub>10</sub> episodes in Central Europe was performed with the CHIMERE model (Bessanget et al., 2008).

The EMEP network is ideal for identifying and studying this type of cross European pollution events. Observational data from several sites have been compared to the EMEP model for the actual period. Combined analysis of the time-series of observed and modelled (including and excluding windblown dust) PM<sub>10</sub> concentrations show clear signals of a dust pollution episode on the 24-25 March at several German sites, at Kollumerwaard (the Netherlands), and at Aspvreten (Sweden), at UK sites on the 25-26 March, and at the Slovenian site Iskrba on the 26-27 March (see Figure 3.8). The series of maps in Figure 3.9 displays the propagation of the dust cloud during the period from 23-26 March 2007, as calculated by the EMEP model. In these maps, it is rather difficult to distinguish between the dust generated in Ukraine and the dust plume originating from Central Asia. Thus, the dust episodes seen in the time-series are apparently a combination of the two.

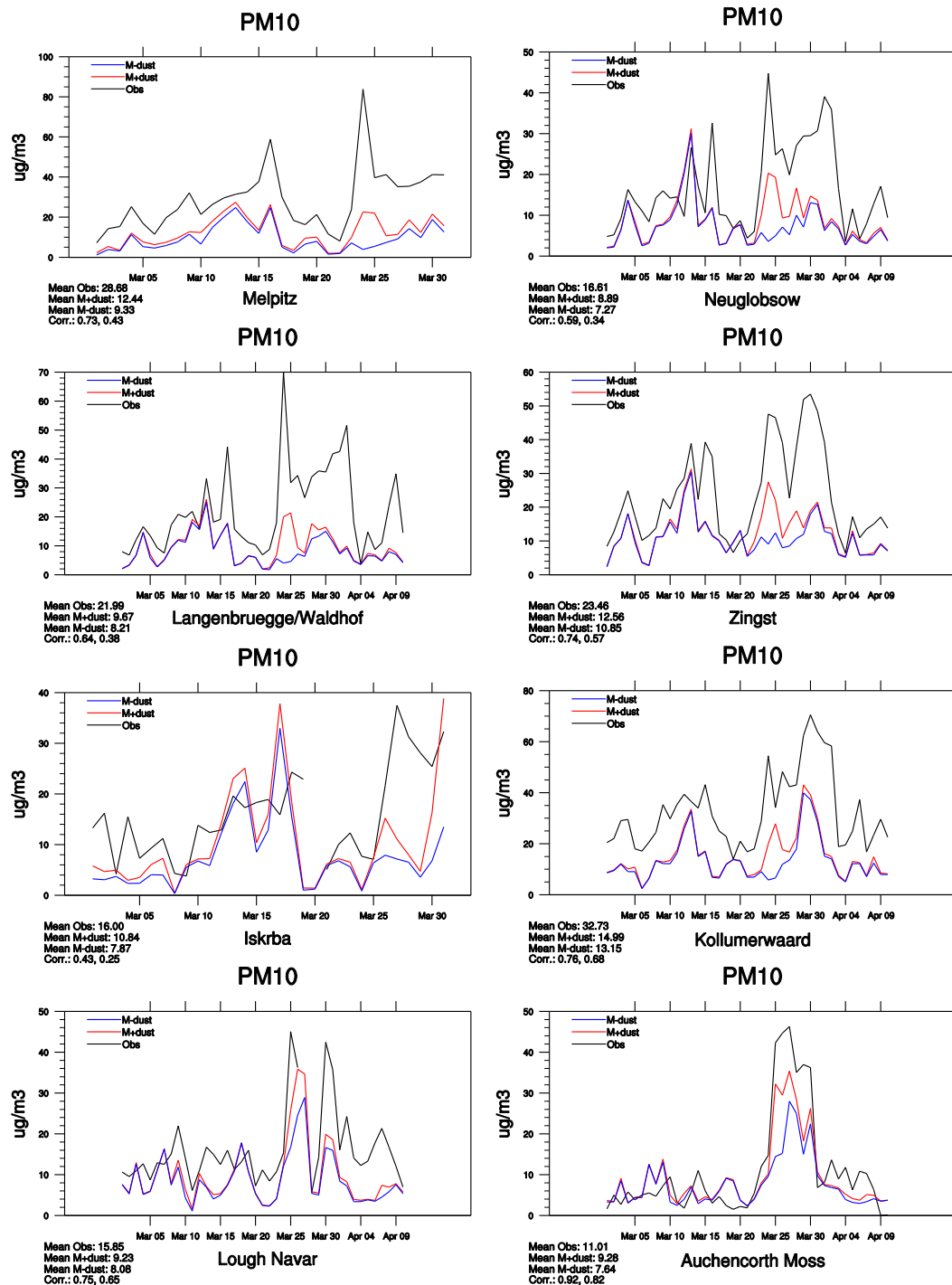


Figure 3.8:  $PM_{10}$  concentrations in March 2007 at Melpitz (DE44), Neuglobsow (DE07), Langenbruegge (DE02), Zingst (DE09), Kollumerwaard (NL09), Iskrba (SI08), Lough Navar (GB06), and Auchencorth Moss (GB48). Observations are shown in black lines, whereas model calculations including mineral dust is red and without dust is blue.

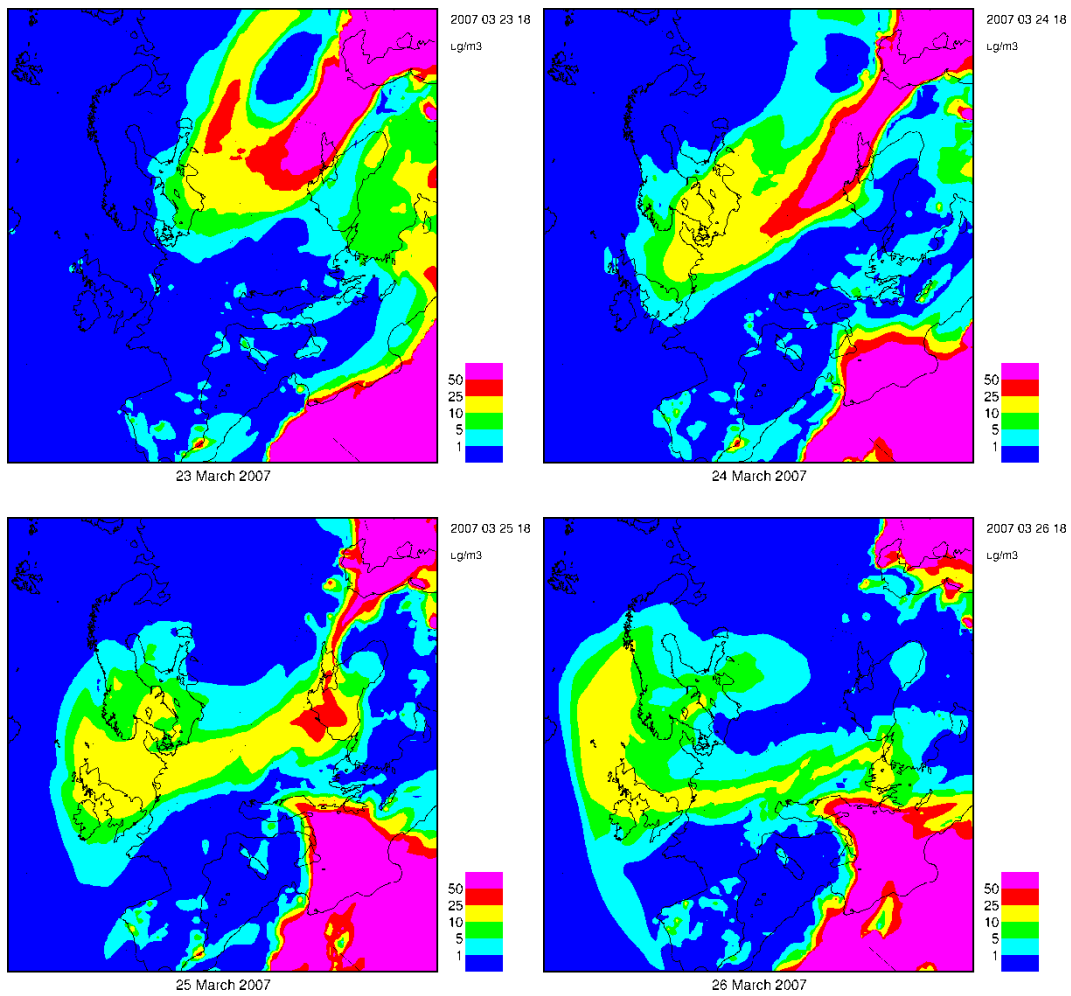


Figure 3.9: Model calculated maps of windblown dust concentrations during the period 23 to 26 March 2007.

## 4 References

- AEA (2008) UK Air Quality Forecasting: A UK particulate episode from 24<sup>th</sup> March to 2<sup>nd</sup> April 2007. Didcot (AEAT/ENV/R/2566 Issue 1, January 2008).  
URL: [http://www.airquality.co.uk/reports/cat12/0802071455\\_AQF\\_Partepi0307-final\\_final.pdf](http://www.airquality.co.uk/reports/cat12/0802071455_AQF_Partepi0307-final_final.pdf).
- Amann, M., Asman, W., Bertok, I., Cofala, J., Heyes, C., Klimont, Z., Posch, M., Schöpp, W. and Wagner, F. (2006) Emission control scenarios that meet the environmental objectives of the Thematic Strategy on Air Pollution. Laxenburg, International Institute for Applied Systems Analysis (IIASA) (NEC Scenario Analysis Report Nr. 2).  
URL: <http://www.iiasa.ac.at/rains/reports/NEC2-final.pdf>.
- Amann, M., Bertok, I., Cofala, J., Heyes, C., Klimont, Z., Rafaj, P., Schöpp, W. and Wagner, F. (2008) National emission ceilings for 2020 based on the 2008 Climate & Energy Package. Laxenburg, IIASA (NEC Scenario Analysis Report Nr. 6).  
URL: <http://www.iiasa.ac.at/rains/reports/NEC6-final110708.pdf>.
- Andersson-Sköld, Y. and Simpson, D. (2001) Secondary organic aerosol formation in Northern Europe: a model study. *J. Geophys. Res.*, 106D, 7357–7374.
- Bessagnet B., Menut, L., Aymoz, G., Chepfer, H. and Vautard, R. (2008) Modelling dust emissions and transport within Europe: the Ukraine March 2007 event. *J. Geophys. Res.-Atmospheres*, 113, D15202, doi:10.1029/2007JD009541.
- Birmili, W., Schepanski, K., Ansmann, A., Spindler, G., Tegen, I., Wehner, B., Nowak, A., Reimer, E., Mattis, I., Müller, K., Brüggemann, E., Gnauk, T., Herrmann, H., Wiedensohler, A., Althausen, D., Schladitz, A., Tuch, T. and Löschau, G. (2008) A case of extreme particulate matter concentrations over Central Europe caused by dust emitted over the southern Ukraine. *Atmos. Chem. Phys.*, 8, 997-1016.
- Bruggeman. D.A.G. (1935) Berechnung verschiedener physikalischer Konstanten von heterogenen Substanzen. 1. Dielektrizitätskonstanten und Leitfähigkeiten der Mischkörper aus isotropen Substanzen. *Ann. Phys.*, 24, 636-664.
- Chu, D.A., Kaufman, Y.J., Zibordi, G., Chern, J.D., Mao, J., Li, C. and Holben, B.N. (2003) Global monitoring of air pollution over land from the Earth Observing System-Terra Moderate Resolution Imaging Spectroradiometer (MODIS). *J. Geophys. Res.*, 108D, 4661, doi: 10.1029/2002JD003179.
- Chýlek, P., Videen, G., Geldart, D.J.W., Steven Dobbie, J. and Tso, H.C.W. (2000) Effective medium approximations for heterogeneous particles. In: *Light scattering by nonspherical particles*. Ed. by M.I. Mishchenko, J.W. Hovenier and L.D. Travis. San Diego, Academic Press. pp. 274-308

- Denier van der Gon, H.A.C., Visschedijk, A.J.H., Dröge, R., Mulder, M., Johansson, C. and Klimont, Z. (2009) A high resolution emission inventory of particulate elemental carbon and organic carbon for Europe in 2005. 7<sup>th</sup> International Conference on Air Quality – Science and Application. Istanbul, Turkey.
- Deuzé, J.-L., Bréon, F.-M., Devaux, C., Goloub, P., Herman, M., Lafrance, B., Maignan, F., Marchand, A., Nadaf, L., Perry, G. and Tanré, D. (2001) Remote sensing of aerosols over land surfaces from POLDER-ADEOS 1 Polarized measurements, *J. Geophys. Res.*, *106D*, 4913-4926.
- Donahue, N.M., Robinson, A.L. and Pandis, S.N. (2009) Atmospheric organic particulate matter: From smoke to secondary organic aerosol. *Atmos. Environ.*, *43(1)*, 94 – 106.
- Donahue, N.M., Robinson, A.L., Stanier, C.O. and Pandis, S.N. (2006) Coupled partitioning, dilution, and chemical aging of semivolatile organics. *Environ. Sci. Technol.*, *40(8)*, 2635–2643.
- EEA/CEIP (2008) Mareckova K., R.Wankmueller, M.Wiesser, S.Poupa, B.Muik, M.Anderl. Inventory review 2008 stage 1 and 2 and Gridded data. Vienna, EEA/CEIP. URL: <http://www.ceip.at/review-process/review-2008/>.
- EEA/CEIP (2009) Mareckova K., R.Wankmueller, M.Wiesser, S.Poupa, B.Muik, M.Anderl. Inventory review 2009 stage 1 and 2 and Gridded data and LPS data. Vienna, EEA/CEIP. URL: <http://www.ceip.at/review-process/review-2009/>.
- Elvidge, C.D., Baugh, K.E., Tuttle, B.T., Howard, A.T., Pack, D.W., Milesi, C. and Erwin, E.H. (2007) A twelve year record of national and global gas flaring volumes estimated using satellite data: final report to the World Bank. Boulder, NOAA National Geophysical Data Center. URL: [http://www.ngdc.noaa.gov/dmsp/interest/DMSP\\_flares\\_20070530\\_b.pdf](http://www.ngdc.noaa.gov/dmsp/interest/DMSP_flares_20070530_b.pdf)
- EMEP (2004) An initial outlook into the future development of fine particulate matter in Europe. In: *Transboundary particulate matter in Europe*. Ed. by K. Tørseth. Kjeller, Norwegian Institute for Air Research (EMEP Report 4/2004).
- EMEP (2008a) Transboundary particulate matter in Europe. EMEP status report 4/2008. Kjeller, Norwegian Institute for Air Research (EMEP Report 4/2008).
- EMEP (2008b) Transboundary acidification, eutrophication and ground level ozone in Europe in 2006. EMEP status report 2008. Ed. by L. Tarrasón, and Á, Nyíri. Oslo, Norwegian Meteorological Institute (EMEP Report 1/2008).
- EMEP (2009) Transboundary acidification, eutrophication and ground level ozone in Europe in 2007. Oslo, Norwegian Meteorological Institute (EMEP Status Report 1/2009).
- EMEP/EEA (2009) EMEP/CORINAIR emission inventory guidebook — 2009. TFEIP-endorsed draft. (EEA technical report). Available at: <http://www.eea.europa.eu/publications/emep-eea-emission-inventory-guidebook-2009>.

- Gelencsér, A., May, B., Simpson, D., S´anchez-Ochoa, A., Kasper-Giebl, A., Puxbaum, H., Caseiro, A., Pio, C. and Legrand, M. (2007) Source apportionment of PM<sub>2.5</sub> organic aerosol over Europe: primary/secondary, natural/anthropogenic, fossil/biogenic origin. *J. Geophys. Res.*, *112*, D23S04, doi:10.1029/2006JD008094.
- Giglio, L., van der Werf, G.R., Randerson, J.T., Collatz, G.J. and Kasibhatla, P. (2006) Global estimation of burned area using MODIS active fire observations. *Atmos. Chem. Phys.*, *6*, 957-974.
- Hallquist, M., Wenger, J.C., Baltensperger, U., Rudich, Y., Simpson, D., Claeys, M., Dommen, J., Donahue, N.M., George, C., Goldstein, A.H., Hamilton, J.F., Herrmann, H., Hoffmann, T., Iinuma, Y., Jang, M., Jenkin, M.E., Jimenez, J.L., Kiendler-Scharr, A., Maenhaut, W., McFiggans, G., Mentel, Th. F., Monod, A., Prévôt, A.S.H., Seinfeld, J.H., Surratt, J.D., Szmigielski, R., and Wildt, J. (2009) The formation, properties and impact of secondary organic aerosol: current and emerging issues. *Atmos. Chem. Phys.*, *9*, 5155-5235.
- Hjellbrekke, A.-G. and Fjæraa, A.M. (2009) Data report 2007. Acidifying and eutrophying compounds. Kjeller, Norwegian Institute for Air Research (EMEP/CCC-Report 1/2009).
- Hoff, R. and Christopher, S. (2009) Critical review: Remote sensing of particulate pollution from space: Have we reached the promised land? *J. Air Waste Manage. Assoc.*, *59*, 645-675.
- Holzer-Popp, T., Schroedter, M. and Gesell, G. (2000) High resolution aerosol maps exploiting the synergy of ATSR-2 and GOME. *Earth Obs. Q.*, *65*, 19-24.
- Holzer-Popp, T., Schroedter-Homscheidt, M., Breitkreuz, H.-K., Martynenko, D. and Klüser, L. (2009) Benefits and limitations of the synergistic aerosol retrieval SYNAER (2009). In: *Satellite Aerosol Remote Sensing Over Land*. Ed. by A.A. Kokhanovsky and G. de Leeuw. UK, Springer, Praxis Publishing.
- Holzer-Popp, T., Schroedter-Homscheidt, M., Breitkreuz, H., Martynenko, D. and Klüser, L. (2008) Synergetic aerosol retrieval from SCIAMACHY and AATSR onboard ENVISAT. *Atmos. Chem. Phys.*, *8*, 7651-7672.
- Kahn, R.A., Gaitley, B.J. and Martonchik, J.V. (2005) Multiangle Imaging Spectroradiometer (MISR) global aerosol optical depth validation based on 2 years of coincident Aerosol Robotic Network (AERONET) observations. *J. Geophys. Res.*, *110*, D10S04, doi: 10.1029/2004JD004706.
- Kiss, G., Varga, B., Galambos, I. and Ganszky, I. (2002) Characterization of water-soluble organic matter isolated from atmospheric fine aerosol. *J. Geophys. Res.*, *107D*, 8339, doi: 10.1029/2001JD000603.
- Klimont, Z. and Kupiainen, K. (2009, in prep.) Future of BC and OC emissions in Europe.
- Klimont, Z., Cofala, J., Bertok, I., Amann, M., Heyes, C., Gyarmas, F. (2002) Modelling particulate emissions in Europe a framework to estimate reduction potential and control costs. Laxenburg, IIASA (Interim Report IR-02-076).

- Koelemeijer, R.B.A., Homan, C.D. and Matthijsen, J. (2006) Comparison of spatial and temporal variations of aerosol optical thickness and particulate matter over Europe. *Atmos. Environ.*, *40*, 5304-5315.
- Kokhanovsky, A.A. and de Leeuw, G., eds. (2009) Satellite aerosol remote sensing over land. Berlin/Chichester, Springer-Praxis Publishing.
- Kokhanovsky, A.A., von Hoyningen-Huene, W. and Burrows, J.P. (2006) Atmospheric aerosol load as derived from space. *Atmos. Res.*, *81*, 176-185.
- Kulmala, M., Asmi, A., Lappalainen, H.K., Carslaw, K.S., Poschl, U., Baltensperger, U., Hov, Ø., Brenquier, J.-L., Pandis, S.N., Facchini, M.C., Hansson, H.-C., Wiedensohler, A. and O'Dowd, C.D. (2009) Introduction: European integrated project on aerosol cloud climate and air quality interactions (EUCAARI) – integrating aerosol research from nano to global scales. *Atmos. Chem. Phys.*, *9*, 2825–2841.
- Kupiainen, K. and Klimont, Z. (2004) Primary emissions of submicron and carbonaceous particles in Europe and the potential for their control. Laxenburg, International Institute for Applied Systems Analysis (IIASA) (IR-04-79).
- Kupiainen, K. and Klimont, Z. (2007) Primary emissions of fine carbonaceous particles in Europe. *Atmos. Environ.*, *41*, 2156-2170.
- Lane, T.E., Donahue, N.M. and Pandis, S.N. (2008a) Effect of NO<sub>x</sub> on secondary organic aerosol concentrations. *Environ. Sci. Technol.*, *42*, 6022–6027.
- Lane, T.E., Donahue, N.M. and Pandis, S.N. (2008b) Simulating secondary organic aerosol formation using the volatility basis-set approach in a chemical transport model. *Atmos. Environ.*, *42*, 7439–7451.
- Legrand, M. and Puxbaum, H. (2007) Summary of the carbosol project: Present and retrospective state of organic versus inorganic aerosol over Europe. *J. Geophys. Res.*, *112*, D23S01, doi:10.1029/2006JD008271.
- Levy, R.C., Remer, L.A., Mattoo, S., Vermote, E.F. and Kaufman, Y.J. (2007) Second-generation operational algorithm: Retrieval of aerosol properties over land from inversion of Moderate Resolution Imaging Spectroradiometer spectral reflectance. *J. Geophys. Res.*, *112*, doi:10.1029/2006JD007811.
- Liu, Y., Koutrakis, P. and Kahn, R. (2007) Estimating fine particulate matter component concentrations and size distributions using satellite-retrieved fractional aerosol optical depth: Part 1-Method development. *J. Air Waste Manage. Assoc.*, *57*, 1351-1359.
- Maxwell-Garnett, J.C. (1904) Colours in metal glasses and in metallic films. *Philos. Trans. R. Soc. A*, *203*, 385-420.
- Mishchenko, M.I., Cairns, B., Kopp, G., Schueler, C.F., Fafaul, B.A., Hansen, J.E., Hooker, R.J., Itchkawich, T., Maring, H.B., and Travis, L.D. (2007) Accurate monitoring of terrestrial aerosols and total solar irradiance: introducing the Glory Mission, *Bull. Am. Meteorol. Soc.*, *88*, 677–691.

- Myhre, C.L., Toledano, C., Myhre, G., Stebel, K., Yttri, K.E., Aaltonen, V., Johnsrud, M., Frioud, M., Cachorro, V., de Frutos, A., Lihavainen, H., Campbell, J.R., Chaikovsky, A.P., Shiobara, M., Welton, E.J. and Tørseth, K. (2007) Regional aerosol optical properties and radiative impact of the extreme smoke event in the European Arctic in spring 2006. *Atmos. Chem. Phys.*, 7, 5899-5915.
- Pathak, R.K., Presto, A.A., Lane, T.E. et al. (2007) Ozonolysis of  $\alpha$ -pinene: parameterization of secondary organic aerosol mass fraction. *Atmos. Chem. Physics*, 7(14), 3811–3821.
- Pettus, A. (2009) Agricultural fires and Arctic climate change: a special CATF report. Boston, Clean Air Task Force. URL: [http://www.catf.us/publications/reports/Agricultural\\_Fires\\_and\\_Arctic\\_Climate\\_Change.pdf](http://www.catf.us/publications/reports/Agricultural_Fires_and_Arctic_Climate_Change.pdf)
- Pio, C.A., Legrand, M., Oliveira, T., Afonso, J., Santos, C., Caseiro, A., Fialho, P., Barata, F., Puxbaum, H., Sánchez-Ochoa, A., Kasper-Giebl, A., Gelencsér, A., Preunkert, S. and Schock, M. (2007) Climatology of aerosol composition (organic versus inorganic) at non-urban sites on a west-east transect across Europe. *J. Geophys. Res.*, 112, D23S02, doi: 10.1029/2006JD008080.
- Presto, A.A. and Donahue, N.M. (2006) Investigation of  $\alpha$ -pinene + ozone secondary organic aerosol formation at low total aerosol mass. *Environ. Sci. Technol.*, 40, 3536–3543.
- Remer, L.A., Tanré, D. and Kaufman, Y.J. (2006) Algorithm for remote sensing of tropospheric aerosol from MODIS: Collection 5. Product ID: MOD04/MYD04). Greenbelt, USA, NASA Goddard Space Flight Center. [http://modis.gsfc.nasa.gov/data/atbd/atbd\\_mod02.pdf](http://modis.gsfc.nasa.gov/data/atbd/atbd_mod02.pdf)
- Robinson, A.L., Donahue, N.M., Shrivastava, M.K., Weitkamp, E.A., Sage, A.M., Grieshop, A.P., Lane, T.E., Pierce, J.R. and Pandis, S.N. (2007) Rethinking organic aerosols: Semivolatile emissions and photochemical aging. *Science*, 315, 1259–1262.
- Schaap, M., Apituley, A., Timmermans, R.M.A., Koelemeijer, R.B.A. and de Leeuw, G. (2009) Exploring the relation between aerosol optical depth and PM<sub>2.5</sub> at Cabauw, the Netherlands, *Atmos. Chem. Phys.*, 9, 909-925.
- Schmid, H., Laskus, L., Abraham, H.J., Baltensperger, U., Lavanchy, V., Bizjak, M., Burba, P., Cachier, H., Crow, D., Chow, J., Gnauk, T., Even, A., ten Brink, H.M., Giesen, K.-P., Hitzenberger, R., Hueglin, C., Maenhaut, W., Pio, C., Carvalho, A., Putaud, J.-P. and Toom-Sauntry, D. (2001) Results of the “carbon conference” international aerosol carbon round robin test stage I. *Atmos. Environ.*, 35, 2111–2121.
- Shrivastava, M.K., Lane, T.E., Donahue, N.M., Pandis, S.N. and Robinson, A.L. (2008) Effects of gas particle partitioning and aging of primary emissions on urban and regional organic aerosol concentrations. *J. Geophys. Res.*, 113, D18301, doi:10.1029/2007JD009735.

- Simpson, D., Yttri, K.E., Klimont, Z., Kupiainen, K., Caseiro, A., Gelencsér, A., Pio, C., Puxbaum, H. and Legrand, M. (2007) Modeling carbonaceous aerosol over Europe: Analysis of the CARBOSOL and EMEP EC/OC campaigns. *J. Geophys. Res.*, 112, D23S14, doi:10.1029/2006JD008158.
- Stohl, A., Berg, T., Burkhardt, J.F., Fjæraa, A.M., Forster, C., Herber, A., Hov, Ø., Lunder, C., McMillan, W.W., Oltmans, S., Shiobara, M., Simpson, D., Solberg, S., Stebel, K., Ström, J., Tørseth, K., Treffeisen, R., Virkkunen, K. and Yttri, K.E. (2007) Arctic smoke – record high air pollution levels in the European Arctic due to agricultural fires in Eastern Europe. *Atmos. Chem. Phys.*, 7, 511-534.
- Tsyro, S., Yttri, K.E. and Aas, W. (2009) Measurement and model assessment of Particulate Matter in Europe, Status 2007. In: *Transboundary Particulate Matter in Europe. EMEP Status report 4/2009*. Kjeller, Norwegian Institute for Air Research (EMEP Report 4/2009).
- Turpin, B. and Lim, H.-J. (2001) Species contributions to PM<sub>2.5</sub> mass: concentrations: Revisiting common assumptions for estimating organic mass. *Aerosol Sci. Technol.*, 35, 602-610.
- UNECE (2009) Guidelines for reporting emission data under the Convention on Long-range Transboundary Air Pollution (ECE/EB.AIR/97). Available at: [http://www.ceip.at/fileadmin/inhalte/emep/reporting\\_2009/Rep\\_Guidelines\\_ECE\\_EB\\_AIR\\_97\\_e.pdf](http://www.ceip.at/fileadmin/inhalte/emep/reporting_2009/Rep_Guidelines_ECE_EB_AIR_97_e.pdf)
- Veefkind, J.P., de Leeuw, G., Durkee, P.A., Russell, P.B., Hobbs, P.V. and Livingston, J.M. (1999) Aerosol optical depth retrieval using ATSR-2 data and AVHRR data during TARFOX. *J. Geophys. Res.*, 104D, 2253-2260.
- von Hoyningen-Huene, W., Freitag, M. and Burrows, J.B. (2003) Retrieval of aerosol optical thickness over land surfaces from top-of-atmosphere radiance. *J. Geophys. Res.*, 108, D4260, doi: 10.1029/2001JD002018.
- von Hoyningen-Huene, W., Kokhanovsky, A. and Burrows, J.P. (2008) Retrieval of Particulate Matter from MERIS Observations. In: *Advanced Environmental Monitoring*. Ed. by J.K. Young and U. Platt. Dordrecht, Springer.
- Yttri, K.E., Aas, W., Bjerke, A., Cape, J.N., Cavalli, F., Ceburnis, D., Dye, C., Emblico, L., Facchini, M.C., Forster, C., Hanssen, J.E., Hansson, H.C., Jennings, S.G., Maenhaut, W., Putaud, J.P. and Tørseth, K. (2007a) Elemental and organic carbon in PM<sub>10</sub>: a one year measurement campaign within the European Monitoring and Evaluation Programme EMEP. *Atmos. Chem. Phys.*, 7, 5711–5725, [www.atmos-chem-phys.net/7/5711/2007/](http://www.atmos-chem-phys.net/7/5711/2007/).

## **APPENDIX A**

### **Overview of PM emissions reporting**



Table A.1: Overview of PM reporting - sectoral emissions 2000, 2005, and 2007.

Country	PM <sub>2.5</sub>			PM <sub>10</sub>		
	2000	2005	2007	2000	2005	2007
Albania						
Armenia						
Austria	x	x	x	x	x	x
Azerbaijan						
Belarus		x	x		x	x
Belgium	x	x	x	x	x	x
Bosnia and Herzegovina						
Bulgaria			x			x
Canada	x	x	x	x	x	x
Croatia	x	x	x	x	x	x
Cyprus	x	x	x	x	x	x
Czech Republic		x	x		x	x
Denmark	x	x	x	x	x	x
Estonia	x	x	x	x	x	x
European Community	x	x	x	x	x	x
Finland	x	x	x	x	x	x
France	x	x	x	x	x	x
Georgia						
Germany	x	x	x	x	x	x
Greece						
Hungary	x	x	x	x	x	x
Iceland						
Ireland	x	x	x	x	x	x
Italy	x	x	x	x	x	x
Kazakhstan						
Kyrgyzstan						
Latvia	x	x	x	x	x	x
Liechtenstein						
Lithuania		x	x		x	x
Luxembourg						
Malta	x	x	x	x	x	x
Monaco						
Montenegro						
Netherlands	x	x	x	x	x	x
Norway	x	x	x	x	x	x
Poland	x	x	x	x	x	x
Portugal	x	x	x	x	x	x
Republic of Moldova	x	x		x	x	
Romania			x		x	x
Russian Federation		x	x		x	x
Serbia						
Slovakia	x	x	x	x	x	x
Slovenia	x	x	x	x	x	x
Spain	x	x	x	x	x	x
Sweden	x	x	x	x	x	x
Switzerland	x	x	x	x	x	x
TFY Republic of Macedonia						
Turkey						
Ukraine		x			x	
United Kingdom	x	x	x	x	x	x
United States of America						
<b>No of countries which reported sectoral emissions</b>	<b>27</b>	<b>32</b>	<b>32</b>	<b>27</b>	<b>33</b>	<b>32</b>

Note: x indicates that Party reported sectoral PM emissions for particular year.



## **APPENDIX B**

### **Tables and figure to Chapter 2**

Time-series of the concentrations of PM<sub>10</sub>, PM<sub>2.5</sub> and their components as calculated with the EMEP model and measured during EMEP intensive periods in June 2006 and January 2007



*Table B.1: Comparison of calculated with the EMEP model and measured concentrations of PM<sub>10</sub> for EMEP stations for 2007. Here, Obs – the measured mean, Mod – the calculated mean, Bias is calculated as  $\Sigma(\text{Mod}-\text{Obs})/\text{Obs} \times 100\%$ , R– the temporal correlation coefficient and RMSE – the Root mean Square Error=  $[1/Ns\Sigma(\text{Mod}-\text{Obs})^2]^{1/2}$ .*

Code	Station	Obs	Mod	Bias	R	RSME
AT02	Illmitz	20.76	8.07	-61	0.64	16.64
AT05	Vorhegg	8.52	10.36	22	0.56	7.99
AT48	Zoebelboden	9.77	9.76	0	0.58	7.57
CH01	Jungfrauoch	3.34	6.80	103	0.50	8.69
CH02	Payerne	19.30	8.24	-57	0.64	14.51
CH03	Taenikon	18.61	9.03	-52	0.65	13.40
CH04	Chaumont	10.63	8.35	-21	0.77	5.58
CH05	Rigi	10.64	7.84	-26	0.70	6.81
CY02	Ayia Marina	28.22	19	-32	0.66	18.34
DE01	Westerland/Wenningsted	18.61	11.09	-40	0.53	11.28
DE02	Langenbruegge/Waldhof	15.79	7.38	-53	0.62	11.48
DE03	Schauinsland	9.40	7.75	-18	0.70	6.34
DE07	Neuglobsow	14.00	6.34	-55	0.60	10.37
DE08	Schmuecke	10.42	7.50	-28	0.61	7.56
DE09	Zingst	15.40	8.37	-46	0.57	10.82
DE44	Melpitz	21.67	8.27	-61	0.66	15.84
DK05	Keldsnor	22.00	11.44	-48	0.42	14.68
ES07	Viznar	20.58	11.78	-43	0.45	16.90
ES08	Niembro	19.78	19.47	-2	0.28	12.12
ES09	Campisabalos	7.78	6.41	-18	0.52	5.27
ES10	Cabo de Creus	18.56	11.75	-37	0.48	9.73
ES11	Barcarrota	15.91	8.34	-48	0.23	13.73
ES12	Zarra	14.29	10.05	-30	0.55	9.22
ES13	Penausende	10.71	8.01	-25	0.47	7.39
ES14	Els Torms	17.51	11.87	-32	0.49	10.70
ES15 <sup>*)</sup>	Risco Llano	10.17	8.93	-12	0.50	8.69
ES16	O Savinao	12.06	10.74	-11	0.60	5.87
FR09	Revin	20.90	9.83	-53	0.71	13.36
FR13	Peyrusse Vieille	15.21	10.71	-30	0.21	9.48
IT01	Montelibretti	31.47	12.00	-62	0.38	23.55
NL07	Eibergen	26.19	11.00	-58	0.71	17.97
NL09	Kollumerwaard	25.77	10.28	-60	0.67	17.40
NL10	Vreededepeel	23.82	12.68	-46	0.73	14.88
NO01 <sup>**)</sup>	Birkenes	5.60	2.62	-53	-	-
PL05	Diabla Gora	15.84	6.80	-57	0.69	12.16
SE11 <sup>*)</sup>	Vavihill	15.09	6.24	-59	0.54	10.89
SE12	Aspvreten	9.59	3.36	-65	0.69	7.73
SE35	Vindeln	6.56	1.36	-79	0.59	6.03
SI08	Iskrba	15.47	8.54	-45	0.54	9.84
GB06	Lough Navar	12.88	6.12	-52	0.65	8.08
GB36	Harwell	21.54	7.62	-64	0.76	15.08
GB43	Narberth	18.07	8.36	-53	0.71	11.36
GB48	Auchencorth Moss	6.44	5.69	-11	0.77	4.54

<sup>\*)</sup> Fewer than 180 days with measurement data

<sup>\*\*)</sup> Annual average concentrations are compared  
*Italic font* – hourly measurements with TEOM

*Table B.2: Comparison of calculated with the EMEP model and measured concentrations of PM<sub>2.5</sub> for EMEP stations for 2007. Here, Obs – the measured mean, Mod – the calculated mean, Bias is calculated as  $\Sigma(\text{Mod-Obs})/\text{Obs} \times 100\%$ , R – the temporal correlation coefficient and RMSE – the Root mean Square Error =  $[1/N_s \Sigma(\text{Mod-Obs})^2]^{1/2}$ .*

Code	Station	Obs	Mod	Bias	R	RSME
AT02	Illmitz	16.11	6.93	-57	0.64	12.68
CH02	Payerne	12.43	6.79	-45	0.59	9.67
CH05	Rigi	7.86	6.25	-20	0.75	4.84
DE02	Langenbruegge/Waldhof	11.29	6.07	-46	0.63	8.43
DE03	Schauinsland	6.51	6.71	3	0.73	4.37
DE44	Melpitz	17.44	6.8	-61	0.68	13
ES07	Viznar	10.78	6.22	-42	0.36	7.39
ES08	Niembro	11.71	9.75	-16	0.65	6.21
ES09	Campisabalos	6.82	4.36	-36	0.39	5.52
ES10	Cabo de Creus	10.01	7.24	-27	0.58	5.44
ES11	Barcarrota	8.22	5.97	-27	0.38	5.28
ES12	Zarra	8.83	7.09	-19	0.5	5.25
ES13	Penausende	6.45	5.88	-8	0.54	3.76
ES14	Els Torms	12.29	8.83	-28	0.55	6.94
ES15 <sup>*)</sup>	Risco Llano	7.03	6.07	-13	0.49	4.79
ES16	O Savinao	7.95	7.48	-5	0.68	4.11
IT01	Montelibretti	21.87	8.44	-61	0.38	16.41
IT04	Ispra	25.59	12.81	-49	0.1	26.9
NO01 <sup>**)</sup>	Birkenes	3.30	1.75	-47	-	-
<i>SE11</i>	<i>Vavihill</i>	<i>9.04</i>	<i>4.21</i>	<i>-53</i>	<i>0.84</i>	<i>5.65</i>
<i>SE12</i>	<i>Aspvreten</i>	<i>6.73</i>	<i>2.32</i>	<i>-65</i>	<i>0.72</i>	<i>5.76</i>
SI08	Iskrba	10.09	6.9	-31	0.45	6.56
GB36	Harwell	11.6	5.25	-54.8	0.82	7.26
GB48	Auchencorth Moss	4.04	3.38	-16.4	0.84	3.29

<sup>\*)</sup> Fewer than 180 days with measurement data

<sup>\*\*) Annual average concentrations are compared  
*Italic font* – hourly measurements with TEOM</sup>

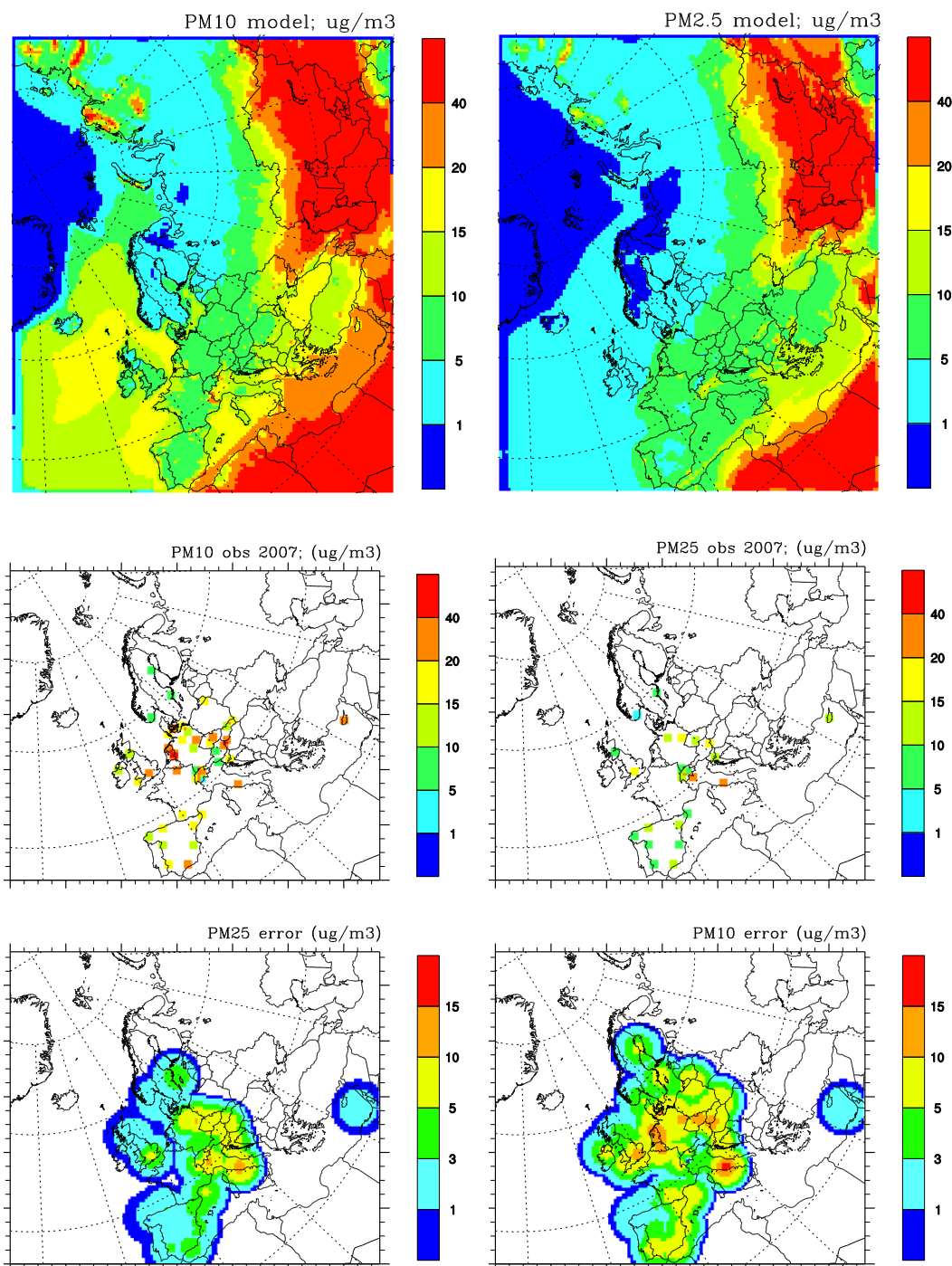
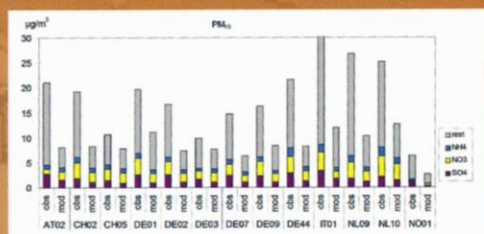


Figure B.1: Annual mean concentrations of PM<sub>10</sub> (left) and PM<sub>2.5</sub> (right) in 2007: upper row – the model calculations, middle row – the EMEP measurements, and lower row – the interpolated differences between measured and modelled PM concentrations.

# emep

Chemical Co-ordinating Centre of EMEP  
Norwegian Institute for Air Research  
P.O. Box 100, N-2027 Kjeller, Norway



ccc  
NILU  
Norwegian Institute for Air Research  
P.O. Box 100  
NO-2027 Kjeller  
Norway  
Phone: +47 63 89 80 00  
Fax: +47 63 89 80 50  
E-mail: [kjetil.torseth@nilu.no](mailto:kjetil.torseth@nilu.no)  
Internet: [www.nilu.no](http://www.nilu.no)



ciam  
International Institute for  
Applied Systems Analysis  
(IIASA)  
A-2361 Laxenburg  
Austria  
Phone: +43 2236 80 70  
Fax: +43 2236 71 31  
E-mail: [amann@iiasa.ac.at](mailto:amann@iiasa.ac.at)  
Internet: [www.iiasa.ac.at](http://www.iiasa.ac.at)

umweltbundesamt<sup>u</sup>

ciamp  
Umweltbundesamt GmbH  
Spittelauer Lände 5  
1090 Vienna  
Austria  
Phone: +43-(0)1-313 04  
Fax: +43-(0)1-313 04/5400  
E-mail:  
[emep.emissions@umweltbundesamt.at](mailto:emep.emissions@umweltbundesamt.at)  
Internet:  
<http://www.umweltbundesamt.at/>



msc-e  
Meteorological Synthesizing  
Centre-East  
Krasina pereulok, 16/1  
123056 Moscow  
Russia  
Phone +7 495 981 15 66  
Fax: +7 495 981 15 67  
E-mail: [msce@msceast.org](mailto:msce@msceast.org)  
Internet: [www.msceast.org](http://www.msceast.org)



msc-w  
Norwegian Meteorological  
Institute (met.no)  
P.O. Box 43 Blindern  
NO-0313 OSLO  
Norway  
Phone: +47 22 96 30 00  
Fax: +47 22 96 30 50  
E-mail: [emep.mscw@met.no](mailto:emep.mscw@met.no)  
Internet: [www.emep.int](http://www.emep.int)